MODIFIED PECTIN STRUCTURE FOR TARGETED DIVALENT CATION BINDING AND ASSOCIATED FUNCTIONALITIES IN FOOD MODEL SYSTEMS

Miete CELUS

Promotor:
Prof. M. Hendrickx, KU Leuven

Members of the examination committee:
Prof. I. Vankelecom, KU Leuven, chairman
Prof. T. Grauwet, KU Leuven
Prof. I. Foubert, KU Leuven (Campus Kulak)
Prof. I. Fraeye, KU Leuven (Technologiecampus Gent)
Prof. K. Dewettinck, UGent

Dissertation presented
in partial fulfilment of
the requirements
for the degree of
Doctor of Bioscience
Engineering (PhD)

December 2018

Doctoraatsproefschrift nr. 1545 aan de faculteit Bio-ingenieurswetenschappen van de KU Leuven.

© 2018 KU Leuven, Science, Engineering & Technology
Uitgegeven in eigen beheer, Miete Celus, Leuven

Alle rechten voorbehouden. Niets uit deze uitgave mag worden vermenigvuldigd en/of openbaar gemaakt worden door middel van druk, fotokopie, microfilm, elektronisch of op welke andere wijze ook zonder voorafgaandelijke schriftelijke toestemming van de uitgever.

All rights reserved. No part of the publication may be reproduced in any form by print, photoprint, microfilm, electronic or any other means without written permission from the publisher.

SAMENVATTING

Pectine is een celwandpolysacharide dat voornamelijk geëxtraheerd wordt uit de afvalstromen van de citrus- en appelverwerkende industrie en vaak gebruikt wordt als additief in onder andere groenten- en fruitgebaseerde levensmiddelen. De voornaamste toepassing is als gelerend agens omwille van zijn capaciteit om tweewaardige kationen te binden, zoals Ca^{2+}. Deze functionaliteit van pectine wordt grotendeels beïnvloed door zijn structurele eigenschappen, in het bijzonder door de graad van methylverestering (*degree of methylesterification*, DM) en graad van bloksgewijsheid (*absolute degree of blockiness*, DB_{abs}). De relatie tussen deze structuureigenschappen van pectine en de Ca^{2+} binding of gelering werden reeds uitgebreid bestudeerd. Desalniettemin ontbreekt tot op heden een fundamenteel inzicht in de interactie tussen pectine en Ca^{2+}. Bovendien is zeer weinig informatie beschikbaar over hoe de structuureigenschappen van pectine de binding met andere tweewaardige kationen beïnvloeden, zoals Fe^{2+} of Zn^{2+}. Nochtans bestaat de hypothese dat de binding van dergelijke kationen aan pectine kan leiden tot andere specifieke functionaliteiten. Zo kan de binding van essentiële divalente kationen (zoals Zn^{2+}) aan pectine bijvoorbeeld leiden tot een verlaagde biotoegankelijkheid tijdens de vertering, wat mogelijk resulteert in mineraal deficiënties. Pectine is immers een dieetvezel die niet wordt afgebroken tijdens de vertering in de dunne darm. Daarnaast wordt verondersteld dat de binding van Fe^{2+} aan pectine kan resulteren in een vertraging van de lipide oxidatie in emulsie-gebaseerde levensmiddelen en dus bijdraagt tot het antioxiderend vermogen van pectine. Op die manier zou pectine kunnen fungeren als natuurlijk antioxidant en zo het gebruik van artificiële antioxidanten zoals ethyleendiaminetetra-azijnzuur (EDTA) mogelijk reduceren, wat interessanter geacht wordt voor de consument. Bijgevolg is het doel van dit doctoraat om fundamenteel inzicht te verwerven in het effect van de DM en DB_{abs} van pectine op de interactie met Fe^{2+}, Zn^{2+} of Ca^{2+} en de geassocieerde functionaliteiten, in het bijzonder het antioxiderend vermogen en de rol in de Zn^{2+} biotoegankelijkheid.

Pectinestalen met vergelijkbare graad van methylverestering (DM) maar verschillende patronen (DB_{abs}) werden aangemaakt via enzymatische (gebruik makend van wortel pectine methylesterase) of basische (met NaOH) demethylesterificatie startend van hoog-methylveresterd citruspectine. In eerste instantie werd de interactie van deze pectinestalen met Fe^{2+}, Zn^{2+} of Ca^{2+} bestudeerd via evenwichts-adsorptie experimenten. Dit resulteerde in adsorptie-isothermen die werden gemodelleerd op basis van het Langmuir adsorptie-isotherm model ter

kwantificatie van de maximale bindingscapaciteit en gerelateerde interactie-energie. De resultaten van deze studie toonden aan dat pectine met afnemende DM of toenemende DB_{abs} meer Fe^{2+}, Zn^{2+} of Ca^{2+} kon binden. De maximale bindingscapaciteit werd bovendien voornamelijk beïnvloed door de DM, terwijl de interactie-energie eerder door de DB_{abs} bepaald werd. De pectinestalen vertoonden de hoogste bindingscapaciteit en interactie-energie voor Zn^{2+}, gevolgd door Ca^{2+} en Fe^{2+}. Daarnaast werden ook de thermodynamische eigenschappen van de pectine-kation interacties, in het bijzonder de pectine-Zn^{2+} binding, bestudeerd door isotherme titratie calorimetrie (ITC). Deze resultaten vormden een aanvulling op deze van de evenwichts-adsorptie experimenten. ITC toonde immers aan dat de Zn^{2+} binding aan pectine een endotherme reactie is, waarbij een positieve entropieverandering de ongunstige endothermische enthalpieverandering domineerde. De pectine-Zn^{2+} interactie verloopt daarnaast via een twee-staps mechanisme met eerst monocomplexatie en de vorming van *point-like cross-links*, gevolgd door dimerizatie.

Vervolgens werd bestudeerd in welke mate de DM en DB_{abs} van pectine en de gerelateerde interactie met Zn^{2+} een invloed hadden op de Zn^{2+} biotoegankelijkheid. Dit werd verwezenlijkt door het uitvoeren van een *in vitro* gesimuleerde vertering van pectineoplossingen die werden aangereikt met Zn^{2+}. Een afnemende DM of toenemende DB_{abs} resulteerde in een dalende Zn^{2+} biotoegankelijkheid, wat te wijten is aan een grotere bindingscapaciteit van pectine. Desalniettemin bleken kleinere hoeveelheden Zn^{2+} biotoegankelijk te zijn dan verwacht kon worden op basis van de eerder vastgestelde maximale Zn^{2+}-bindingscapaciteit van pectine. Dit wijst op mogelijke binding van Zn^{2+} aan galzouten of enzymen die tijdens de *in vitro* gesimuleerde vertering werden toegevoegd. Daarnaast werd de mogelijk competitie tussen Ca^{2+} en Zn^{2+} voor binding aan pectine tijdens de digestie onderzocht en een lage concentratie Ca^{2+} (ongeveer 0.33 mM) had geen significant effect op de Zn^{2+} biotoegankelijkheid.

Met het oog op het gebruik van natuurlijke antioxidanten ter reductie van synthetische, werd tot slot het antioxiderend vermogen van de pectinestalen bestudeerd in lijnzaad/zonnebloem olie-in-water (o/w) emulsies (5% w/v), die werden aangereikt met Fe^{2+}. Het peroxidegetal werd bepaald in functie van de bewaartijd. Laag DM pectine en een verhoogde pectine concentratie hadden een positief effect op het antioxiderend vermogen omwille van een verhoogde Fe^{2+} bindingscapaciteit. Het antioxiderend vermogen van pectine was echter lager dan dit van EDTA. Bovendien destabiliseerde pectine de o/w emulsies door flocculatie (*bridging* of *depletion flocculation*).

Deze doctoraatsthesis toonde duidelijk het effect aan van de DM en DB_{abs} van pectine op de kation bindingscapaciteit en gerelateerde functionaliteiten. De resultaten verschaffen een fundamenteel inzicht in de structuur-functie relatie van pectine wat op zijn beurt kan bijdragen tot optimalisatie van *ex situ* pectine functionaliteiten in verscheidene toepassingen, waaronder het verhogen van de product viscositeit zonder in te boeten in de nutritionele waarde van het product. Bovendien vormen deze resultaten een basis voor de toepassing van pectine als een natuurlijk antioxidant en verder onderzoek naar de *in situ* functionaliteiten van pectine.

ABSTRACT

Extracted pectin is currently widely used as a food additive in plant-based products, particularly in gelling applications, due to its ability to bind divalent cations, especially Ca^{2+}. This pectin functionality has been reported to be largely influenced by its structural properties, in particular the degree and pattern of methylesterification (DM) and blockiness (DB_{abs}), which are a measure for the percentage and distribution of methylesterified galacturonic acid units, respectively. Although the role of these structural properties in Ca^{2+}-binding and gelling has been widely explored, fundamental insights into these interactions are limited. Moreover, scarce information is available on the role of the pectin properties in the interaction with other divalent cations, despite the hypothesized ability of pectin to bind these divalent cations yielding specific functionalities. For instance, given that pectin is a dietary fiber and thus not digestible in the small intestine, its interaction with essential divalent cations, such as Zn^{2+}, could result in reduced mineral bioaccessibilities during digestion, potentially contributing to mineral deficiencies. Additionally, binding of Fe^{2+} has been considered to confer pectin a lipid antioxidant capacity in emulsion-based products, thereby retarding lipid oxidation. Exploring this pectin functionality could promote its use as a natural antioxidant which is more appealing to consumers compared to synthetic additives, such as ethylenediaminetetraacetic acid (EDTA). Therefore, this doctoral thesis aimed to provide fundamental insights into the effect of pectin DM and DB_{abs} on its interaction with Fe^{2+}, Zn^{2+}, or Ca^{2+} and associated functionalities, particularly the lipid antioxidant capacity and its role in the Zn^{2+} *in vitro* bioaccessibility.

Pectin samples with comparable methylesterification degrees (DM) but different patterns of methylester distribution (DB_{abs}) were generated through enzymatic (using carrot pectin methylesterase) or alkaline (using NaOH) demethylesterification of high methylesterified citrus pectin. First, the interaction of these pectin samples with Fe^{2+}, Zn^{2+}, or Ca^{2+} was explored through equilibrium adsorption experiments, followed by generation of adsorption isotherms based on the Langmuir adsorption isotherm model to quantify their maximum binding capacities and associated interaction energies. Results of this study showed that decreasing pectin DM or increasing DB_{abs} promoted the Fe^{2+}-, Zn^{2+}-, or Ca^{2+}-binding capacity of pectin, with the maximum binding capacity being mainly determined by the DM and the interaction energy by DB_{abs}. With regard to cation type, the highest maximum binding capacity and interaction energy were exhibited for Zn^{2+} compared to Ca^{2+} and Fe^{2+}. Additionally, insights into

the thermodynamics of the pectin-cation interaction, particularly pectin-Zn^{2+} binding, were obtained using isothermal titration calorimetry (ITC). Results obtained complemented those from the equilibrium adsorption experiment. The binding of Zn^{2+} to pectin was found to be an endothermic interaction, in which a positive entropy change dominated the unfavorable endothermic enthalpy change. Moreover, the pectin-Zn^{2+} interaction occurred according to a two-step mechanism involving first monocomplexation and the formation of point-like cross-links, followed by dimerization.

The role of pectin DM and DB_{abs}, and associated pectin-Zn^{2+} interaction, in directing Zn^{2+} bioaccessibility was subsequently studied through *in vitro* simulated digestion of Zn^{2+}-enriched pectin solutions. Decreasing DM or increasing DB_{abs} resulted in decreased Zn^{2+} bioaccessibilities due to higher Zn^{2+}-binding capacities. However, lower amounts of Zn^{2+} than expected (based on the established maximum Zn^{2+}-binding capacity of pectin) were bioaccessible, suggesting binding of Zn^{2+} to the bile salts and probably to enzymes added during the *in vitro* simulated digestion. Exploration of the possible competition between Ca^{2+} and Zn^{2+} for binding to pectin during digestion revealed that low Ca^{2+} levels (approximately 0.33 mM) had no significant influence on Zn^{2+} bioaccessibility.

In view of identifying (potential) natural antioxidants to reduce synthetic ones, the lipid antioxidant capacity of the derived pectins in Fe^{2+}-enriched linseed/sunflower oil-in-water (o/w) emulsions (5% w/v) was explored by determination of the peroxide value as a function of storage time. Low DM pectin and increased pectin concentration promoted the lipid antioxidant capacity, due to an increased Fe^{2+}-binding capacity. However, EDTA exhibited still a higher antioxidant capacity compared to low DM pectin. Moreover, pectin was found to destabilize the o/w emulsions by bridging or depletion flocculation.

This doctoral thesis clearly demonstrated the role of DM and DB_{abs} in directing pectin cation-binding capacity and associated functionalities. The results obtained provide fundamental insights into the pectin structure-function relation which in turn can contribute to optimization of *ex situ* pectin functionalities in several applications, including product structure build-up while maintaining the nutritional value of the food product. Moreover, these findings form a basis for potential exploitation of pectin as an antioxidant as well as exploring pectin functionalities *in situ*.

LIST OF NOTATIONS

LIST OF ABBREVIATIONS

Ara	Arabinose
$\overline{BN}$	Number of averaged-sized non-methylesterified domains per molecule
$\overline{BS}$	Average size of non-methylesterified domains
CNBr	Cyanogen bromide
DAc	Degree of acetylation
DB	Degree of blockiness
DB_{abs}	Absolute degree of blockiness
DBMe	Degree of blockiness of high methylesterified stretch
$DB_{abs}Me$	Absolute degree of blockiness of high methylesterified stretch
DM	Degree of methylesterification
DP	Degree of polymerization
EDTA	Ethylenediaminetetraacetic acid
FFA	Free fatty acid
FT-IR	Fourier transform infra-red
Fuc	Fucose
Gal	Galactose
GalA	Galacturonic acid
Glu	Glucose
HG	Homogalacturonan
HM	High methylesterified
HPAEC	High-performance anion exchange chromatography
HPSEC	High-performance size exclusion chromatography
ICP-MS	Inductively coupled plasma mass spectrometry
ITC	Isothermal titration calorimetry

LM	Low methylesterified
LSSO	Linseed/sunflower oil
MALLS	Multi-angle laser light scattering
Man	Mannose
MWCO	Molecular weight cut-off
NHS	N-hydroxysuccinimide
NMD	Non-methylesterified domain
o/w	Oil-in-water
PAD	Pulsed amperometric detector
PG	Polygalacturonase
PME	Pectin methylesterase
PMEI	Pectin methylesterase inhibitor
Rha	Rhamnose
RG I	Rhamnogalacturonan I
RG II	Rhamnogalacturonan II
SEM	Scanning electron microscopy
TFA	Trifluoroacetic acid
Xyl	Xylose

LIST OF SYMBOLS

$\boldsymbol{\theta}_j$	Fraction of site j occupied by the ligand
ΔG	Gibbs free energy change (J/mol)
ΔH	Enthalpy change (J/mol)
ΔQ	Differential heat (J)
ΔS	Entropy change (J/mol.K)
C	C-pectin – alkaline (chemically) demethylesterified citrus pectin
C_0	Initial cation concentration (g/L)

C_e	Equilibrium cation concentration (g/L)
CP95	Commercial high methylesterified citrus pectin
d_{32}	Surface-weighted mean particle size (µm)
d_{43}	Volume-weighted mean particle size (µm)
H_c	Height of cream layer (cm)
H_e	Total height of the emulsion (cm)
K_a	Binding constant (mM^{-1})
K_j	Binding constant for process j
K_L	Langmuir constant – Interaction energy (mM^{-1})
[L]	Free ligand concentration (M)
L_t	Total ligand concentration (M)
M_n	Number average molar mass (Da)
M_w	Weight average molar mass (Da)
n	Stoichiometric ratio – binding capacity (mol cation/mol GalA)
n_j	Total stoichiometric ratio for process j
P	P-pectin – enzymatically demethylesterified citrus pectin
P_t	Total macromolecule concentration (M)
Q	Total heat produced (J)
q_e	Equilibrium cation-binding capacity (mol cation/mol GalA)
q_{max}^{G}	Maximum binding capacity (mol cation/mol GalA)
q_{max}^{C}	Maximum binding capacity (mol cation/mol COO^-)
T	Temperature (K)
V_0	Initial volume of the sample cell (L)
V_{in}	Volume inside membrane (L)
V_{out}	Volume outside membrane (L)

TABLE OF CONTENTS

SAMENVATTING I

ABSTRACT V

LIST OF NOTATIONS VII

TABLE OF CONTENTS XI

CONTEXT AND RESEARCH OBJECTIVES XVII

PART I: LITERATURE REVIEW 1

1 PECTIN STRUCTURE, CATION BINDING AND FUNCTIONALITY 3

1.1 INTRODUCTION 3

1.2 INFLUENCE OF PECTIN MOLECULAR STRUCTURE ON THE DIVALENT CATION-BINDING CAPACITY OF PECTIN 5

1.2.1 General description of pectin molecular structure in view of divalent cation binding 5

1.2.2 DM and distribution pattern of non-methylesterified GalA units 7

1.2.3 Chain length 11

1.2.4 Other structural characteristics 12

1.3 BINDING MECHANISMS BETWEEN PECTIN AND DIVALENT CATIONS 14

1.4 INFLUENCE OF CATION TYPE ON THE BINDING CAPACITY OF PECTIN 18

1.5 INFLUENCE OF EXTRINSIC FACTORS ON THE CATION-BINDING CAPACITY OF PECTIN 21

1.6 PECTIN FUNCTIONALITIES BASED ON CATION INTERACTIONS 23

1.6.1 Cation-induced gelation 23

1.6.1.1 Ca^{2+}-induced gelation 23
1.6.1.2 Gelation induced by other divalent cations 26
1.6.2 Antioxidant capacity 27
1.6.3 Role of pectin in the digestive tract 29
1.6.3.1 Mineral bioaccessibility or bioavailability 29
1.6.3.2 Role of pectin in excretion of toxic minerals 34
1.6.3.3 Role of pectin in lipid digestion and cholesterol synthesis 34
1.6.4 Other pectin functionalities 35

1.7 CONCLUSION AND RESEARCH OBJECTIVE 36

PART II: EXPERIMENTAL WORK 37

2 DEMETHYLESTERIFICATION AND STRUCTURAL CHARACTERIZATION OF PECTINS 39

2.1 INTRODUCTION 39

2.2 MATERIALS AND METHODS 40
2.2.1 Materials 40
2.2.2 Kiwi PMEI extraction and purification for preparation of PMEI-sepharose gel 41
2.2.3 Carrot PME extraction and purification 42
2.2.4 PME and PMEI activity determination 42
2.2.5 Demethylesterification of citrus pectin 43
2.2.5.1 Enzymatic demethylesterification with carrot PME 43
2.2.5.2 Alkaline demethylesterification 43
2.2.6 Characterization of the demethylesterified pectin samples 44
2.2.6.1 Determination of the degree of methylesterification 44
2.2.6.2 Estimation of the absolute degree of blockiness 44
2.2.6.3 Determination of GalA and neutral sugar content 45
2.2.6.4 Determination of molar mass distribution 46
2.2.6.5 Determination of the intrinsic cation concentration 46
2.2.7 Statistical data analysis 46

2.3 RESULTS AND DISCUSSION 47
2.3.1 Degree and pattern of methylesterification of the pectin samples 47
2.3.2 GalA content and neutral sugar composition 49
2.3.3 Molar mass distributions 50
2.3.4 Intrinsic cation concentration of the pectin samples 51

2.4 CONCLUSION 53

3 INFLUENCE OF PECTIN DEGREE AND PATTERN OF METHYLESTERIFICATION ON INTERACTION WITH ZN^{2+} OR CA^{2+} AND ASSOCIATED ZN^{2+} BIOACCESSIBILITY 55

3.1 INTRODUCTION 55

3.2 MATERIALS AND METHODS 56
3.2.1 Materials 56
3.2.2 Determination of adsorption isotherms of pectin for Zn^{2+} and Ca^{2+} 56
3.2.3 *In vitro* simulated digestion of Zn^{2+}-enriched pectin samples 58
3.2.4 Statistical data analysis 59

3.3 RESULTS AND DISCUSSION 59
3.3.1 Adsorption isotherms of pectin samples for Zn^{2+} or Ca^{2+} in general 59
3.3.2 Influence of pectin DM and DB_{abs} on the maximum Zn^{2+}- or Ca^{2+}-binding capacity 61
3.3.2.1 q_{max}^{G} values 61
3.3.2.2 q_{max}^{C} values 64
3.3.3 Influence of pectin DM and DB_{abs} on interaction energy between pectin and Zn^{2+} or Ca^{2+} 67
3.3.4 Influence of cation type (Zn^{2+} or Ca^{2+}) on interactions with pectin 69
3.3.5 *In vitro* bioaccessibility of Zn^{2+} 69

3.4 CONCLUSION 73

4 ISOTHERMAL TITRATION CALORIMETRY FOR ASSESSING THE ZN^{2+}-BINDING CAPACITY OF PECTIN 75

4.1 INTRODUCTION 75

4.2 MATERIALS AND METHODS 76
4.2.1 Materials 76
4.2.2 Isothermal titration calorimetry 76
4.2.3 Statistical data analysis 78

4.3 RESULTS AND DISCUSSION 78
4.3.1 Isothermal titration calorimetry in general 78
4.3.2 Influence of pectin DM and DB_{abs} on Zn^{2+}-binding capacity 82
4.3.3 Influence of pectin DM and DB_{abs} on binding constant of pectin-Zn^{2+} interaction 85
4.3.4 Influence of pectin DM and DB_{abs} on entropy and enthalpy change for pectin-Zn^{2+} interaction 86

4.4 CONCLUSION 89

5 INFLUENCE OF PECTIN DEGREE AND PATTERN OF METHYLESTERIFICATION ON FE^{2+} INTERACTION 91

5.1 INTRODUCTION 91

5.2 MATERIALS AND METHODS 92
5.2.1 Materials 92
5.2.2 Determination of adsorption isotherms of pectin for Fe^{2+} 92
5.2.3 Statistical data analysis 94

5.3 RESULTS AND DISCUSSION 94
5.3.1 Adsorption isotherms of pectin samples for Fe^{2+} in general 94
5.3.2 Influence of pectin DM and DB_{abs} on the maximum Fe^{2+}-binding capacity 96
5.3.3 Influence of pectin DM and DB_{abs} on interaction energy between pectin and Fe^{2+} 99

5.4 CONCLUSION 101

6 INFLUENCE OF PECTIN DEGREE AND PATTERN OF METHYLESTERIFICATION ON PHYSICAL AND OXIDATIVE STABILITY OF OIL-IN-WATER EMULSIONS 103

6.1 INTRODUCTION 103

6.2 MATERIALS AND METHODS 105
6.2.1 Materials 105
6.2.2 Emulsion preparation 105
6.2.3 Physical characterization of emulsion stability 106
6.2.3.1 Particle electrical charge 106
6.2.3.2 Creaming index 107
6.2.3.3 Particle size distribution 107
6.2.3.4 Microstructure 107
6.2.4 Determination of emulsion oxidative stability 108
6.2.5 Statistical data analysis 108

6.3 RESULTS AND DISCUSSION 108
6.3.1 Emulsion physical stability 108
6.3.1.1 Particle electrical charge measurements 109

6.3.1.2 Emulsion particle size, creaming index and microstructure 112
6.3.2 Emulsion oxidative stability 117

6.4 CONCLUSION 122

PART III: GENERAL CONCLUSIONS AND PERSPECTIVES 123

7 GENERAL CONCLUSIONS AND FUTURE PERSPECTIVES 125

LIST OF REFERENCES 133

LIST OF PUBLICATIONS 147

CONTEXT AND RESEARCH OBJECTIVES

Nowadays, there is an increased consumer awareness towards the consumption of more fruit-, vegetable-, and legume-based food products, containing naturally sourced ingredients. In such plant-based food products, pectin, a cell wall polysaccharide exhibits a major role in determining product textural quality, an important attribute for consumer acceptability. Pectin also serves as a dietary fiber, contributing to improved health benefits of these food products by for instance promoting the cardiovascular health or reducing the risk of cancers. Besides its functionality *in situ*, pectin is more commonly extracted from citrus peel or apple pomace on commercial scale and used as a natural additive (*ex situ*), which is more appealing to consumers. These *ex situ* pectin functionalities can be mainly attributed to its capacity to bind divalent cations via the negatively chargeable non-methylesterified galacturonic acid (GalA) units of homogalacturonan, the linear pectin subdomain. The structural properties of pectin, and in particular the degree (DM) and pattern (degree of blockiness, DB) of methylesterification are reported to largely determine the cation-binding capacity of pectin and associated functionalities. It is hypothesized that pectin with decreasing DM or increasing DB interacts to a higher extent with divalent cations due to higher number or longer blocks of negatively charged carboxyl groups.

To date, commercially available pectin is widely used as a gelling or thickening agent in among others fruit- and vegetable-based food products for structure build-up due to its ability to crosslink with divalent cations, such as Ca^{2+}, Zn^{2+}, or Fe^{2+}. Despite the potential use of both *in situ* and *ex situ* pectin in product structure build-up, attributed to their cation-binding ability, the polyanionic nature of pectin might negatively influence the bioaccessibility of the bound cations, hence their absorption in the small intestine during digestion. For instance, it is hypothesized that essential minerals bound to pectin may not be released during digestion, potentially promoting mineral deficiencies. With regard to the Fe^{2+}-binding ability of pectin, this pectin-cation interaction can additionally contribute to a specific functionality as it confers pectin a possible antioxidant capacity in oil-in-water emulsion-based food products. Chelation of these pro-oxidative metal ions, thus partitioning them away from the oil-water interface, retards the lipid oxidation. To this extent, pectin might be used as a natural antioxidant and as such reduce synthetic ones as for instance ethylenediaminetetraacetic acid (EDTA), which is currently widely used in food products sensitive to oxidation, such as dressings or mayonnaises.

Consequently, while the cation-binding capacity of pectin is of great importance and an interesting area of research in exploring several pectin functionalities, it is a big challenge for food technologists and nutritionists to optimize multiple pectin functionalities. For instance, promoting pectin-cation interactions for product structure build-up or antioxidant capacity in foods, without compromising the product's mineral nutritional value, remains a challenge and probably requires fundamental insights into the relation between pectin structure and cation-binding capacity. The role of pectin structure in the Ca^{2+}-binding and associated gelling has received a lot of focus. However, studies systematically exploring the binding capacity of other divalent cations such as Fe^{2+} or Zn^{2+} and related binding constants of pectins with targeted modified structures are scarce, despite its potential role in distinct functionalities (e.g., antioxidant capacity). The main objective of this doctoral thesis is therefore to obtain a fundamental understanding of the relation between pectin structure (with main focus on DM and DB, which are pectin properties of major interest in relation to cation binding) and the Fe^{2+}-, Zn^{2+}-, or Ca^{2+}-binding capacity. This is followed by elucidation of the effect of these pectin structural properties on the *in vitro* Zn^{2+} bioaccessibility (as Zn^{2+} deficiency is reported to be a highly prevalent nutritional problem worldwide) and its lipid antioxidant capacity in oil-in-water emulsions, serving as food model systems. A schematic overview of the thesis contents and research strategy to achieve this objective is given in **Figure 1**.

Chapter 1 reviews the literature on pectin structure and its influence (of mainly the HG subdomain) on the cation-binding capacity and functionalities, including cation-induced gelation, lipid antioxidant capacity and mineral bioaccessibility. Binding mechanisms between pectin and specific cations are also discussed. The literature review is followed by five chapters of experimental work performed to reach the objective of this doctoral thesis. **Chapter 2** describes the generation and characterization of the demethylesterified pectin samples used in subsequent chapters to gain insights into the role of the DM and DB in directing the cation-binding capacity and functionalities of pectin. The Zn^{2+}- and Ca^{2+}-binding capacities of the pectin samples are explored in **Chapter 3**, followed by a study on its role in the *in vitro* Zn^{2+} bioaccessibility. Besides exploring the Zn^{2+}-binding capacity of the pectins through an equilibrium adsorption experiment (Chapter 3), in **Chapter 4**, an alternative method, namely isothermal titration calorimetry (ITC), was employed in order to gain fundamental insights into the binding thermodynamics. **Chapter 5** explores the Fe^{2+}-binding capacity of the pectin samples through an equilibrium adsorption experiment and **Chapter 6**, finally, is a study on the effect of pectin on the oxidative (lipid antioxidant capacity) and physical stability of oil-in-water emulsions.

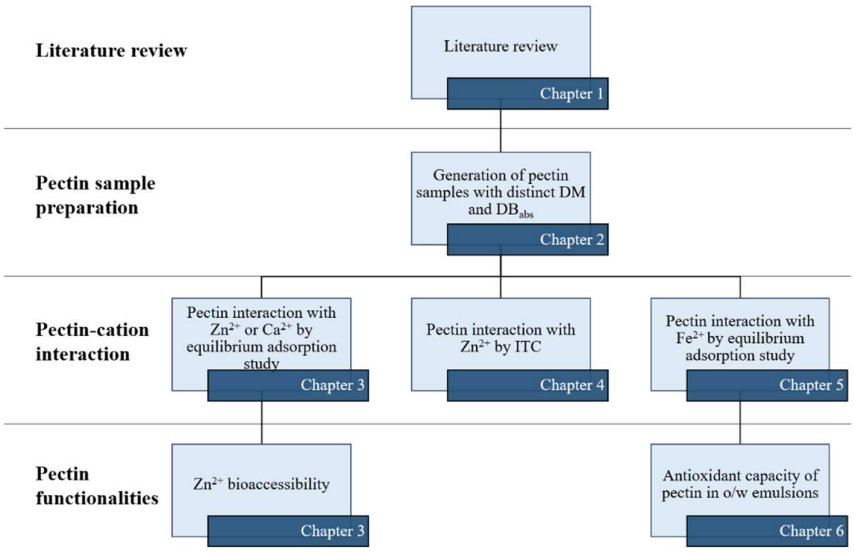

Figure 1: Schematic overview of the research strategy of the doctoral thesis.

PART I: LITERATURE REVIEW

CHAPTER 1

PECTIN STRUCTURE, CATION BINDING AND FUNCTIONALITY[1]

1.1 INTRODUCTION

Nowadays, consumer diets are changing towards more fruit-, vegetable-, and legume-based food products. Such plant-based products are reported to be part of sustainable diets, which are characterized by a low environmental impact and high nutritional value (van Dooren, Douma, Aiking, & Vellinga, 2017). These products also contain dietary fibers, of which pectin, a cell wall polysaccharide, is of particular interest due to its multiple functionalities and health benefits (May, 1990; Thakur, Singh, Handa, & Rao, 1997; Wicker et al., 2014). Pectin is naturally present in fruit- or vegetable-based products, resulting in *in situ* pectin functionalities (Christiaens et al., 2012; Sila et al., 2009), or it is used as a food additive, after extraction from citrus peel or apple pomace, during food processing to impart specific product characteristics (Sila et al., 2009; Willats, Knox, & Mikkelsen, 2006). An important part of the pectin functionalities explored, both *in situ* or in systems with added extracted pectin, are associated with its ability to bind divalent cations (Renard & Jarvis, 1999). Such cations are naturally present in food products (mostly in low concentrations) or introduced during processing or cooking (Gao et al., 2017).

[1] This chapter is based on following paper:
Celus, M., Kyomugasho, C., Van Loey, A., Grauwet, T., and Hendrickx, M. (2018). Influence of pectin structural properties on the interaction with divalent cations and its associated functionalities. *Comprehensive reviews in food science and food safety*, 17: 1576-1594.

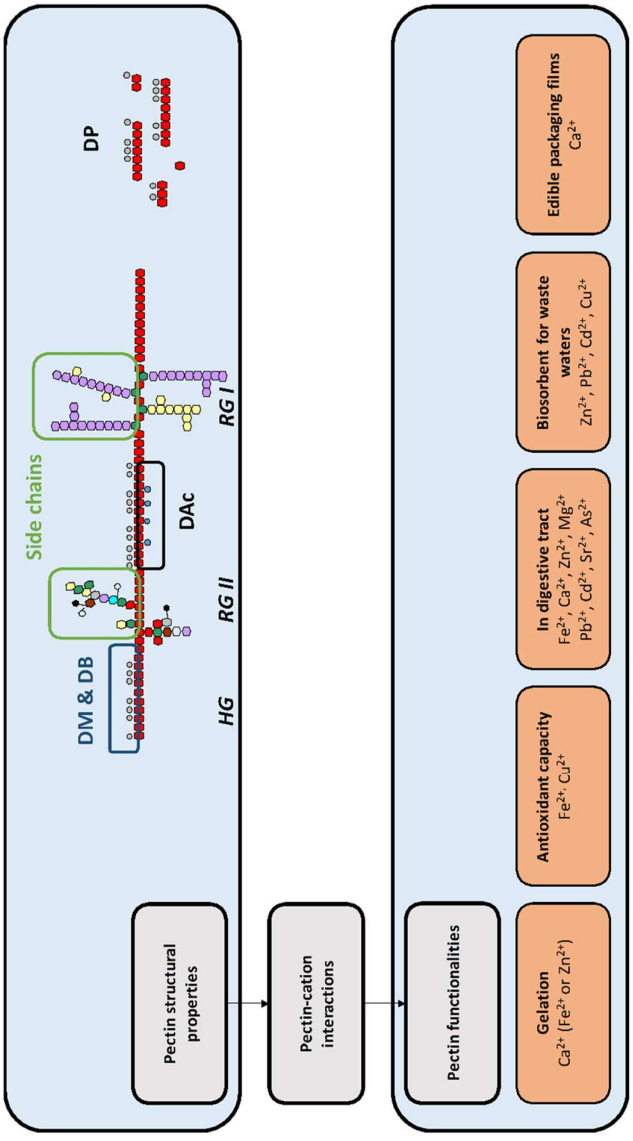

Figure 1.1: Schematic overview of the topics covered in this literature review; which pectin structural properties influence the cation-binding capacity and associated functionalities (main cation types involved in the functionalities are indicated). The pectin molecular structure is schematically presented, with HG: homogalacturonan, RG I and II: rhamnogalacturonan I and II. Red hexagons present the galacturonic acid units, grey dots represent the methylesters and blue dots the acetylesters. Other colored hexagons represent different neutral sugars. DM = degree of methylesterification, DB = degree of blockiness, DAc = degree of acetylation, and DP = degree of

For instance, pectin *in situ* can self-associate in the cell wall via cation-mediated electrostatic interactions, thereby partially regulating the rigidity of plant cell walls (Fang et al., 2009), whereas extracted pectin is used as a functional additive such as gelling agent based on Ca^{2+} cross-linking (Renard & Jarvis, 1999; Thakur et al., 1997).

Pectin exhibits a wide range of molecular structures, with distinct functional groups possibly influencing the cation binding. This pectin structural diversity can occur between different pectin sources, but also within one pectin source (Fraeye, Duvetter, Doungla, Van Loey, & Hendrickx, 2010b). Moreover, the structural properties of (extracted) pectin can be modified through enzymatic or chemical conversions to direct its functionality. To date, several studies exploring the cation-binding capacity of pectin have been conducted, using pectin from several sources as well as distinct structurally modified pectins. This literature review therefore aims to give an overview of the research progress on the interaction (mechanisms) between pectin and distinct divalent cations, and associated functional properties. Particularly, the role of the molecular structure of extracted pectin in its cation-binding capacity will be discussed. In this context, citrus, apple, or sugar beet pectins will be mainly considered as they are most likely to be used in *ex situ* applications. Although pectin has been reported to bind monovalent and multivalent ions, this review will focus on the interaction of pectin with selected divalent cations that are mainly present in food matrices or that are of common application and contribute to divalent cation-associated pectin functionalities. The pectin structural and functional properties described in this review are presented in a schematic overview in **Figure 1.1**.

1.2 INFLUENCE OF PECTIN MOLECULAR STRUCTURE ON THE DIVALENT CATION-BINDING CAPACITY OF PECTIN

1.2.1 General description of pectin molecular structure in view of divalent cation binding

This section will only briefly discuss the pectin structural composition, as it has already been reviewed thoroughly by several authors (Caffall & Mohnen, 2009; Ridley, O'Neill, & Mohnen, 2001; Vincken et al., 2003a; Voragen, Coenen, Verhoef, & Schols, 2009). Structurally, pectin is a complex biomacromolecule mainly present in the middle lamella and primary cell wall of fruits and vegetables (Voragen et al., 2009). It is comprised of covalently linked polysaccharides, rich in galacturonic acid (GalA), with the three main building blocks being homogalacturonan (HG), and rhamnogalacturonan I and II (RG I and II) (**Figure 1.1**) (Caffall & Mohnen, 2009). HG is the predominant and linear pectin domain with a backbone consisting of α-1,4-

linked GalA units which can be methylesterified at their C-6 position or O-acetylated at the C-2 or C-3, as can be seen in **Figure 1.2** (Ridley et al., 2001). The percentage of methylesterified or O-acetylated GalA units within the HG substructure is defined as the degree of methylesterification (DM) or degree of acetylation (DAc), respectively. Pectin DM is considered to be the most important structural parameter in relation to the cation-binding capacity of pectin (Kohn, 1975; Thibault & Ralet, 2003; Vincken et al., 2003a). Non-methylesterified GalA residues can be negatively charged at pH values above the pKa of pectin (2.9-4.1) (Ralet, Dronnet, Buchholt, & Thibault, 2001; Sriamornsak, 2003), giving pectin the ability to interact with cations. In this context, the lower the DM of pectin, the higher the number of non-methylesterified GalA residues present and, therefore, the higher the cation-binding capacity.

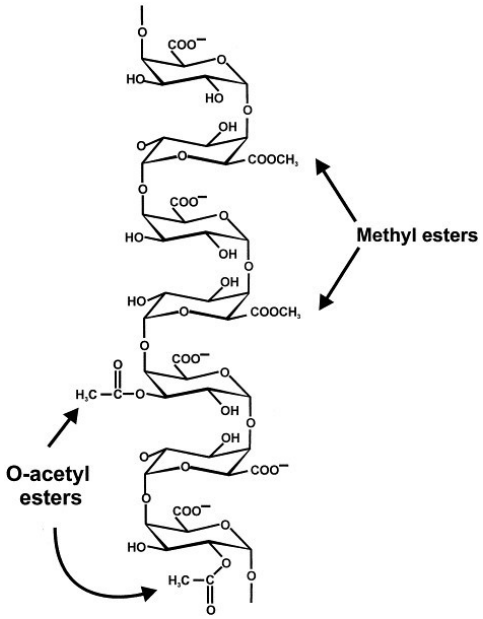

Figure 1.2: Schematic overview of the homogalacturonan substructure of pectin, with indication of methylesters at C-6 position and O-acetylesters on C-2 or C-3 position. Reprinted, with permission, from Ridley, B., L., O'Neill, M.A., and Mohnen, D. (2001). Pectins: Structure, biosynthesis, and oligogalacturonide-related signaling. *Phytochemistry*, *57,* 929-967. Copyright (2018).

In contrast to HG, RG I and II are more branched pectin domains. RG I is composed of the repeating disaccharide [→4)-α-D-GalA-(1→2)-α-L-rhamnose-(1→] with different side chains at the C-4 position of rhamnose, which are composed of neutral sugars, mainly D-galactose and/or L-arabinose (Voragen et al., 2009). RG II is

structurally the most complex heteropolysaccharide, comprised of an HG backbone of approximately nine α-1,4-linked GalA units with four structurally conserved side chains, consisting of twelve different monosaccharides (Caffall & Mohnen, 2009). It is generally accepted that the pectin backbone consists of (alternating) covalently linked HG and RG I and II, referring to 'smooth' and 'hairy' regions, respectively (Coenen, Bakx, Verhoef, Schols, & Voragen, 2007; De Vries, Rombouts, Voragen, & Pilnik, 1982). However, an alternative model in which the pectin backbone may be composed of RG I with HG as a side chain was proposed by Vincken et al. (2003b). Yapo (2011) further introduced the 'living thing-like' model, in which the pectin backbone is composed of alternating two HG and one RG I substructures, with the former containing side chains of RG II. Nevertheless, the molecular pectin organization is currently still under debate, since no conclusive evidence to confirm or reject the models has been presented (Christiaens et al., 2015b; Coenen et al., 2007).

Although the cation-binding potential of pectin and associated functional properties are reported to be influenced by its major structural domains (HG, RG I, and II), only the influence of HG, the linear subdomain has been widely explored (Fraeye et al., 2010; Hwang & Kokini, 1992; Ngouémazong et al., 2012b; Sousa, Nielsen, Armagan, Larsen, & Sørensen, 2015; Ventura, Jammal, & Bianco-Peled, 2013). The branched domains have received limited attention with minor information available on the influence of selectively modified pectin structures, in terms of side chains, on the cation-binding capacity. Since most of the commercially available pectin largely consists of HG (e.g., citrus or apple pectin, mainly due to industrial extraction processes), the main focus of this literature review will be on the linear HG substructure and its relation with the cation-binding capacity. Therefore, the following sections will provide a detailed look into the DM, the distribution pattern of non-methylesterified GalA units, and the chain length of HG, representing the structural properties mainly related to the cation-binding capacity of pectin. Other structural characteristics such as the acetylation degree, side chains in RG I and II or neutral sugars will be briefly addressed.

1.2.2 DM and distribution pattern of non-methylesterified GalA units

Of the many structural properties of pectin, the degree of methylesterification (DM) has received much attention as it is considered to be the main factor influencing its cation-binding capacity (Kohn, 1975; Thibault & Ralet, 2003; Vincken et al., 2003a). This parameter has been used to classify pectin for cation-binding related functionality, with pectin of DM above 50% and below 50% being typically classified as high (HM) and low (LM) methylesterified pectin, respectively (Thakur et al.,

1997). LM pectin exhibits a higher charge density (Ralet et al., 2001; Thibault & Rinaudo, 1985) due to its higher number of negatively chargeable carboxyl groups (non-methylesterified carboxyl groups) compared to HM pectin, which infers that the cation-binding capacity of pectin increases with decreasing DM.

The influence of pectin DM on its cation-binding has mostly been studied through equilibrium adsorption studies in which targeted demethylesterified pectin samples are dissolved in aqueous solutions in presence of cations. The number of cations bound to pectin are then estimated from the free cation concentrations, determined either by spectrophotometry (Khotimchenko, Kolenchenko, & Khotimchenko, 2008), or by potentiometry or conductimetry through establishing the activity coefficients of cations (Dronnet, Renard, Axelos, & Thibault, 1996; Garnier, Axelos, & Thibault, 1994; Ralet et al., 2001; Renard & Jarvis, 1999; Tanhatan-Nasseri, Crépeau, Thibault, & Ralet, 2011; Thibault & Rinaudo, 1985). More recently, isothermal titration calorimetry (ITC) is used to study the thermodynamics of the pectin-cation-binding interactions (Assifaoui et al., 2015; Fang et al., 2008). Irrespective of the methodology used, all studies reveal a higher amount bound and stronger interactions between cations and pectin with decreasing DM, for all types of cations studied (e.g., Zn^{2+}, Ca^{2+}, Cu^{2+}, and Pb^{2+}).

In addition to the DM, the intramolecular distribution of the non-methylesterified carboxyl groups within a pectin chain plays an important role in determining pectin's anionic nature and associated functionality (Cameron, Kim, Galant, Luzio, & Tzen, 2015; Vincken et al., 2003a). However, the influence of the distribution pattern of non-methylesterified GalA units on the cation-binding capacity of pectin is less described in literature compared to DM. The pattern of methylesterification within a pectin chain was first quantified by Daas, Meyer-Hansen, Schols, De Ruiter and Voragen (1999) as the degree of blockiness (DB) and represents the relative occurrence of blocks of non-methylesterified GalA units. Besides the DB, the absolute number of non-methylesterified GalA units present in blocks can be expressed as the absolute degree of blockiness (DB_{abs}). The DB and DB_{abs} were originally established by (exhaustive) enzymatic degradation of pectin using endo-polygalacturonase (endo-PG) of *K. fragilis*, which requires at least four consecutive non-methylesterified GalA units in order to hydrolyze the linkage between two non-methylesterified GalA units (Daas et al., 1999). The DB was then quantified as the ratio of released mono-, di-, and trigalacturonic acid units by the enzyme to the total amount of non-methylesterified GalA units (Daas et al., 1999), whereas the DB_{abs} was defined as the number of released GalA oligomers in the endo-PG digest to the total number of GalA

units in the pectin polymer, thus without correction of the DM (Guillotin et al., 2005). These two parameters are schematically presented in **Figure 1.3** (Fraeye et al., 2010b).

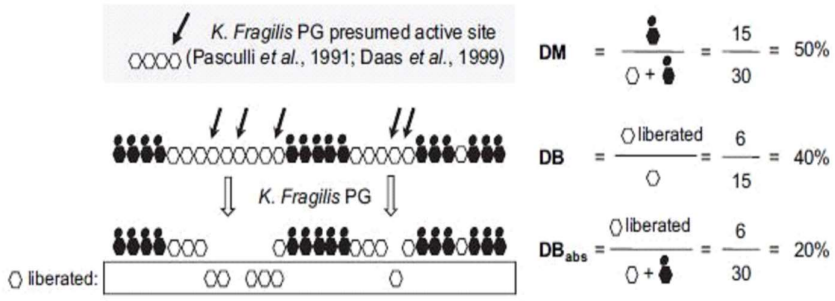

Figure 1.3: Simplified scheme of the principle of pectin digestion by *K. fragilis* polygalacturonase (PG) and calculation of degree of methylesterification (DM), degree of blockiness (DB), and absolute degree of blockiness (DB_{abs}). Methylesterified and non-methylesterified GalA residues are represented by black and white hexagons, respectively. This PG enzyme is thought to cleave linkages between GalA residues when at least four non-methylesterified GalA residues are present in a sequence. Depending on the locations of PG attack and the type of PG used, other digestion schemes are possible. Non-methylesterified mono-, di-, and triGalA liberated, which are quantified, are collected in the rectangle and denoted as white hexagons ''liberated''. Reprinted, with permission, from Fraeye, I., Duvetter, T., Doungla, E., Van Loey, A., and Hendrickx, M. (2010). Fine-tuning the properties of pectin-calcium gels by control of pectin fine structure, gel composition and environmental conditions. Trends in food science and technology, 21, 219-228. Copyright (2018).

Ralet et al. (2012) extended the concept of DB and DB_{abs}, to DB and DB_{abs} of highly methylesterified stretches (DBMe and DB_{abs}Me) based on HG digestion by pectin lyase, a pectin-degrading enzyme which exhibits increased activity with increasing pectin DM. As such, pectin samples which are highly degradable by pectin lyase, constitute of long methylesterified stretches. The combination of DB, DB_{abs}, DBMe and DB_{abs}Me are assumed to quantify the total proportion of degradable zones within a pectin sample (Ralet et al., 2012). In addition, Cameron, Luzio, Goodner, and Williams (2008) defined the pectin intramolecular distribution of methylesters using the average size of non-methylesterified domains (NMDs) per molecule ($\overline{BS}$) and number of averaged-sized NMDs per molecule ($\overline{BN}$). These parameters were calculated from the molar concentrations of non-methylesterified GalA units and pectin after a limited endo-PG treatment. The $\overline{BS}$ is then determined as the average number of demethylesterified blocks released from a molecule multiplied by the block length and divided by the average sum of blocks per molecule, while $\overline{BN}$ is defined as the ratio of the average sum of blocks per molecule to the average demethylesterified block size released (Kim, Williams, Luzio, & Cameron, 2017). According to Kim et

al. (2017), decreasing pectin DM was associated with increasing DB, DB_{abs} or $\overline{BS}$, but resulted in a decreased estimated $\overline{BN}$. Nevertheless, since the DB and DB_{abs} are the most commonly reported parameters to express the distribution pattern of methylesters, these will be mainly used in the next sections.

As reported by Fraeye et al. (2009) and Sila et al. (2009), targeted pectin modification through chemical or enzymatic conversion reactions can be applied to generate differences in pectin DM and DB (or DB_{abs}), thereby influencing the number and distribution pattern of negatively chargeable carboxyl groups, hence cation-binding capacity. While chemical demethylesterification involves an alkaline treatment (titration with a sodium hydroxide solution), which results in a random removal of methylesters (Limberg et al., 2000), enzymatic demethylesterification is accomplished by the action of pectin methylesterase (PME), which catalyzes the hydrolysis of the methylester bond at C-6 of GalA units (Jolie, Duvetter, Van Loey, & Hendrickx, 2010). Two types of PME can be distinguished, namely PMEs with an alkaline (mostly plant PME) or acidic (microbial PME) pI. On the one hand, plant PMEs hydrolyze methylesters in a blockwise manner, via a single-chain or multiple-attack mechanism. The former includes hydrolysis of the methylesters up to the end of the pectin chain or until a blocking residue is reached prior to dissociation of the enzyme-substrate complex, while hydrolysis via the multiple-attack mechanism is comprised of a limited average number of subsequent methylesters per enzyme attack. Demethylesterification by microbial PMEs, on the other hand, occurs via a multiple-chain mechanism, which includes hydrolysis of only one methylester before dissociating, resulting in more randomly distributed demethylesterified GalA units (Cameron et al., 2008; Jolie et al., 2010; Limberg et al., 2000; Willats et al., 2001). As such, the two demethylesterification methods result in different distributions of (non-)methylesterified GalA units, with higher DB and DB_{abs} or DBMe and DB_{abs}Me values for enzymatically demethylesterified pectins (particularly when using plant PMEs) compared to alkaline demethylesterified pectins of comparable DM (Ngouémazong et al., 2011; Ralet et al., 2012). Therefore, enzymatically demethylesterified pectins consist of few long methylesterified stretches, alternated with few long stretches of non-methylesterified GalA units and thus exhibit a higher number or longer blocks of successive negatively chargeable carboxyl groups, which make them more sensitive to cations, resulting in a higher cation-binding capacity (Ralet, Crépeau, Buchholt, & Thibault, 2003). Despite the limited number of studies described in literature, Ralet et al. (2003, 2001), Tanhattan-Nasseri et al. (2011) and Tibault and Rinaudo (1985) reported indeed lower calcium activity coefficients for

enzymatically demethylesterified pectins (citrus, sugar beet, or apple pectin) compared to alkaline demethylesterified pectins for a comparable DM, implying a stronger binding of Ca^{2+} to enzymatically demethylesterified pectins. In other words, pectins with a comparable DM but higher DB or DB_{abs} exhibit stronger interactions with cations, which can be explained by the formation of dimers between two pectin chains as described for pectin-cation interactions (Section 1.3) (Braccini & Pérez, 2001; Fang et al., 2008). For this type of ionic interaction, a higher number or longer blocks of consecutive non-methylesterified GalA units, and thus a higher DB or DB_{abs}, results in stronger interactions between the pectin chains and divalent cations (Luzio & Cameron, 2008; Voragen et al., 2009).

1.2.3 Chain length

The pectin polymer chain length can be quantified as the degree of polymerization (DP), which is defined as the ratio of the number average molar mass (M_n) to the molar mass of one GalA unit within a pectin chain (194.14 kDa – 18 kDa of H_2O = 176.14 Da). Despite the fact that DM is considered to be an important property in the cation-binding capacity of pectin, this structural parameter is not taken into account with the calculation of DP, resulting in a possible overestimation of DP (particularly for high DM pectins). Nevertheless, the effect of DM is considered to be relatively low as methyl groups only account for a small molar mass compared to GalA. Although the DP is suggested to play an important role in determining the cation-binding capacity of pectin (Kohn, 1975), it continues to receive only limited attention. This is possibly due to the laborious and time-consuming preparation of selectively designed pectins with different molar mass (Kohn, 1975). The few studies available in literature generally observed an increased cation binding of pectin with increasing DP for pectins of a given DM, which can be attributed to the presence of a higher number of binding sites (Kohn & Luknár, 1977; Kohn, 1987; Kyomugasho et al., 2018). This is particularly true for oligomeric pectin fragments, as cation binding to such pectin fragments is considered to be purely electrostatic (Kohn, 1987). For instance, Kohn (1987) observed that as the DP of pectin increased until DP 7 (M_n ~ 1.2 kDa), there were decreased activity coefficients for several divalent cations (e.g., Ca^{2+}, Zn^{2+}, Cu^{2+}), suggesting stronger cation binding with increasing DP. These low molar mass pectin samples bind cations such as Ca^{2+} probably without formation of cooperative junction zones (i.e., the binding of a cation to the carboxyl groups of two opposite pectin chains, stabilized by van der Waals interactions and hydrogen bonds, see Section 1.3) (Kyomugasho et al., 2018). A further increase in DP from 10 to 30 (M_n ~ 1.8 and 5.3 kDa, respectively) was accompanied by a clear drop in Ca^{2+} activity

according to Kohn and Luknár (1977), implying stronger Ca^{2+}-binding in this range of DPs. They attributed this sudden decrease of Ca^{2+} activity coefficient to an intermolecular Ca^{2+}-binding in aggregates of the macromolecules.

Although it is generally accepted that a certain minimum DP is necessary to induce binding via the egg-box model (binding between two pectin chains, see Section 1.3), there is no consensus on the exact chain length. While Liners et al. (1992) observed (indirectly) pectin dimerization induced by Ca^{2+} cross-linking from a DP of 9, Powell (1982) found a critical chain length of 14 residues (measured by circular dichroism). An overview of the studies estimating the minimum chain length involved in egg-box formation is given by Fraeye et al. (2010b), suggesting a range of minimum DPs between 6 and 14. For pectins with DPs of 30 to 64 (M_n ~ 5.3 to 11.3 kDa), Kohn and Luknár (1977) did not observe significantly stronger interactions between Ca^{2+} and pectin. However, more recently, Kyomugasho et al. (2018) performed equilibrium adsorption experiments and found that the Ca^{2+}-binding capacities and interaction energies of citrus pectin of a given DM (32%) increased with increasing weight average molar mass (6.2 to 52 kDa).

In contrast to the hypothesis of the previously cited studies that an increased chain length of pectin is associated with increased cation binding, Khotimchenko, Makarova, Khozhaenko and Kovalev (2017) concluded that low molar mass pectins (5-12 kDa) can bind to a higher extent with metal ions than high molar mass pectin (20-48 kDa). The authors explain this by the potential of low molar mass pectins to change their orientation and form a higher number of bonds with cations. Nevertheless, no other study has confirmed this result so far. Given the high discrepancies between the few studies mentioned, more research is needed in order to provide better insight into the effect of the chain length of pectin on its cation-binding capacity.

1.2.4 Other structural characteristics

This section describes the other structural properties of pectin reported to influence its cation binding, namely the degree of acetylation and the presence of neutral sugar side chains. The role of these structural properties is only briefly discussed, given that the current literature review is focused on pectins commercially used in pectin-cation-associated functionalities. These pectins include particularly citrus and apple pectin, in which the degree of acetylation and neutral sugar side chains play a limited role as these pectins naturally exhibit a low degree of acetylation [e.g., approximately 2.5% in citrus pectin (Kyomugasho et al., 2017)] and the method of commercial extraction

of these pectins (acid extraction) degrades the side chains, generating more linear pectin (Massiot, Rouau, & Thibault, 1988).

The degree of acetylation (DAc) is defined as the ratio of the number of acetyl groups to the GalA units within the pectin chain. It is reported that both GalA units in HG and RG I can be acetylated, with the extent of acetylation of each substructure varying depending on the pectin source (Broxterman, Picouet, & Schols, 2017). For instance in sugar beet, 80-90% of the acetyl groups are located in the HG subdomain, while in carrot most of the acetyl groups are present in the RG I region (Broxterman et al., 2017; Ralet et al., 2003). The presence of acetyl groups on C-2 or C-3 of GalA residues in the HG substructure (**Figure 1.2**) can negatively influence the pectin cation-binding capacity by hindering the dimerization of pectin chains (Kohn & Furda, 1968; Ralet et al., 2003; Renard & Jarvis, 1999). This steric hindrance of the acetyl groups is according to Kohn & Furda (1968) larger when there is a shorter distance between free carboxyl groups, i.e. in pectins with lower DM. The few studies available on the effect of the DAc on the cation binding of pectin (Ca^{2+}, Zn^{2+}, or Pb^{2+}) reported a decreased cation binding with increasing pectin DAc (Kohn & Furda, 1968; Ralet et al., 2003; Renard & Jarvis, 1999). For instance, sugar beet pectin, which is known to be highly acetylated (35% average) (Pérez, Mazeau, & Hervé du Penhoat, 2000), exhibits poor chelating capacity and lower cation affinity compared to citrus pectin with a comparable charge density (Dronnet et al., 1996; Ralet et al., 2003). Moreover, Ralet et al. (2003) observed no significant differences in Ca^{2+}-binding properties between sugar beet pectins with different patterns of non-methylesterified GalA residues, due to the high number of acetyl groups hindering the dimerization. Renard and Jarvis (1999) suggested several possibilities for the reduced cation-binding capacity of high acetylated pectins, including (i) blocking of the hydroxyl groups active in chelation mechanisms, (ii) physically impeding access of the ions, or (iii) preventing H-bonds between adjacent galacturonic acid residues, thus changing the chain conformation. Besides, acetyl groups can preclude the action of PME, resulting in only small blocks of demethylesterified GalA units (Oosterveld, Beldman, Searle-Van Leeuwen, & Voragen, 2000), which in turn limit the cation-binding capacity of pectin.

To the best of our knowledge, data on the influence of the neutral sugars on the cation-binding capacity of pectin are very scarce. Moreover, no consensus can be reached. For instance, Ralet et al. (2003) concluded that the inter-chain association between pectins is not hindered by arabinose and galactose side chains, whereas Khotimchenko, Khozhaenko, Kovalev, and Khotimchenko (2012) attributed the

higher Ce^{3+}-binding capacities for pectins isolated from seagrasses compared to commercial citrus pectin to the presence of side chains in their HG subdomain. However, it should be noted that in the former, the DM of the pectins was generally lower (7.9-10.2%) compared to the DM of citrus pectin (60%), which increases the cation binding. Moreover, no clear interaction mode has been reported between pectin and trivalent cations such as Ce^{3+}, whereas the binding between pectin and divalent cations is known to occur according to the egg-box model for most of the cations (Section 1.3). In order to clearly define the role of neutral sugars in the cation-binding capacity of pectin, there is a need to generate selectively modified pectin structures in which neutral sugar side chains are systematically altered without compromising other structural properties such as DM or chain length.

1.3 BINDING MECHANISMS BETWEEN PECTIN AND DIVALENT CATIONS

The binding mechanisms between the GalA units of pectin and distinct divalent cations are reported to be cation type-dependent as they are associated with the affinities of the cations for water (Huynh, Lerbret, Neiers, Chambin, & Assifaoui, 2016). In general, the higher the affinity for water, the more difficult the interaction between pectin and the cation (Huynh, Chambin, Maire du Poset, & Assifaoui, 2018). Huynh et al. (2016) studied the binding mechanism(s) of Mg^{2+}, Ca^{2+}, Ba^{2+}, or Zn^{2+} to polygalacturonate and they reported that Mg^{2+} exhibits the highest affinity for water, followed by Zn^{2+}, Ca^{2+}, and finally Ba^{2+}. Mg^{2+} and Zn^{2+} exhibit tighter interactions with water, resulting in a monodentate coordination with GalA, whereas interaction between GalA and Ba^{2+} or Ca^{2+} was through bidentate coordination, as measured by means of molecular dynamics simulations (Assifaoui et al., 2015; Huynh et al., 2016). Monodentate binding defines the interaction between a cation and one oxygen atom of the carboxylate group of GalA, while bidentate coordination includes binding to two oxygen atoms, which implies a release of one or two water molecules from the hydration shell of the cations, respectively (Huynh et al., 2016). Mg^{2+} binds to pectin via polycondensation, due to its very high affinity for water, whereas the other cations were found to bind via the generally accepted two-step mechanism (**Figure 1.4**). This two-step binding mechanism is transposed from the alginate-cation interaction, in particular from its interaction with Ca^{2+}, given that the polygalacturonate chain is very similar to the polyguluronate chain of alginate (Fang et al., 2008; Ventura et al., 2013). In the first step, at low cation concentrations, monocomplexation and point-like cross-links occur, which implies the binding of a divalent cation with one GalA unit and the formation of a GalA-cation-GalA bridge between two pectin chains, respectively

(Siew & Williams, 2005; Ventura et al., 2013). The formation of such monocomplexation and point-like cross-links is illustrated in **Figure 1.4** and applies to both LM and HM pectin. This first step in binding is associated with an endothermic binding as determined by isothermal titration calorimetry (Assifaoui et al., 2015). Subsequently, dimerization of LM pectin chains occurs (in step two of cation binding) when the cation concentration increases above a threshold molar ratio (R^*), resulting in an ordered structure (Assifaoui et al., 2015; Fang et al., 2008; Huynh et al., 2016) (**Figure 1.4**). This interaction is an exothermic process (Assifaoui et al., 2015). HM pectin is reported to only interact with cations via a single-step process, without dimerization (Fang et al., 2008).

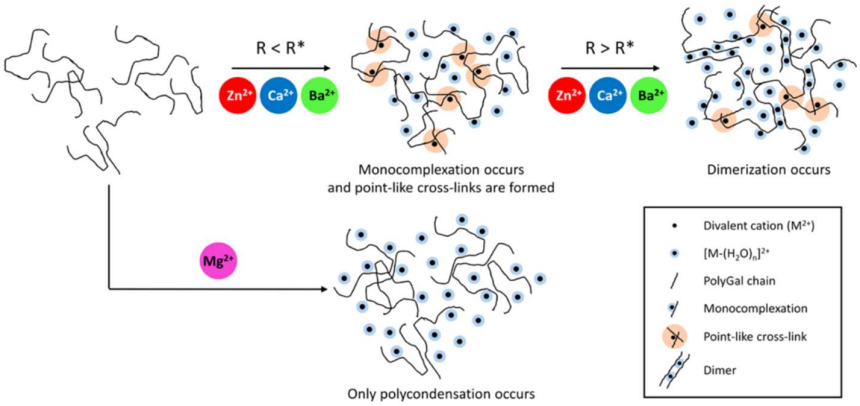

Figure 1.4: Schematic representation of the association steps between polygalacturonate (PGA) and divalent cations (Zn^{2+}, Ca^{2+}, Ba^{2+}, and Mg^{2+}). R is the molar ratio ($[Me^{2+}]/[GalA]$) and R^* is the threshold molar ratio at which transition from monocomplexation and point-like cross-links to dimerization occurs. Reprinted, with permission, from Huynh, U. T. D., Lerbret, A., Neiers, F., Chambin, O., and Assifaoui, A. (2016). Binding of divalent cations to polygalacturonate: A mechanism driven by the hydration water. *Journal of Physical Chemistry B*, 120, 1021–1032. Copyright (2018).

According to the reported two-step binding mechanism, Ngouémazong et al. (2012c) suggested pectin chain entanglements at low Ca^{2+} concentration, rather than cross-linking. At higher Ca^{2+} concentration, the entangled network is converted into a cross-linked network, due to the formation of dimers. The dimerization between pectin chains is assumed to follow the egg-box model, which was originally described for Ca^{2+}-binding to alginate by Grant et al. (1973) and slightly adjusted by Braccini and Pérez (2001) to the so-called 'shifted egg-box' model. The latter model describes a strong inter-chain association via cation bonding, with a shift of 1.7 Å orientation of one pectin chain to another chain. As such, cooperative junction zones are formed

wherein the cations are entrapped. In addition to electrostatic interactions, van der Waals interactions and hydrogen bonds stabilize the junction zones (Braccini & Pérez, 2001). To date, the egg-box model of binding has mainly been described for pectin-Ca^{2+} binding, but it can be assumed to be applicable for interactions between pectin and other divalent cations. Moreover, Assifaoui et al. (2015) reported that the egg-box model is more appropriate in Zn^{2+}-binding than Ca^{2+} as they found that Zn^{2+} interacts with both carboxyl and hydroxyl groups, comparable to the egg-box model, whereas Ca^{2+} is reported to only bind via carboxyl groups.

Table 1.1 shows the threshold molar ratios at which cation-mediated dimerization between pectin chains occurs, as observed by several authors. The molar ratio between cation and pectin has been defined differently in literature, either as $R = 2[Me^{2+}]/[COO^-]$ (Fraeye et al., 2010b), or as $[Me^{2+}]/[COO^-]$ (Assifaoui et al., 2015; Fang et al., 2008). Huynh et al. (2016) reported a molar ratio of $[Me^{2+}]/[GalA]$, which equals the molar ratio of $[Me^{2+}]/[COO^-]$, since they studied the interaction between polygalacturonate (DM ~ 0%) and divalent cations. Theoretically, the threshold molar ratio, expressed as $[Me^{2+}]/[COO^-]$ for formation of the egg-box model equals 0.25 (Fraeye et al., 2010b; Maire du Poset, Lerbret, Zitolo, Cousin, & Assifaoui, 2018). However, Huynh et al. (2016) suggested that the threshold molar ratio depends on the cation type and associated stability of the point-like cross-links formed with pectin, which in turn is related to their water affinity. For instance, Ba^{2+} shows the lowest affinity for water, resulting in less stable point-like cross-links, which implies a higher threshold molar ratio required for the formation of dimers (Huynh et al., 2016). Assifaoui et al. (2015) and Fang et al. (2008) reported the occurrence of dimerization at a higher molar ratio of Ca^{2+}, namely 0.25, compared to Huynh et al. (2016) who suggested a molar ratio of 0.05. However, in general, the values reported for Ca^{2+} are still lower than for Ba^{2+}, indicating a higher stability of the point-like cross-links for Ca^{2+}. According to Huynh et al. (2016), the point-like cross-links formed in the presence of Zn^{2+} exhibited the highest stability (compared to Ca^{2+} and Ba^{2+}), which can be attributed to its potential to partially covalently bind with other electronegative groups.

Table 1.1: Comparison of the threshold molar ratio (R^*) reported by different authors, indicating the molar ratio R at which a transition from monocomplexes or point-like cross-links to dimerization of pectin chains occurs. Me^{2+} = divalent cation, GalA = galacturonic acid, and nd. = not determined.

Reference	Definition R	Ca^{2+}	Zn^{2+}	Ba^{2+}
Huynh et al. (2016)	R= $[Me^{2+}]/[GalA]$	0.05	0.3	0.35
Assifaoui et al. (2015)	R= $[Me^{2+}]/[COO^-]$	0.25	0.35	nd.
Fang et al. (2008)	R= $[Me^{2+}]/[COO^-]$	0.25	nd.	nd.

For the formation of dimers, cations need to be entrapped in cavities formed by two pectin chains. As such, cations with very large or small hydrated ionic radii can be hypothesized to not fit into the cavities, leading to lower affinities or amounts bound by pectin (Kyomugasho et al., 2017). Besides its high affinity for water, this might explain the lower amount of Mg^{2+} bound to pectin as a higher effective hydrated diameter of Mg^{2+} (0.8 nm) is reported compared to the other cations (~ 0.6 nm) (Kyomugasho et al., 2017). Nevertheless, Tansel (2012) reported lower values of hydrated radii for these cations, with a similar hydrated radius for Mg^{2+} (0.3-0.47 nm) compared to Zn^{2+} (0.40-0.43 nm), Ca^{2+} (0.41-0.42 nm), or Fe^{2+} (0.43 nm). As contrasting information about the hydrated radii of cations can be found, it is not straightforward to associate cation radii to the binding mechanism or capacity to pectin. More profound studies in which the cation radius can be clearly linked with the interaction mode and binding capacity are recommended to improve the interpretation of the findings available in the literature.

In the case of cation binding to alginate, the dimerization in the second step is typically followed by a weaker inter-dimer aggregation during Ca^{2+}-induced gelation (Braccini & Pérez, 2001; Fang et al., 2008). Although this inter-dimerization is also assumed for pectin (Braccini & Pérez, 2001; Ngouémazong et al., 2012a), it was not observed by Fang et al. (2008), who attributed this to the presence of methylesters or amide groups along the pectin chain, hindering the lateral association of pectin dimers. Moreover, the two-step binding mechanism described above is only seen for Ca^{2+}, Zn^{2+}, or Ba^{2+}. Information on the binding mechanism between pectin and Fe^{2+} is missing, despite iron being an essential mineral present in many food products and the suggested pectin-Fe^{2+}-mediated functionalities (see Section 1.6 and Chapter 6).

1.4 INFLUENCE OF CATION TYPE ON THE BINDING CAPACITY OF PECTIN

As already hinted at in the previous section, the nature of the cation type is an important parameter in determining the interaction with pectin. This section will therefore compare the binding capacities and affinities of pectin for distinct cation types. It is generally observed that pectin shows the highest affinity for Cu^{2+} and Pb^{2+} (Braudo et al., 1996; Dronnet et al., 1996; Haug & Smidsrød, 1970; Kartel, Kupchik, & Veisov, 1999; Kohn, 1975, 1987; Nair, Asp, Nyman, & Persson, 1987). This might be explained by their higher average electronegative values (Allred, 1961) compared to the other alkali-earth or transition metal ions commonly explored. Interactions between pectin and Cu^{2+} or Pb^{2+} are mainly of interest in the context of excretion of these toxic metals from the human body (Section 1.6.3.2) or their removal from waste waters (Section 1.6.4). With regard to the common food-related cations, pectin shows in general the highest affinity for Zn^{2+} followed by Ca^{2+} and Mg^{2+} (Assifaoui et al., 2015; Dronnet et al., 1996; Haug & Smidsrød, 1970; Huynh et al., 2016; Renard & Jarvis, 1999; Schlemmer, 1989), although Surabhi, Williams and Elzagheid (2017) suggest higher affinities for Ca^{2+} than Zn^{2+}. In the case of Fe^{2+}, which is an important cation in terms of lipid oxidation or biological functions, only scarce information is available on its interaction with pectin. It was suggested that a higher amount of Fe^{2+} can bind to pectin compared to Ca^{2+} or Zn^{2+}, based on the results of a bioaccessibility study by Kyomugasho et al. (2017) or from a dialysis experiment performed by Surabhi et al. (2017). Although Fe^{2+} exhibits a hydrated radius (0.43 nm) similar to Ca^{2+} (0.41-0.42 nm) and Zn^{2+} (0.40-0.43 nm) (Tansel, 2012), a higher electronegativity has been reported for Fe^{2+} (Allred, 1961), which probably explains the higher affinity of pectin for Fe^{2+}. On the contrary, Dronnet et al. (1996) remark that the selectivity scale of pectins for various cations cannot be easily related to any property of these ions including the hydrated radius. They conclude that identification of the conformation of the pectin salts can contribute to a better understanding of the binding modes and differences in affinity. The order of affinity can be of importance when there is competition between the cations for pectin. For instance during digestion of pectin-cation systems, the cation exhibiting the strongest binding with pectin will theoretically have a lower number of free (bioaccessible) cations.

Due to the diversity in experimental designs by different authors, it is not straightforward to compare binding capacities of pectins for distinct cations. The interaction between pectin and cations can be characterized by several binding parameters, which are commonly estimated by (spectrophotometric) determination of

the equilibrium adsorption isotherm. Such an adsorption isotherm describes the retention of a ligand on an adsorbent at a constant temperature as a function of the remaining ligand concentration (Foo & Hameed, 2010; Limousin et al., 2007). Adsorption isotherms can be quantitatively described by several empirical models that are typically defined by certain physicochemical parameters, indicating the binding mechanism, surface properties, and the binding affinity of the adsorbent (Foo & Hameed, 2010; Ho, Huang, & Huang, 2002). Several adsorption isotherm models have been developed (Foo & Hameed, 2010), with the Langmuir and Freundlich isotherm models being most widely used (Limousin et al., 2007). For instance, the interaction between pectin and Zn^{2+} or Ca^{2+} has successfully been described by the Langmuir isotherm (Khotimchenko et al., 2008; Kyomugasho et al., 2018), which assumes a monolayer adsorption of the cations at a finite number of identical binding sites (galacturonic acid units) (Foo & Hameed, 2010). To the best of our knowledge, only these two abovementioned authors have determined the maximum cation-binding capacity for Zn^{2+} or Ca^{2+} and associated interaction energy of citrus pectin samples with distinct DMs through equilibrium adsorption experiments and then modeled the results obtained based on the Langmuir adsorption model (**Table 1.2**). The maximum Zn^{2+}-binding capacities reported by Khotimchenko et al. (2008) are however expressed in other units (mg cation/g pectin) than the results of Kyomugasho et al. (2018) (mol cation/mol GalA). Given the anhydrogalacturonic acid content (%) of the pectin samples, the molar mass of galacturonic acid in a pectin chain (176.14 g/mol) and the molar mass of Zn^{2+} (65.38 g/mol), the maximum binding capacities (obtained by Khotimchenko et al. 2008) can be converted to mol Zn^{2+}/mol GalA to allow comparison, as can be seen in **Table 1.2**. In this context, the maximum Ca^{2+}-binding capacity (~ 0.4 mol Ca^{2+}/mol GalA) for enzymatically demethylesterified citrus pectin with a DM around 33% is in between the maximum Zn^{2+}-binding capacities for alkaline demethylesterified pectin with a DM of 40% (approximately 0.30 mol Zn^{2+}/mol GalA) and 20% (approximately 0.43 mol Zn^{2+}/mol GalA), as observed by Khotimchenko et al. (2008). Despite the comparable maximum binding capacities, clearly lower values of pectin-Zn^{2+} interaction energy (expressed as L/mmol) were reported compared to pectin-Ca^{2+} interactions by Kyomugasho et al. (2018). This higher interaction energy between pectin and Ca^{2+} hypothesizes a higher affinity for Ca^{2+} compared to Zn^{2+}, which is in contrast with the order of affinity as mentioned before. However, since only a limited number of studies have explored the maximum binding capacity and associated interaction energy between pectin and cations such as Zn^{2+} or Ca^{2+}, no conclusive comparisons between the cation-pectin interactions can be made.

Moreover, different methodologies are used to demethylesterify the citrus pectin sample, which can influence the binding capacity as mentioned before (Section 1.2.2).

Table 1.2: Overview of maximum binding capacities for Zn^{2+} and Ca^{2+} and associated interaction energies ± standard deviation (if reported) as estimated by equilibrium adsorption isotherms or by isothermal titration calorimetry for demethylesterified citrus pectin samples with distinct degrees of methylesterification (DM, %) as reported by different authors. (E) indicates enzymatically demethylesterified citrus pectin, (C) refers to alkaline demethylesterified pectin samples, while (U) refers to an unknown method of demethylesterification. The values between brackets are the original data reported by Khotimchenko et al. (2008), expressed as mg/g pectin for the maximum binding capacity or mL/mg for the interaction energy. For the conversion of the binding capacity from mg/g pectin to mol/mol GalA or the interaction energy from mL/mg to L/mmol, a galacturonic acid (GalA) content of 0.794, 0.704 and 0.666 g GalA/g pectin for pectin with DM of 60.2, 40.1 and 18.8%, respectively, a M_w of GalA within a pectin chain of 176.14 g/mol and a M_w of Zn^{2+} of 65.38 g/mol are used. nd = not determined.

Reference	DM (%) of citrus pectin	Zn^{2+} maximum binding capacity (mol/mol GalA)	Interaction energy for Zn^{2+} (L/mmol)	Ca^{2+} maximum binding capacity (mol/mol GalA)	Interaction energy for Ca^{2+} (L/mmol)
Khotimchenko et al. (2008) ***Equilibrium adsorption isotherm***	60.2 (C)	0.26 (75.7)	$8.5x10^{-4}$ (0.0013)	nd.	nd.
	40.1 (C)	0.30 (79.4)	$57.5x10^{-4}$ (0.088)	nd.	nd.
	18.8 (C)	0.43 (105.2)	$68.6x10^{-4}$ (0.105)	nd.	nd.
Kyomugasho et al. (2018) ***Equilibrium adsorption isotherm***	32 ± 3 (E)	nd.	nd.	0.40 ± 0.02	372.1 ± 97.5
Assifaoui et al. (2010) ***Isothermal titration calorimetry***	30 (U)	0.07 ± 0.04	21.5 ± 7.6	0.19 ± 0.03	20.5 ± 0.3

Besides the use of equilibrium adsorption experiments and fitting of the generated adsorption isotherms with adsorption models, isothermal titration calorimetry (ITC) is a recently used tool to study the cation-binding capacity of pectin and factors influencing this ability (Assifaoui et al., 2015; Fang et al., 2008). With regard to the binding capacities, some discrepancies were found between values determined by equilibrium adsorption experiments and ITC (**Table 1.2**). Khotimchenko et al. (2008) and Kyomugasho et al. (2018) observed higher Zn^{2+}- or Ca^{2+}-binding capacities,

measured by equilibrium adsorption experiments, compared to values determined by Assifaoui et al. (2015) using ITC. In addition, ITC measurements revealed higher binding constants between pectin and Zn^{2+} compared to the interaction energies obtained by equilibrium adsorption experiments, while a lower binding constant was observed for Ca^{2+} by ITC compared to the equilibrium adsorption experiment (Assifaoui et al., 2015). The differences observed between these studies can possibly be explained by the difference in parameters measured. However, since only a limited number of studies are available, more studies are required to profoundly compare results of ITC measurement and equilibrium adsorption experiments.

1.5 INFLUENCE OF EXTRINSIC FACTORS ON THE CATION-BINDING CAPACITY OF PECTIN

The divalent cation-binding capacity of pectin can be influenced by several intrinsic as well as extrinsic factors. Intrinsic factors include pectin characteristics, varying from DM, DB, chain length, acetylation etc., which are described in Section 1.2. In addition to cation concentration and cation type discussed in Sections 1.3 and 1.4, other well-described extrinsic factors which are of particular interest in relation to pectin-cation interactions, including the pH of pectin solutions, the ionic strength, as well as pectin concentration, will be reviewed in this section.

The pH of a pectin solution is of great importance in determining the cation-binding capacity of pectin. A pH of at least one log unit above the pKa of pectin (2.9-4.1) is required to ensure more than 50% dissociated carboxyl groups and, therefore, a sufficient pectin charge density for the formation of ionic cross-links. A pH below this value would lead to protonation of non-methylesterified GalA units, resulting in a reduced binding capacity. According to Khotimchenko et al. (2008), at pH values lower than 2, pectin usually precipitates, thereby further reducing the binding capacity. A pH of 5 is found to be optimal for Ca^{2+}-binding by LM pectin (Schlemmer, 1989; Surabhi et al., 2017) as well as for Zn^{2+}-binding (Khotimchenko et al., 2008; Nair et al., 1987; Schlemmer, 1989). A further increase of pH does not alter the binding capacity for Ca^{2+} or Zn^{2+}, as reported by Nair et al. (1987) and Schlemmer (1989), while a decrease in Ca^{2+}- or Zn^{2+}-binding capacity has been observed by Surabhi et al. (2017) and Khotimchenko et al. (2008). At pH values higher than 8, polysaccharides such as pectin become unstable [e.g., due to depolymerization (Van Buggenhout, Sila, Duvetter, Van Loey, & Hendrickx, 2009)], explaining the decreased binding capacity (Khotimchenko et al., 2008). In addition, at very high pH values (~ 12) hydrocomplexes of the cation can be formed, such as $Zn(OH)_4^{2-}$. These

hydrocomplexes are characterized by a larger hydrated radius and are more difficult to dissociate, which results in limited interactions with pectin (Khotimchenko et al., 2008).

The ionic strength of pectin solutions is reported to influence their divalent cation binding. Most of the reported divalent cation-binding capacities are determined in pectin systems dissolved in pure water (ion-free solutions) and then enriched with divalent cations of interest. As such, the influence of the presence of monovalent ions on the amount of divalent cations bound to pectin is usually excluded, as suggested by Lips, Clark, Cutler and Durand (1991). Addition of monovalent ions, i.e., an increased ionic strength, to a pectin solution enriched with divalent cations is associated with a decreased pectin affinity for the divalent cations, as the charges on the pectin polymer are screened (Dronnet et al., 1996; Garnier et al., 1994; Tibbits, MacDougall, & Ring, 1998). Garnier et al. (1994), Dronnet et al. (1996) and Renard and Jarvis (1999) observed indeed less binding between pectin and Zn^{2+} or Ca^{2+} upon addition of 0.1 M Na^{+} (NaCl or $NaNO_3$). Moreover, the decrease in binding affinity is larger with increasing monovalent cation concentration (Lips et al., 1991) and with increasing pectin DM (Renard & Jarvis, 1999). The presence of monovalent cations in pectin solutions could also influence the binding mode between pectin and divalent cations. For instance, in the absence of monovalent cations, the interaction between pectin and Ca^{2+} is reported to be anti-cooperative and cooperative in the presence of monovalent cations (Dronnet et al., 1996; Garnier et al., 1994), which implies a decrease and increase, respectively, in affinity of the divalent cation for pectin as the binding reaction proceeds (Dronnet et al., 1996). The anti-cooperativity in the divalent cation-enriched pectin solutions (in absence of monovalent cations) can be attributed to the typical behavior of polyelectrolytes in water, given that the electrostatic potential decreases upon divalent cation binding, resulting in less evident binding. The cooperative effect observed at high ionic strength is, according to Garnier et al. (1994), due to the screening of the polyelectrolyte effects. The difference in binding mode is, moreover, dependent on the divalent cation type (Pb^{2+}, Ca^{2+}, or Zn^{2+}) and pectin structure (DM, DAc) (Dronnet et al., 1996; Renard & Jarvis, 1999). Cooperative binding between low DM pectin and Pb^{2+} is observed both in the absence and in the presence of monovalent cations, whereas for pectin with a higher DM, this interaction is reported to be anti-cooperative. In addition, divalent cations that strongly bind to pectin, such as Cu^{2+}, show cooperative binding to citrus pectin and to acetylated sugar beet pectin, while Ca^{2+} and Zn^{2+} bind in an anti-cooperative mode to sugar beet pectin, but in a cooperative mode to citrus pectin.

While pH and ionic strength have been largely explored in relation to pectin-divalent cation interactions, more research on pectin concentration is necessary for a better understanding of the effect of this extrinsic factor on the divalent cation-binding capacity of pectin. Garnier et al. (1994) reported stronger pectin-Ca^{2+} interaction with increasing pectin concentration in the presence of monovalent cations, while in the absence of monovalent cations, the Ca^{2+}-binding was independent of the (LM) pectin concentration. Moreover, at lower DM, a higher affinity for Ca^{2+} was observed compared to high DM pectin, but this effect decreased with increasing pectin concentration. This can be explained by the higher number of binding sites available, leveling out the effect of DM on the binding capacity.

1.6 PECTIN FUNCTIONALITIES BASED ON CATION INTERACTIONS

1.6.1 Cation-induced gelation

1.6.1.1 Ca^{2+}-induced gelation

Ca^{2+}-induced pectin gelation is the most widely exploited pectin functionality, which is based on the ability of pectin to bind divalent cations (particularly Ca^{2+}) and the formation of a three-dimensional network of cross-linked pectin molecules (Thakur et al., 1997). This gelation mechanism typically involves formation of pectin dimers through binding of Ca^{2+} to negatively charged carboxyl groups of two pectin chains, resulting in junction zones. The junction zones are then stabilized by van der Waals forces, hydrogen bonds, hydrophobic interactions and electrostatic interactions between two polymer chains (Fraeye et al., 2010b). Ca^{2+}-induced pectin gelation occurs typically with LM pectin, given its increased potential to electrostatically interact with cations at pH values higher than the pKa to form a cross-linked network. HM pectin is also reported to gel in the presence of cations (Tibbits et al., 1998), but to a lesser extent than LM pectin. HM pectin mainly gels via hydrogen bonds and hydrophobic interactions between two pectin chains in acidic medium (pH < pKa) and in the presence of at least 55% soluble solids (Thibault & Ralet, 2003; Willats et al., 2006). This section focuses on cation-induced gelation of LM pectin, and particularly on Ca^{2+}-induced gelation as this cation is widely used in gelling applications and has been largely explored by several researchers. Considering that the influence of pectin structure and extrinsic factors on properties of pectin-Ca^{2+} gels has already been reviewed by Fraeye et al. (2010b) and that the intrinsic and extrinsic factors promoting Ca^{2+}-binding capacity as discussed in Sections 1.2 and 1.5 logically promote Ca^{2+}-

induced gelation, the present section will only briefly discuss the influence of these factors, highlighting the more recent findings.

Briefly, by decreasing pectin DM and increasing the sequences of successive non-methylesterified GalA units along the pectin chain, pectin-Ca^{2+} interaction is promoted (both interaction energy and maximum Ca^{2+}-binding capacity), leading to formation of egg-boxes, thereby yielding stronger gels (Fraeye et al., 2009; Kyomugasho et al., 2016; Ngouémazong et al., 2012a, 2012c; Powell et al., 1982; Ström et al., 2007). According to Kyomugasho et al. (2016), this increased gel strength is complemented by a higher number of strand-like microstructures.

With regard to pectin chain length, decreasing pectin molar mass leads to decreased gel strength, given the associated lower Ca^{2+}-binding capacity and interaction energy (Capel, Nicolai, Durand, Boulenguer, & Langerdorff, 2005; Fraeye et al., 2009; Kyomugasho et al., 2018; Rolin, Nielsen, & Glahn, 1998). The influence of limited reduction in pectin molar mass can be partially compensated by increasing the Ca^{2+} concentration (Fraeye et al., 2009; Kyomugasho et al., 2018), while drastic pectin depolymerization (to for instance, low molar mass of ~ 6 kDa) results in the loss of gelling ability (Capel et al., 2005; Kyomugasho et al., 2018). **Figure 1.5** illustrates microstructures of Ca^{2+}-mediated gels, visualized by cryo-scanning electron microscopy (cryo-SEM), of 1% pectin solutions with decreasing molar mass. As can be seen from **Figure 1.5**, decreased pectin molar mass resulted in less entangled network formation for a given stoichiometric ratio ($2[Ca^{2+}]/[COO^-]$).

The influence of the degree of acetylation of pectin and presence of neutral sugars on Ca^{2+}-induced pectin gelation is particularly important in sugar beet pectin, which is, as discussed earlier (Section 1.2.4), characterized by a substantial number of acetylated GalA units and neutral sugar side chains. These properties are generally reported to limit the exploitation of sugar beet pectin in Ca^{2+}-induced pectin gelation applications. Sugar beet pectin is for instance shown to form weaker gels compared to citrus pectin (Kyomugasho et al., 2016), due to the acetyl groups sterically hindering Ca^{2+} cross-linking (Ralet et al., 2003; Renard & Jarvis, 1999). The limited Ca^{2+}-induced pectin interaction was evident in cryo-SEM images of sugar beet gels showing less strand-like microstructures compared to citrus pectin with a similar DM (Kyomugasho et al., 2016). In fact, according to Rolin et al. (1998), sugar beet pectin is actually not able to form strong gels due to its O-acetyl groups. Besides, while the higher content of neutral sugars such as rhamnose, arabinose, or galactose in commercially available sugar beet pectin compared to citrus pectin has been reported

to limit its application in Ca^{2+}-induced gelling applications, available information is contradictory. On the one hand, Rolin et al. (1998) suggest that neutral sugar side chains reduce the gelling capacity of sugar beet pectin by causing kinks in the pectin molecular structure, preventing the association of two pectin chains. On the other hand, other authors have reported that hydrolyzing side chains of pectin (carrot or apple pectin) results in significantly less strong gels (Hwang & Kokini, 1992; Ngouémazong et al., 2012b; Sousa et al., 2015) due to reduced overall entanglement of the pectin (Ngouémazong et al., 2012b; Sousa et al., 2015). As such, more research is needed in order to draw a clear conclusion on the influence of neutral sugars on the cation-induced gelation of pectin.

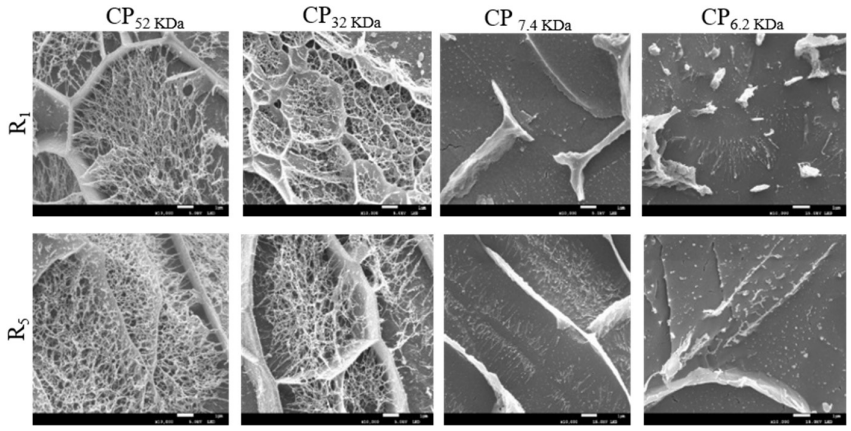

Figure 1.5: Microstructure of Ca^{2+}-mediated gels (measured by cryo-SEM) of 1% citrus pectin with distinct molar mass at stoichiometric ratios of 1 and 5 (R values, with R= 2[Ca^{2+}]/[COO^-]). Scale bars = 1 μm. Reprinted, with permission, from Kyomugasho, C., Munyensanga, C., Celus, M., Van de Walle, D., Dewettinck, K., Van Loey, A., and Hendrickx, M.E. (2018). Molar mass influence on pectin-Ca^{2+} adsorption capacity, interaction energy and associated functionality: gel microstructure and stiffness. *Food Hydrocolloids*, 85, 331-342. Copyright (2018).

Finally, in addition to intrinsic factors, Ca^{2+}-induced gelation can be optimized by controlling the Ca^{2+} concentration as well as pH of the systems. According to Fraeye et al. (2010b), by increasing the Ca^{2+} concentration, pectin solutions gradually transition from a sol phase to a gel. This dependency is mostly expressed as a function of the stoichiometric ratio R, as discussed earlier (Section 1.3), rather than the total Ca^{2+} concentration (Fraeye et al., 2010b). At a low Ca^{2+} concentration, i.e., below the threshold molar ratio (R^*, Section 1.3), weaker gels are formed due to the formation of monocomplexes and point-like cross-links between pectin and Ca^{2+} (Kyomugasho et al., 2018; Ventura et al., 2013), while increasing the Ca^{2+} concentration (> R^*) of

pectin solutions results in pectin dimerization and a more intertwined strand-like microstructure, generating gels with increased strength (Fraeye et al., 2009; Kyomugasho et al., 2016, 2018; Ngouémazong et al., 2012a, 2012c). Some authors observed a maximum gel strength at a certain Ca^{2+} concentration, beyond which the strength is not influenced by the Ca^{2+} concentration (Han et al., 2017; Kyomugasho et al., 2016, 2018; Ngouémazong et al., 2012a). This so-called 'saturating' Ca^{2+} concentration depends on the distribution pattern of methylesters, with an R value of ~ 1 (with $R = 2[Ca^{2+}]/[COO^{-}]$) for pectins with more blockwise distributed methylesters (achieved by demethylesterification using plant PME), whereas pectin with a random distribution of methylesters with a comparable DM exhibits higher R values (Ngouémazong et al., 2012a). According to Kyomugasho et al. (2018), the maximum Ca^{2+}-binding capacity of enzymatically demethylesterified citrus pectin (DM 32%) is reached at an R value of approximately 1, which can explain the maximum gel strength at this R value. Further Ca^{2+} addition (R = 5) reveals a more cross-linked network by cryo-SEM (**Figure 1.5**), despite no clear evidence of an increase in gel strength (Kyomugasho et al., 2018). It can be suggested that addition of Ca^{2+} to pectin solutions, even when the maximum binding capacity is reached, can still induce network formation, without necessarily significantly increasing the gel strength (Kyomugasho et al., 2018). The induced network formation is probably related to inter-dimerization, whereby formed dimers associate via weak electrostatic interactions (Braccini & Pérez, 2001).

With regard to the pH of the pectin system, limited ionic cross-linking and thus weaker gels with a less intertwined fibrous network are found at low pH values (< 3) (Han et al., 2017; Kyomugasho et al., 2016; Lootens et al., 2003), while at pH values above the pKa value (4.5-7), pectin is able to interact more with Ca^{2+}, resulting in more compact and stronger gels (Han et al., 2017; Kyomugasho et al., 2016). Han et al. (2017) found a maximal gel strength at a pH between 3.5 and 5, and a further increase in pH (6.3-6.6) was associated with a gradual decrease in gel strength, due to a predominant electrostatic repulsion between the pectin chains.

1.6.1.2 Gelation induced by other divalent cations

Although Ca^{2+} is the most commonly explored divalent cation-induced gelation, LM pectin can also form gels in the presence of other divalent cations, including Zn^{2+} and Fe^{2+} (Huynh et al., 2018; Kyomugasho et al., 2016). In the presence of Zn^{2+} and Fe^{2+}, gels with a denser and more cross-linked network were generated compared to Ca^{2+}-gels, according to Kyomugasho et al. (2016). They attributed this to a stronger binding of these cations to pectin, which can be confirmed by the reported higher affinities of

Zn^{2+} and Fe^{2+} for pectin compared to Ca^{2+} (Section 1.4). Addition of Mg^{2+} to pectin solutions was found to induce gels with a more open microstructure and less intertwined network compared to Ca^{2+} (as well as Zn^{2+} and Fe^{2+}) (Kyomugasho et al., 2016). This can be explained by the different binding mechanisms, with binding of Mg^{2+} to pectin via polycondensation (Huynh et al., 2016), while Ca^{2+} binds through the above-mentioned two-step mechanism (monocomplexation/point-like cross-links and dimerization). There is a general scarcity of information on the use of other divalent cations (except Ca^{2+}) to induce the gel formation, which might be due to: (i) the limited use of other cations in food applications, (ii) Ca^{2+} being the most predominant divalent cation naturally present in many food matrices, (iii) the tendency of Zn^{2+}-mediated gels to aggregate (Assifaoui et al., 2015), or (iii) the color and taste of Zn^{2+}- or Fe^{2+}-mediated gels, which are less appealing to consumers. Nevertheless, it might be interesting to explore gelation induced by other divalent cations as they have been shown to form a more cross-linked network, potentially leading to a better structure build-up.

1.6.2 Antioxidant capacity

Pectin is suggested to possess a lipid antioxidant capacity, which is largely associated with its ability to bind Fe^{2+}, as this cation is considered to be the most important pro-oxidant of lipid oxidation in food products (Mei, Decker, & McClements, 1998). Transition metals such as Fe^{2+} are mostly present in the aqueous phase of food oil-in-water (o/w) emulsions, in which they accelerate the oxidation of lipids, located at the droplet surface (McClements & Decker, 2000). Chelation of Fe^{2+}, thus removing this pro-oxidant from the vicinity of the oil-water interface, is an effective strategy to inhibit or retard lipid oxidation. To date, EDTA is widely used for this purpose. However, with the growing demand to replace artificial additives by natural alternatives, the ability of anionic natural polysaccharides such as pectin to retard lipid oxidation by binding Fe^{2+} has been explored by a few researchers (Chen, McClements, & Decker, 2010; Huang, Lu, Wang, & Wu, 2011; Shimada, Okada, Matsuo, & Yoshioka, 1996; Xu, Liu, Luo, Liu, & McClements, 2017). Although Cu^{2+} is also known to accelerate lipid oxidation (Schaich, Shahidi, Zhong, & Eskin, 2013), the interaction between pectin and Fe^{2+} is considered more important here given that Fe^{2+} is more (naturally) abundant in food products (Katsuda, McClements, Miglioranza, & Decker, 2008). Moreover, pectin exhibits a higher affinity for Cu^{2+} compared to Fe^{2+}, as described before (Section 1.4), implying that the former would be more strongly bound, thus less available to catalyze the lipid oxidation reaction.

Despite the fact that several pectin structural properties, such as DM, DB, DP, or DAc, have been suggested to direct its cation-chelating capacity and thus its lipid antioxidant capacity, only the effect of pectin DM on the oxidative stability of o/w emulsions has been reported in the literature. The lipid antioxidant capacity of pectin is reported to be more pronounced at low DM, due to the higher number of negative charges, which is associated with a higher Fe^{2+}-binding capacity (Chen et al., 2010). In addition to the pectin molecular structure, extrinsic factors such as the pectin concentration and pH are reported to influence lipid oxidation. For instance, Chen et al. (2010) found that an increase in pectin concentration from 0.02 to 0.05% w/v in the aqueous phase of menhaden o/w emulsions (2.5% w/v) stabilized by Brij 35 (0.25% w/v) resulted in decreased lipid oxidation, regardless of the DM. Despite the fact that a further increase in pectin concentration from 0.05 to 0.1% w/v did not lead to a clear difference in lipid antioxidant capacity of LM or HM pectin according to Chen et al. (2010), it can be suggested that increasing pectin concentration results in a decrease in lipid oxidation, given the higher number of negatively charged carboxyl groups present to bind Fe^{2+}. However, in contrast to the reported lipid antioxidant capacities of pectin, Qiu, Zhao, Decker and McClements (2015) observed an increased lipid oxidation upon addition of 0.1% w/v citrus pectin to a fish o/w emulsion (2.5% w/v) and attributed this to the potential presence of residual transition metals in the pectin sample, promoting lipid oxidation. Therefore, it is advised to carefully verify the intrinsic cation concentration of the pectin samples before using pectin as an antioxidant in o/w emulsions. Besides the pectin concentration, the pH of the emulsions has also been reported to influence the lipid antioxidant capacity of pectin. Pectin exhibits a higher lipid antioxidant capacity in emulsions at pH 7 compared to those at pH 3.5, which can be explained by a higher number of negatively charged carboxyl groups at pH 7, implying a higher Fe^{2+} chelating capacity (Xu et al., 2017). Moreover, Fe^{2+} exhibits an increased solubility in water with decreasing pH values from 7 to 3, thus also possibly increasing lipid oxidation at lower pH values, given that the ions are readily available at the oil-water interface (Mei et al., 1998).

It is noteworthy that the lipid antioxidant capacity of pectin is not solely associated with its Fe^{2+}-chelating capacity. Citrus pectin has been reported to exhibit radical-scavenging ability, thus acting as an electron donor to terminate the free-radical lipid oxidation reaction (Huang et al., 2011; Matsumura et al., 2003). However, this pectin characteristic is considered to be of secondary importance in determining the lipid antioxidant capacity of pectin. Furthermore, pectin is known to increase the viscosity of o/w emulsions (Dickinson, 2003), thereby possibly retarding the diffusion of dissolved oxygen through the oil-water interface, which could promote the oxidative

stability of emulsions (Shimada et al., 1996). Moreover, it can be hypothesized that an increase in emulsion viscosity also restricts the diffusion of Fe^{2+} through the aqueous phase towards the oil-water interface and into the lipid phase. The oxidative stability of emulsions can also be promoted by using pectin as a coating to encapsulate lipid droplets in addition to emulsifiers (Katsuda et al., 2008). In this case, the decrease in lipid oxidation cannot be directly related to the lipid antioxidant capacity of pectin, but rather to the altered emulsion droplet charge and thickness of the interfacial region (Katsuda et al., 2008; McClements & Decker, 2018).

1.6.3 Role of pectin in the digestive tract

Besides its importance in human digestion as a dietary fiber, pectin also plays a major role in the digestive tract attributed to its divalent cation-binding ability. On the one hand, the binding of essential minerals such as Fe^{2+} and Zn^{2+} is hypothesized to reduce their bioaccessibility, as the bound ions may not be released during digestion, and are thus not available for absorption in the small intestine (Raes, Knockaert, Struijs, & Van Camp, 2014). On the other hand, pectin is widely used for complexing toxic minerals such as Pb^{2+} or Cd^{2+} leading to their excretion from the human body, when pectin is fermented in the colon (Eliaz, Hotchkiss, Fishman, & Rode, 2006). Based on its potential fermentation in the colon, pectin has also been proposed to be suitable as a colon-specific drug-delivery vehicle (Wicker et al., 2014). Furthermore, pectin is also reported to indirectly influence lipid digestion by binding divalent cations important for lipid digestion as well as increasing the viscosity of the digest (Cervantes-Paz et al., 2017). This section discusses the role of pectin structural properties in mineral bioaccessibility, excretion of heavy metals, lipid digestion, and hypothesized cholesterol-lowering properties.

1.6.3.1 Mineral bioaccessibility or bioavailability

Pectin is considered as an anti-nutritional factor since it might reduce the mineral bioavailability or bioaccessibility (Raes et al., 2014). The term bioaccessibility is defined as the amount of nutrients released from the ingested food matrix and potentially available for absorption from the small intestine after digestion, whereas bioavailability is a measure of the rate and extent to which nutrients are absorbed in the circulatory system and become available for physiological functions in the body (Grundy et al., 2016; Raes et al., 2014). A decreased bioaccessibility can potentially promote mineral deficiencies, particularly of essential minerals such as Zn^{2+} and Fe^{2+}, which are reported to be highly prevalent nutritional problems worldwide (Raes et al., 2014).

During digestion, the influence of the gastric phase is reported to be minimal (if any), given that at this very low pH (1-3), the carboxyl groups of pectin are protonated and therefore no significant binding between pectin and cations occurs. Indeed, at a pH of 1-2 (approaching the acidity of the stomach) a high release of Zn^{2+} and Fe^{3+} from pectin was found by Debon and Tester (2001) and Miyada, Nakajima, and Ebihara (2011). However, during intestinal digestion (pH 6-7), the carboxyl groups of pectin become negatively charged and pectin-divalent cation interactions are thus promoted. As such, this digestion phase is suggested to be the most important in mineral bioaccessibility, as bound divalent cations may not be released and therefore not available for absorption, given that pectin is non-digestible in the small intestine (Bosscher, Van Caillie-Bertrand, Van Cauwenbergh, & Deelstra, 2003). On the contrary, other researchers suggest that pectin can be fermented in the colon by the microflora, releasing the bound divalent cations, thereby increasing the potential for cation absorption (Cummings & Macfarlane, 1991; Dongowski, Lorenz, & Proll, 2002). However, considering that the small intestine is the main site for mineral absorption, their suggested release in the colon may not promote their absorption. Moreover, the potentially released cations in the colon could be utilized by the colonic microflora and are thus not available for human absorption. This section will therefore focus on the effect of pectin structural properties on the mineral bioaccessibility and bioavailability in the small intestine during digestion.

***In vitro* bioaccessibility of divalent minerals**

Considering the role of pectin structural properties in determining pectin-divalent cation interactions, they probably in turn influence mineral bioaccessibility, a pectin-cation-associated functionality. An overview of the reported *in vitro* bioaccessibilities of Zn^{2+}, Ca^{2+}, and Fe^{2+} in the presence of pectin from different sources is presented in **Table 1.3**. First, decreasing pectin DM (of citrus and sugar beet) resulted in a decreased *in vitro* mineral bioaccessibility, as pectin-cation interactions are promoted, making these strongly bound minerals unavailable for absorption (Bosscher et al., 2003; Kyomugasho et al., 2017). Moreover, at a given DM, the influence of the pectin source on *in vitro* bioaccessibility of these cations is clear, with higher bioaccessibilities obtained in the presence of sugar beet pectin than citrus pectin. This can be attributed to the structural properties of sugar beet pectin, which is typically characterized by a higher degree of acetylation and branching compared to citrus pectin, properties that limit the divalent cation-binding capacity of pectin (Kyomugasho et al., 2017). To the best of our knowledge, no effect of methylesterification pattern has been studied in relation to the mineral bioaccessibility.

Table 1.3: Overview of Zn^{2+}, Ca^{2+}, or Fe^{2+} bioaccessibilities (BAC) or bioavailabilities (BAV) ± standard deviation (if reported) in presence of pectin with distinct DMs determined via *in vitro* and *in vivo* studies as reported by different authors. (E) and (U) refer to an enzymatic and unknown method of demethylesterification, respectively. DM = degree of methylesterification, ns = not specified, nd = not determined, conc. = concentration.

***In vitro* studies**						
Reference	**Pectin conc. (%) + source**	**DM (%)**	**Cation concentration**	**Zn^{2+} BAC (%)**	**Ca^{2+} BAC (%)**	**Fe^{2+}/Fe^{3+} BAC (%)**
Bosscher et al. (2003)	3% Citrus	>65 (U)	ns.	8.4 ± 0.9	11.7 ± 0.7	2.3 ± 0.5
	3% Citrus	26-31 (U)	ns.	7.0 ± 0.7	14.2 ± 1.4	2.1 ± 0.1
Kyomugasho et al. (2017)	1% Citrus	95	5 mM	~ 75	~ 90	~ 10
	1% Citrus	65 (E)	5 mM	~ 10	~ 60	~ 2.5
	1% Citrus	35 (E)	5 mM	~ 8	~ 40	~ 1.5
	1% Citrus	16 (E)	5 mM	~ 5	~ 25	~ 1
	1% Sugar beet	60 (E)	5 mM	~ 60	~ 80	~ 14
	1% Sugar beet	35 (E)	5 mM	~ 50	~ 55	~ 3
***In vivo* studies**						
Reference	**Pectin conc. (%) + source**	**DM (%)**	**Cation conc.**	**Zn^{2+} BAV (%)**	**Ca^{2+} BAV (%)**	**Fe^{2+}/Fe^{3+} BAV (%)**
Bagheri and Guénguen (1985) In pigs	2.5% Apple	72.5 (U)	8.54 g/kg Ca^{2+} 0.118 g/kg Zn^{2+}	12.3 ± 5.9	28.1 ± 3.8	nd.
	2.5% Apple	39.9 (U)	8.50 g/kg Ca^{2+} 0.126 g/kg Zn^{2+}	< 0	0.42 ± 7.5	nd.
Kim (1998) In rats	80g/kg diet ns.	73 (U)	214-217 mg/kg	nd.	nd.	~ 65*
	80g/kg diet ns.	22 (U)	214-217 mg/kg	nd.	nd.	~ 55*
Jaramillo et al. (2015) In humans	250 mg Citrus	55-70 (U)	5 mg	nd.	nd.	60

* data are expressed as amount of Fe^{2+} absorbed as a fraction of the calculated amount that entered the intestine (Kim, 1998).

Besides the pectin structural properties, mineral concentrations have been demonstrated to influence the amount of bioaccessible minerals as well. Enriching pectin solutions with increasing amounts of cations prior to *in vitro* simulated digestion results in enhanced *in vitro* bioaccessibility of Zn^{2+}, Fe^{2+}, and Ca^{2+}, according to Kyomugasho et al. (2017). Pectin can only bind a certain amount of cations, which refers to its maximum binding capacity (**Table 1.2**), such that in the presence of higher cation concentrations, a higher cation amount is not bound and therefore bioaccessible. Analogous to the affinities of pectin for different cations addressed in Section 1.4, the *in vitro* bioaccessibility decreased in the order of Ca^{2+} > Zn^{2+} > Fe^{2+} as shown in **Table 1.3**, indicating the strongest binding with Fe^{2+} (Bosscher et al., 2003; Kyomugasho et al., 2017). The highest bioaccessibility in the presence of similar pectin conditions (e.g., pectin concentration and DM) was observed for Mg^{2+} compared to Ca^{2+}, Zn^{2+}, or Fe^{2+} by Kyomugasho et al. (2017). This is related to a lower amount of Mg^{2+} bound to pectin, which can be explained by the different binding mechanism of Mg^{2+} to pectin, i.e. polycondensation, in comparison to the other divalent cations (Huynh et al., 2016).

Most research conducted on simulated *in vitro* digestion of pectin-containing systems is commonly done on pectin solutions enriched with a single type of mineral and not a combination of minerals. It would be more representative for real food matrices to study the competition effect of several minerals on the bioaccessibility, as these matrices mostly contain a combination of minerals. However, Jaramillo et al. (2015) did not observe a significant difference in Fe^{2+} bioavailability in the presence or absence of Ca^{2+}. This could be explained by the higher affinity of pectin for Fe^{2+} compared to Ca^{2+}. These observations suggest that digestion of food products rich in Zn^{2+}, Fe^{2+}, or Ca^{2+}, would more likely lead to Zn^{2+} or Fe^{2+} deficiencies than to Ca^{2+} deficiency, given the higher affinity of pectin for Zn^{2+} and Fe^{2+} compared to Ca^{2+}. To date, there is limited information on the effect of cation combinations on the bioaccessibility of the individual minerals, probably due to the complexity of the data obtained and their interpretation.

With the growing demand to control mineral deficiencies, several interventions have been proposed, including dietary variation, food supplementation, and fortification. In addition, improvement of nutrient bioaccessibility in plant-based food products, containing anti-nutrients such as pectin, is an important strategy (Gharibzahedi & Jafari, 2017; Raes et al., 2014). The latter can, for instance, be achieved by selective heat-processing of food products to (in)activate pectinases, altering pectin structural properties, and thus cation-binding capacities (Christiaens et al., 2015b; Raes et al.,

2014). To this extent, Kyomugasho, Willemsen, Christiaens, Van Loey and Hendrickx (2015b) processed tomatoes either at high pressure or at high temperature and observed a higher Ca^{2+} and Fe^{2+} bioaccessibility for the high-temperature-blanched tomato-based suspensions. These suspensions were rich in pectin with a high DM, due to inactivation of pectin methylesterase (PME), an enzyme which is responsible for pectin demethylesterification. In the high-pressure-treated tomatoes, pectin with lower DM was found, since PME is considered to be baro-tolerant and thus resists high-pressure processing and is active during subsequent steps (Christiaens et al., 2015b; Kyomugasho et al., 2015b). Besides, cooking of a fruit- and vegetable-based product is also associated with increased mineral bioaccessibilities, as such heat treatments are associated with a beta-elimination reaction. Such reactions are accompanied by a depolymerization of the pectin chain (Van Buggenhout et al., 2009), decreasing the pectin cation-binding capacity as has been explained in Section 1.2.3. Therefore, blanching of the raw food material, thus inactivating PME, followed by cooking of the fruit- and vegetable-based product, thus depolymerizing the pectin chain, is hypothetically an interesting order of processing steps in view of increasing the mineral bioaccessibility. However, it is noteworthy that food processing can also remove or reduce the mineral content and it is advised to carefully select the processing conditions (Fabbri & Crosby, 2016; Gharibzahedi & Jafari, 2017; Raes et al., 2014).

***In vivo* bioavailability of divalent minerals**

Although most studies performed in relation to mineral bioaccessibility, as influenced by pectin, involve simulated *in vitro* digestions, some *in vivo* experiments in humans as well as in pigs have been performed. The role of pectin structural properties in *in vivo* divalent mineral bioavailability has been demonstrated by a number of researchers. In pigs, no significant differences in mineral bioavailability were observed in the presence or absence of HM pectin (Bagheri & Guénguen, 1985; Jaramillo et al., 2015; Lei, Davis, Fang, & Young, 1980), while the presence of LM pectin clearly lowers the *in vivo* mineral absorption in pigs (Bagheri & Guénguen, 1985) and in rats (Kim, 1998) as can been seen from **Table 1.3**. Kim (1998) also reported a clear effect of the DM and molar mass of pectin on Fe^{3+} solubility and absorption in rats, as higher intestinal Fe^{3+} absorption was observed during digestion of a diet enriched with high DM and low molar mass pectin. This is in agreement with the previously discussed results (Section 1.2) that high DM and low DP decrease the divalent cation-binding capacity of pectin, which can result in a higher amount of divalent cations being bioavailable. It should be noted that iron is more easily absorbed as Fe^{2+}. Therefore, if present as Fe^{3+}, it needs to be reduced to Fe^{2+} in order

to be absorbed by the mucosal cells and pass through the cellular membrane of enterocytes (Kim, 1998; Maire du Poset et al., 2018). According to Maire du Poset et al. (2018), incorporation of Fe^{2+} as a cross-linker in pectin-based hydrogels could be used as a promising tool to prevent iron oxidation during digestion. However, the question arises whether this tool can be used to improve Fe^{2+} absorption, as preventing the oxidation of this cation by binding it might still decrease its bioaccessibility or bioavailability.

1.6.3.2 Role of pectin in excretion of toxic minerals

Despite the impaired mineral bioaccessibility as a consequence of pectin-cation interactions in the gastro-intestinal tract, the divalent cation-binding capacity of pectin can be beneficial as it is used for excretion of toxic minerals such as lead, cadmium, strontium, or arsenic (Braudo et al., 1996; Eliaz et al., 2006; Zhao et al., 2008). The ability of pectin to reduce absorption of such heavy metals can on the one hand be attributed to its chelating ability in the small intestine, preventing the absorption and subsequently facilitating the elimination via the feces when fermented in the colon (Eliaz et al., 2006). On the other hand, pectin has been reported to chelate toxic metals in the bloodstream, followed by an urinary excretion (Eliaz et al., 2006). In the latter type of application, modified citrus pectin with shorter-chain molecules is commonly used, as it is easily absorbed into the bloodstream (Zhao et al., 2008). The shorter-chain molecules still possess the ability to bind ions such as Pb^{2+}, as these cations are reported to have a very high affinity for carboxyl groups (Section 1.4). In addition, the modified citrus pectin used for this application is characterized by a reduced number of side chains and reduced DM to enhance the binding capacity (Zhao et al., 2008).

1.6.3.3 Role of pectin in lipid digestion and cholesterol synthesis

The pectin-cation interaction during digestion does not solely influence associated functionalities such as the mineral absorption, but has been reported to also indirectly retard lipid digestion (particularly Ca^{2+} interaction). For instance, binding of Ca^{2+} by pectin can retard lipid hydrolysis given that Ca^{2+} plays an essential role during lipid digestion by removing free fatty acids (FFAs) from the lipid droplet surface, which facilitates the action and access of lipase to lipid droplets (Cervantes-Paz et al., 2017; Espinal-Ruiz, Parada-Alfonso, Restrepo-Sánchez, Narváez-Cuenca, & McClements, 2014; Hu, Li, Decker, & McClements, 2010). Moreover, Ca^{2+} is known to be a co-factor of pancreatic lipase, such that its binding to pectin could lead to decreased lipase activity (Hu et al., 2010). In addition, pectin-Ca^{2+} interactions could result in increased

viscosity or formation of a microgel network, hindering the diffusion of lipase and bile salts and thus retarding the lipid digestion process (Cervantes-Paz et al., 2017; Espinal-Ruiz et al., 2014; Verrijssen et al., 2016). In fact, increased viscosity, possibly due to Ca^{2+}-induced microgels, is reported to be one of the possible mechanisms responsible for the cholesterol-lowering capacity of pectin. A high viscosity might reduce the rate of glucose diffusion and thus its absorption in the small intestine, which consequently causes a decrease in insulin production. Reduced insulin decreases the activity of 3-hydroxy-3-methylglutaryl CoA, an enzyme responsible for the cholesterol synthesis, thereby lowering the cholesterol levels (Wicker et al., 2014). Besides, the formation of pectin-Ca^{2+} microgels can result in an adverse effect on overall nutrient digestion given that the diffusion of other compounds such as proteins or starch-digestive enzymes could also be decreased.

1.6.4 Other pectin functionalities

Pectin has gained interest as a biosorbent for the removal of heavy metals, such as Zn^{2+}, Pb^{2+}, Cd^{2+}, or Cu^{2+} from waste waters, as these metal ions can be toxic to animals and humans. The use of biological materials and, in particular, pectin is desirable compared to traditional metal-removal methods, such as chemical precipitation or membrane processes, due to its effectiveness, safety, and wide availability (Khotimchenko et al., 2008; Schiewer & Patil, 2008). Pectin is abundantly present in waste streams of the citrus, apple, and sugar beet processing industries. Therefore valorizing these waste streams (e.g., citrus peel or sugar beet pulp) to obtain pectin for use as a biosorbent is an interesting area to explore (Christiaens et al., 2015a; Naqash, Masoodi, Rather, Wani, & Gani, 2017). Citrus peel was found to be the most effective in binding Cd^{2+} (Schiewer & Patil, 2008), but also pectin modified with adipic acid (Li, Yang, Zhao, & Xu, 2007) or sugar beet pulp (Castro, Blázquez, González, Muñoz, & Ballester, 2017) were shown to effectively adsorb metal ions. As expected, the metal uptake by these pectins increased with increasing pH as more carboxyl groups were negatively charged (Castro et al., 2017; Schiewer & Patil, 2008).

Besides the use of pectin as a biosorbent, pectin is used in edible packaging, due to its ability to form strong complexes by interacting with divalent cations such as Ca^{2+} (Naqash et al., 2017). It has been used to formulate edible packaging films as part of active food packaging (Espitia, Du, Avena-Bustillos, Soares, & McHugh, 2014). Production of edible films from pectin can be achieved by several methods such as casting, extrusion, spraying, and knife-coating (Espitia et al., 2014).

1.7 CONCLUSION AND RESEARCH OBJECTIVE

This literature review shows that the cation-binding capacity of pectin and its associated functionalities are influenced by many factors, with the pectin molecular structure receiving a lot of attention. The main structural property of pectin explored is the DM, as this is considered to be the most important one, but other structural factors have been shown to also influence the cation-binding capacity and therefore its functionalities. To date, only limited information is available on the influence of targeted designed pectin structures, in terms of distribution pattern of methylesters, chain length or branching, on pectin-cation-associated functionalities (with the exception of Ca^{2+}-induced gelation). Therefore, fundamental research on the determination of the cation-binding capacity of pectins with these distinct structural properties is needed. Moreover, there is a need for an extension of the adsorption studies to other cations, as it has been shown that cation type might influence the binding mechanism and binding characteristics (e.g., binding capacity and binding constant). As such, a better insight can be obtained into the competition between several cations for binding to pectin.

This doctoral thesis therefore aims to explore the role of pectin DM and DB_{abs}, two structural parameters which are considered to largely influence the cation binding, on the binding of Fe^{2+}, Zn^{2+}, or Ca^{2+} through equilibrium adsorption experiments or isothermal titration calorimetry (only Zn^{2+}) (**Chapter 3, 4 and 5**). These cations were chosen as they are frequently present in food products and they are mainly associated with pectin functionality, such as gelling, antioxidant capacity or role in mineral bioaccessibility. The relation between pectin DM and DB and the latter two functionalities will be explored as well in this doctoral thesis (**Chapter 3 and 6**).

PART II: EXPERIMENTAL WORK

CHAPTER 2

Demethylesterification and structural characterization of pectins

CHAPTER 3

Influence of pectin degree and pattern of methylesterification on interaction with Zn^{2+} or Ca^{2+} and associated bioaccessibility

CHAPTER 4

Isothermal titration calorimetry for assessing the Zn^{2+}-binding capacity of pectin

CHAPTER 5

Influence of pectin degree and pattern of methylesterification on Fe^{2+} interaction

CHAPTER 6

Influence of pectin degree and pattern of methylesterification on physical and oxidative stability of oil-in-water emulsions

CHAPTER 2

DEMETHYLESTERIFICATION AND STRUCTURAL CHARACTERIZATION OF PECTINS[2]

2.1 INTRODUCTION

Pectin exhibits a large diversity in structural properties, which confers its variability in both *in situ* and *ex situ* functionality. Pectin extracted from citrus peel or apple pomace is widely used as an additive and mainly consists of linear homogalacturonan (due to the industrial extraction process), of which the degree and pattern of methylesterification (DM and DB, respectively) are of particular importance for the cation-binding capacity and associated functionalities. In order to direct this cation-binding capacity, enzymatic or alkaline pectin demethylesterification is of specific

[2] This chapter is based on following papers:
Celus, M., Kyomugasho, C., Lombardo, S., Thielemans, W., and Hendrickx, M. (2018). Isothermal titration calorimetry to study the influence of citrus pectin degree and pattern of methylesterification on Zn^{2+} interaction. *Carbohydrate Polymers*, 197: 460-468.
Celus, M., Kyomugasho, C., Salvia-Trujillo, L., Van Audenhove, J., Van Loey, A., Grauwet, T., and Hendrickx, M. (2018). Interactions between citrus pectin and Zn^{2+} or Ca^{2+} and associated *in vitro* Zn^{2+} bioaccessibility as affected by degree of methylesterification and blockiness. *Food Hydrocolloids,* 79: 319-330.
Celus, M., Salvia Trujillo, L., Kyomugasho, C., Maes, I., Van Loey, A., Grauwet, T., and Hendrickx, M. (2018). Structurally modified pectin for targeted lipid antioxidant capacity in linseed/sunflower oil-in-water emulsions. *Food Chemistry*, 241: 86-96.
Celus, M., Kyomugasho, C., Jamsazzadeh Kermani, Z., Roggen, K., Van Loey, A., Grauwet, T., and Hendrickx, M. (2017). Fe^{2+} adsorption on citrus pectin is influenced by the degree and pattern of methylesterification. *Food Hydrocolloids*, 73: 101-109

interest in order to generate pectins with different DM and DB. Enzymatically demethylesterified pectins are typically characterized by a higher DB compared to alkaline demethylesterified pectins for a given DM and thus hypothesized to exhibit a higher cation-binding capacity. The DB of pectin may also be presented as the DB_{abs} (absolute degree of blockiness), which is defined as the ratio of the number of non-methylesterified GalA units present in blocks to the total number of GalA units in the pectin chain (Guillotin et al., 2005). The DB_{abs} is according to some authors more informative than DB in understanding the cation-binding capacity of pectin (Guillotin et al., 2005; Slavov et al., 2009; Ström et al., 2007). Therefore, this doctoral thesis will use the DB_{abs} instead of DB.

This chapter describes the preparation and characterization of pectin samples, generated by enzymatic as well as alkaline demethylesterification of commercial citrus pectin with a DM of 95%. Application of both methods of demethylesterification was aimed to create differences in DM as well as DB_{abs} to provide insights into pectin functionality (lipid antioxidant capacity or role in mineral bioaccessibility, the focus of this doctoral thesis) as these pectin structural properties are hypothesized to play a major role. While enzymatic demethylesterification of pectin with plant (carrot) pectin methylesterase (PME) was aimed to generate pectins with a blockwise distribution of non-methylesterified GalA units, alkaline demethylesterification with NaOH will be used to obtain a random removal of methylesters. The prepared demethylesterified pectins samples are further used to gain insights into the influence of these two structural parameters on the cation-binding capacity and associated functionalities.

2.2 MATERIALS AND METHODS

2.2.1 Materials

High methylesterified citrus pectin, with a DM of 95.1 ± 1.8% (CP95), from Sigma-Aldrich Belgium, was used as starting material for the production of pectin samples with different degrees and patterns of methylesterification. Carrots (*Daucus carota* cv. Nerac) and kiwis (*Actinidia deliciosa* cv. Hayward) were purchased from a local shop. The carrots were peeled, cut into 0.2 cm slices, frozen in liquid nitrogen and stored at -40 °C until extraction of PME. Kiwis were stored at room temperature to ripen, followed by extraction of PME inhibitor (PMEI). All chemicals used were of analytical grade.

2.2.2 Kiwi PMEI extraction and purification for preparation of PMEI-sepharose gel

PMEI was extracted from ripe kiwi, purified and coupled to a sepharose gel to obtain a PMEI-Sepharose gel for use in carrot PME purification (Section 2.2.3). First, PMEI was extracted from kiwi as described by Jolie et al. (2009). Ripe kiwi fruits (approximately 1 kg) were peeled, cut into pieces and homogenized at 4 °C (1:1 w/v) in a 5% polyvinylpolypyrrolidone suspension using a blender. After centrifugation of the resulting suspension at 20000 g for 20 min at 4 °C, the pH of the supernatant (containing crude PMEI) was adjusted to 6 with 1 M NaOH. After a filtration step to remove all seeds and other small particles, a crude PMEI-rich extract was obtained. Secondly, the crude PMEI extract was purified by affinity chromatography using an ÄktaPrime™ system (GE Healthcare, Chicago, IL, USA) (Jolie et al., 2009). The PMEI crude extract was mixed end-over-end with orange PME coupled to a CNBr-sepharose 4B gel for at least 2 h at 4 °C. Afterwards, the PMEI coupled to the PME-CNBr-sepharose gel was packed into a column (XK16, GE Healthcare, Chicago, IL, USA) for PMEI separation. After a preliminary wash of the packed gel with 2 mM potassium phosphate buffer (pH 6) containing 0.5 M NaCl, the PMEI was eluted with 20 mM sodium carbonate buffer (pH 9.85) containing 1 M NaCl. The fractions containing PMEI activity were collected, pooled and desalted using Vivaspin 20 centrifugal filters (5 kDa molecular weight cut-off (MWCO), Sartorius, Göttingen, Germany). The purified kiwi PMEI concentrate was dissolved in 10 mM sodium phosphate buffer (pH 6.5), frozen in liquid nitrogen and stored at -80 °C until use in preparation of the PMEI-sepharose gel.

For preparation of the PMEI-sepharose gel, purified kiwi PMEI (approximately 5000 U) dissolved in a 0.2 M carbonate buffer (pH 8.3) containing 0.5 M NaCl was covalently coupled to an NHS (N-hydroxysuccinimide)-activated sepharose 4 Fast Flow matrix (obtained from GE Healthcare, Chicago, IL, USA) by end-over-end mixing at 4 °C overnight as described by Jolie et al. (2009). Subsequently, the PMEI-NHS-sepharose gel was mixed with 1 M Tris-HCl buffer (pH 7.5) for 2 h at 4 °C in order to deactivate all unoccupied sites. Finally, the gel was washed with 0.1 M Tris-HCl buffer (pH 8.5), 0.1 M acetate buffer (pH 4.5), and water and stored in a 20% ethanol solution.

2.2.3 Carrot PME extraction and purification

PME extraction from carrots and purification was performed as described by Jolie et al. (2009). First, frozen carrot slices (see Section 2.2.1) were homogenized using a Grindomix (2 x 20 s at 7500 rpm) and then allowed to melt at room temperature. The homogenate was subsequently washed with demineralized water (1.6:1 w/v) and filtered through a cheese cloth. The pellet obtained was suspended (1:1.3 w/v) in 0.2 M Tris-HCl buffer (pH 8) containing 1 M NaCl and mixed end-over-end overnight at 4 °C in order to extract the PME. The supernatant, obtained after filtration through a cheese cloth, was subjected to sequential ammonium sulphate precipitation. The fraction precipitated at 30% contained impurities which were removed, while the precipitate at 80% ammonium sulphate was separated by centrifugation at 18000 g for 15 min at 4 °C and dissolved in 20 mM Tris-HCl buffer (pH 7), yielding the crude PME extract.

Subsequently, the crude carrot PME extract was coupled to the PMEI-NHS-sepharose gel generated in Section 2.2.2 and purified using affinity chromatography. Briefly, crude PME extract (approximately 2000 U) was first coupled to the PMEI-NHS-sepharose gel by mixing end-over-end at 4 °C for at least 2 h. This gel was then packed into the column (XK 16, GE Healthcare, Chicago, IL, USA), washed with 2 mM potassium phosphate buffer (pH 6) containing 0.5 M NaCl, followed by elution of PME using 50 mM sodium carbonate buffer (pH 9.85) containing 1 M NaCl. The fractions possessing PME activity were pooled and desalted using Vivaspin centrifugal filters (5 kDa MWCO, Sartorius, Göttingen, Germany). The purified PME concentrate was dissolved in 10 mM sodium phosphate buffer (pH 6.5), frozen with liquid nitrogen and stored at -80 °C until use in pectin demethylesterification.

2.2.4 PME and PMEI activity determination

Prior to use of PMEI for the PMEI-sepharose gel preparation (Section 2.2.2) and PME for the PME purification (Section 2.2.3) or pectin demethylesterification (Section 2.2.5.1), their activities were established. The assessment of the PME activity was based on titration with 0.01 M NaOH using an automatic pH-stat titrator (718 STAT titrino, Metrohm, Herisau, Switzerland) as described by Jolie et al. (2009). Purified carrot PME was added to 30 mL of a 0.35% (w/v) apple pectin solution (pH 6.5) containing 0.117 M NaCl at 22 °C. PME catalyzes the de-esterification of methyl groups, resulting in the formation of carboxyl groups which causes a pH drop. To counteract this effect and maintain a constant pH of 7 during the measurement, an automatic pH-stat titrator was employed (titration with 0.01 M NaOH). The PME

activity, in units (U), was defined as the amount of enzyme catalyzing the hydrolysis of 1 µmol of methylesters per min at 22 °C.

The activity of PMEI was measured as its ability to inhibit PME activity. This was determined as the difference between the PME activity of a blank sample (i.e. purified PME extract without PMEI) and the PME activity of a sample with added PMEI (PME:PMEI 1:2 v/v, pre-incubated for 15 min). The PMEI activity assessment was performed in analogous conditions as for PME activity measurements. One unit (U) of PMEI activity was defined as the amount of PMEI blocking 1 U of PME under the abovementioned conditions.

2.2.5 Demethylesterification of citrus pectin

2.2.5.1 Enzymatic demethylesterification with carrot PME

Enzymatic demethylesterification of commercial high methylesterified citrus pectin (CP95) with purified carrot PME was performed as described by Ngouémazong et al. (2011). A 25 mL solution of 0.8% (w/v) CP95 in 0.1 M sodium phosphate buffer pH 7 was incubated with 15 U of the purified carrot PME at 30 °C for different time periods to obtain distinct degrees of methylesterification. Afterwards, the solutions were immediately cooled in an ice bath and adjusted to pH 4.5 using 37% HCl. This pH adjustment was aimed to avoid pectin depolymerization through beta-elimination during the subsequent thermal treatment (4 min at 85 °C), applied to inactivate PME (Ngouémazong et al., 2011).

2.2.5.2 Alkaline demethylesterification

Alkaline demethylesterification was performed according to the method of Fraeye et al. (2009). Commercial high methylesterified citrus pectin (CP95) was dissolved in demineralized water (0.8% w/v) and the resulting pectin solution was adjusted to pH 11 with 0.1 M NaOH. Alkaline demethylesterification occurred at pH 11, leading to a pH drop. The pH was kept constant at pH 11 by titration with 0.1 M NaOH using an automatic pH-stat titrator (718 STAT titrino, Metrohm, Herisau, Switzerland). The reaction was performed at 4 °C to avoid pectin depolymerization (Fraeye et al., 2009). The amount of NaOH added by titration to obtain a specific DM was theoretically determined based on the stoichiometry of the alkaline demethylesterification reaction (Ngouémazong et al., 2011). After addition of the predetermined amounts of NaOH, the demethylesterification was stopped by adjusting the pH to 4.5 (Fraeye et al., 2009).

Subsequently, the enzymatically and alkaline demethylesterified pectin samples were adjusted to pH 6 and dialyzed (Spectra/Por®, MWCO = 12-14 kDa) for 48 h against

demineralized water with approximately 10 refreshments of the dialyzing water. The dialysis was performed to remove salts, particularly Na^+ added during the demethylesterification process. Removal of monovalent ions, including Na^+, was of particular importance since these ions are hypothesized to alter the ionic strength of systems, thereby potentially influencing the cation-binding capacity of pectin, given that the charges on the pectin polymer are screened (Dronnet et al., 1996; Garnier et al., 1994; Renard & Jarvis, 1999). The dialyzed pectin samples were then lyophilized and stored in a desiccator. For further use, the enzymatically demethylesterified pectins will be denoted as P-pectins while the alkaline (chemically) demethylesterified pectins will be denoted as C-pectins.

2.2.6 Characterization of the demethylesterified pectin samples

Commercial high methylesterified citrus pectin (CP95) and the partially demethylesterified pectin samples obtained in Section 2.2.5 were characterized for several structural properties including the DM, GalA and neutral sugars, molar mass distributions, and intrinsic cation concentrations. The absolute degree of blockiness of the pectin samples was estimated based on the polynomial equations established by Ngouémazong et al. (2011).

2.2.6.1 Determination of the degree of methylesterification

Measurement of the DM of the commercially available citrus pectin (CP95) and the demethylesterified pectin samples was performed using Fourier transform infra-red (FT-IR) spectroscopy (Shimadzu FTIR-8400S, Kyoto, Japan) according to the method described by Kyomugasho et al. (2015a). The transmittance was measured at wave numbers from 4000 cm^{-1} to 400 cm^{-1} (100 scans per sample). In order to estimate the DM as a function of the intensity of the peak around 1740 cm^{-1} (C=O stretch) and 1630-1600 cm^{-1} (COO^- stretch), the following standard curve without deconvolution of the spectra was used (Kyomugasho et al., 2015a):

$$\text{DM}\ (\%) = 136.86 \cdot \frac{I(1740)}{I(1740)+I(1600)} + 3.987 \qquad [2.1]$$

2.2.6.2 Estimation of the absolute degree of blockiness

The pattern of methylesterification of the pectin samples can be quantified as the degree of blockiness (DB) or absolute degree of blockiness (DB_{abs}). The DB is the ratio of the number of non-methylesterified GalA units present in blocks to the total non-methylesterified GalA units (Daas et al., 1999), whereas DB_{abs} is defined as the ratio of non-methylesterified GalA units present in blocks to the total amount of GalA units (Guillotin et al., 2005). In this doctoral thesis, only DB_{abs} is taken into account

and was predicted based on parameter estimates of polynomial functions determined by Ngouémazong et al. (2011). The use of these polynomial equations is justified, given that the present study used exactly the same procedures and materials for the targeted pectin modification as described by Ngouémazong et al. (2011). The polynomial functions used were achieved by Ngouémazong et al. (2011) by relating DB_{abs} to DM of tailored pectin samples and are described as follows:

P-pectins: $\mathrm{DB_{abs}} = 0.472\ (\pm 0.03)\ \mathrm{DM}^2 - 1.485\ (\pm 0.04)\ \mathrm{DM} + 1.009$ [2.2]

C-pectins: $\mathrm{DB_{abs}} = -1.998\ (\pm 0.10)\ \mathrm{DM}^3 + 4.595\ (\pm 0.20)\ \mathrm{DM}^2 - 3.598\ (\pm 0.06)\ \mathrm{DM} + 1.000$ [2.3]

2.2.6.3 Determination of GalA and neutral sugar content

To measure the GalA content, pectin samples were first hydrolyzed (in duplicate) with concentrated sulfuric acid according to the method described by Ahmed and Labavitch (1977). The GalA concentration of the hydrolyzed samples was then quantified (in triplicate) by a spectrophotometric method as described by Blumenkrantz and Asboe-Hansen (1973).

The commercial high methylesterified citrus pectin (CP95) and the enzymatically demethylesterified pectin sample with low DM (P13) were additionally characterized for (pectin-related) neutral sugars using high-performance anion-exchange chromatography (HPAEC) combined with pulsed amperometric detection (PAD) as described by Houben, Jolie, Fraeye, Van Loey, and Hendrickx (2011). The pectin samples were first hydrolyzed (in duplicate) with 4 M trifluoroacetic acid (TFA) for 1.5 h at 110 °C. The digest was then dried under a N_2-evaporator (Techne FDB03DD, Cambridge, UK) at 45 °C, subsequently washed with 1 M NH_4OH to remove or neutralize TFA, followed by a second drying under N_2 at 45 °C. The residue was dissolved in ultrapure water (organic free, 18.2 MΩ cm), and filtered (through a 0.45 µm filter) prior to injection (10 µL sample) onto the HPAEC-PAD (Dionex DX600, Sunnyvale, CA, USA). The sample was eluted with 4 mM NaOH at a flow rate of 0.5 mL/min and at 30 °C for 20 min. Neutral sugars, arabinose (Ara), fucose (Fuc), galactose (Gal), glucose (Glu), mannose (Man), rhamnose (Rha), and xylose (Xyl) were identified and quantified using sugar standard solutions at varying concentrations (1-10 ppm). Recovery values were estimated in order to correct for possible degradation of the monosaccharides during the acid hydrolysis. Therefore, sugar standards were also subjected to hydrolysis conditions and the peak areas were compared to the peak areas of the non-hydrolyzed standards.

2.2.6.4 Determination of molar mass distribution

Molar mass distributions of the pectin samples were assessed as described by Shpigelman, Kyomugasho, Christiaens, Van Loey, and Hendrickx (2014) in order to ensure that no depolymerization occurred during the demethylesterification step. High-performance size exclusion chromatography (HPSEC) coupled to a refractive index (RI) detector (Shodex RI-101, Showa Denko K.K., Kawasaki, Japan), a multi-angle laser light scattering detector (MALLS) (PN3621, Postnova Analytics, Landsberg am Lech, Germany), diode array detector (Agilent Technologies, Santa Clara, CA, USA) and a viscometer (PN3310, Postnova analytics, Landsberg am Lech, Germany) was used. Pectin samples were dissolved in ultrapure water (0.2% w/v) and heated for 15 min at 65 °C in order to increase the solubilization of the samples before filtration through a 0.45 µm filter. The filtered pectin solutions (100 µL) were injected (in duplicate) onto a series of Waters columns at 35 °C (Waters, Milford, MA, USA), being Ultra hydrogel 250, 1000 and 2000 with exclusion limits of 8×10^4, 4×10^6 and 1×10^7 g/mol, respectively. A 0.1 M acetic acid buffer (pH 4.4) with 0.1 M $NaNO_3$ was used for elution at a flow rate of 0.5 mL/min. The weight average molar mass was then calculated using the Debye fitting method (2nd order) of the software provided by the manufacturer of the MALLS detector and a *dn/dc* value of 0.146 mL/g was used for all samples.

2.2.6.5 Determination of the intrinsic cation concentration

The concentration of intrinsic cations in the pectin samples was measured by inductively coupled plasma mass spectrometry (ICP-MS). Before analysis, pectin samples were incinerated in a muffle furnace at 550 °C for 22 h and further treated as described by Kyomugasho et al. (2015b). The analysis was performed using an Agilent 7700x ICP-MS (Agilent Technologies, Santa Clara, CA, USA). The concentrations of ^{24}Mg, ^{44}Ca, ^{56}Fe and ^{66}Zn were measured in helium mode using ^{72}Ge as an internal standard. The cations were quantified using reference standard solutions with certified concentrations (Kyomugasho et al., 2015b).

2.2.7 Statistical data analysis

The experimental data were statistically analyzed with the software JMP (JMP 13, SAS Institute Inc., Cary, NC, USA). A one-way analysis of variance (ANOVA) and a Tukey HSD test were carried out to analyze significant differences with a 95% confidence interval ($p \leq 0.05$) between the experimental data.

2.3 RESULTS AND DISCUSSION

2.3.1 Degree and pattern of methylesterification of the pectin samples

Starting from the commercial high methylesterified citrus pectin (CP95), tailored pectins with distinct DMs were obtained via enzymatic (P-pectins) or alkaline (C-pectins) demethylesterification. Samples with similar DM but different DB_{abs} were generated, shown in **Table 2.1,** as a consequence of the method of demethylesterification applied. P-pectins exhibit higher estimated DB_{abs} values compared to C-pectins for a given DM, which can be attributed to the blockwise or random removal of methylesters, respectively. Since only limited depolymerization occurred during this demethylesterification (Section 2.3.2 and 2.3.3) and given that the demethylesterification methods generated pectins with different patterns of methylesterification, P- and C-pectin samples with a similar DM were expected to only differ in DB_{abs} (**Table 2.1**). The DB_{abs} is a measure of the percentage of non-methylesterified GalA units present in blocks in the entire pectin population (Guillotin et al., 2005). In other words, a high DB_{abs} implies a high number or long blocks of successive non-methylesterified GalA units. For the commercial high methylesterified citrus pectin sample (CP95) a DB_{abs} of < 0.74% was established as this value corresponds to the detection limit of the method used to obtain experimental DB_{abs} values on which the polynomial functions are based (Ngouémazong et al., 2011). In general, the DB_{abs} was expected to increase with decreasing DM for both P- and C-pectins, indicating a higher number or longer blocks of successive non-methylesterified GalA units at lower DM, since lowering the DM resulted in an increased number of non-methylesterified GalA units (**Table 2.1**). At a given DM, a lower DB_{abs} was estimated for the C-pectins compared to the P-pectins due to the random demethylesterification of the former. In other words, P-pectins showed a higher number or longer blocks of successive non-methylesterified GalA units than the C-pectins.

The estimated DB_{abs} values from this study are comparable with those of other studies (Ström et al., 2007; Tanhatan-Nasseri et al., 2011). Regarding the alkaline demethylesterified pectin samples, the estimated DB_{abs} values in the present study were very similar to DB_{abs} values reported in literature. For instance, the present study estimated DB_{abs} values of 12.3 ± 0.3% and 43.9 ± 0.9% for C-pectins with DMs of 46 and 20%, respectively, whereas alkaline demethylesterified pectin samples of other studies with similar DMs (45 and 20%) were characterized by DB_{abs} values of 16 and 44%, respectively (Ström et al., 2007; Tanhatan-Nasseri et al., 2011). For the majority of the enzymatically demethylesterified pectin samples, the estimated DB_{abs} values

were also comparable with values from studies of Ström et al. (2007) and Tanhatan-Nasseri et al. (2011). These authors observed DB_{abs} values of 27, 29 and 56% for enzymatic (plant PME) demethylesterified pectin samples with DMs of 70, 60 and 40%, respectively, whereas in the present study DB_{abs} values of 20.6 ± 1.0% (P69), 29.0 ± 1.3% (P60) and 49.9 ± 1.0% (P39) were estimated for pectins with similar DMs. Only a few discrepancies were observed, mostly at lower DMs, and these could be attributed to differences in the pectin type or PME sources used (Ngouémazong et al., 2011).

Table 2.1: Structural characteristics ± standard deviation of the commercial high methylesterified citrus pectin (CP95) and demethylesterified pectin samples, with P representing enzymatically demethylesterified pectins and C the alkaline demethylesterified pectins. DM = the degree of methylesterification, DB_{abs} = the estimated absolute degree of blockiness, GalA = the galacturonic acid content, and M_w = the weight average molar mass. Different letters (a-k) indicate significant ($p \leq 0.05$) differences between the pectin samples for a structural characteristic.

Sample code	DM (%)	DB_{abs} (%)	GalA content (g/g pectin)	M_w (kDa)
CP95	95.1 ± 1.8^{a}	$< 0.74^{j}$	0.69 ± 0.01^{d}	56.1 ± 1.3^{ab}
P69	69.4 ± 1.2^{b}	20.6 ± 1.0^{g}	0.72 ± 0.03^{cd}	65.4 ± 7.3^{a}
P60	59.8 ± 1.4^{c}	29.0 ± 1.3^{f}	0.76 ± 0.02^{c}	64.4 ± 3.0^{a}
P39	39.2 ± 0.9^{e}	49.9 ± 1.0^{d}	0.83 ± 0.02^{a}	56.1 ± 2.3^{ab}
P33	33.0 ± 2.1^{g}	57.1 ± 2.5^{c}	0.70 ± 0.03^{d}	61.7 ± 2.4^{a}
P13	13.0 ± 1.3^{j}	82.4 ± 1.7^{a}	0.72 ± 0.03^{cd}	66.2 ± 0.1^{a}
C67	67.1 ± 0.6^{b}	5.1 ± 0.1^{ij}	0.73 ± 0.02^{cd}	45.7 ± 4.1^{bc}
C58	58.3 ± 1.2^{c}	6.8 ± 0.3^{i}	0.76 ± 0.04^{c}	48.1 ± 2.2^{bc}
C46	45.9 ± 0.5^{d}	12.3 ± 0.3^{h}	0.82 ± 0.01^{ab}	42.6 ± 0.1^{c}
C36	35.9 ± 0.7^{f}	20.8 ± 0.8^{g}	0.77 ± 0.04^{bc}	44.3 ± 0.1^{c}
C30	29.9 ± 0.3^{h}	28.1 ± 0.4^{f}	0.76 ± 0.02^{bc}	43.2 ± 0.1^{c}
C20	20.5 ± 0.4^{i}	43.9 ± 0.9^{e}	0.76 ± 0.02^{bc}	41.1 ± 0.4^{c}
C10	10.0 ± 1.4^{k}	68.4 ± 3.8^{b}	0.85 ± 0.03^{a}	38.7 ± 0.8^{c}

2.3.2 GalA content and neutral sugar composition

The GalA content of the pectin samples varied between 0.69 ± 0.01 and 0.85 ± 0.03 g GalA/g pectin (**Table 2.1**). Despite some significant ($p \leq 0.05$) differences in GalA content observed between the pectin samples, the pectin samples were generally considered to contain a similar concentration of GalA units.

Table 2.2: Summary of galacturonic acid content (repeated from Table 2.1) and (pectin-related) neutral sugars (mg/g pectin) ± standard deviation of commercial high methylesterified citrus pectin (CP95) and an enzymatically demethylesterified citrus pectin (P13), with GalA = galacturonic acid, Fuc = fucose, Rha = rhamnose, Ara = arabinose, Gal = galactose, Glu = glucose, Xyl = xylose, Man = mannose and DL = detection limit. The letter 'a' indicates no significant ($p > 0.05$) differences between the pectin samples for a pectin property.

Pectin property	CP95	P13
GalA (mg/g pectin)	688.78 ± 10.08[a]	717.55 ± 30.56[a]
Fuc (mg/g pectin)	0.16 ± 0.01[a]	0.16 ± 0.01[a]
Rha (mg/g pectin)	10.06 ± 0.99[a]	9.15 ± 1.34[a]
Ara (mg/g pectin)	0.40 ± 0.02[a]	0.37 ± 0.03[a]
Gal (mg/g pectin)	45.85 ± 6.03[a]	46.55 ± 2.30[a]
Glu (mg/g pectin)	4.32 ± 0.47[a]	4.12 ± 0.09[a]
Xyl (mg/g pectin)	0.59 ± 0.19[a]	0.59 ± 0.02[a]
Man (mg/g pectin)	< DL	< DL
GalA/(Fuc + Rha + Ara + Gal + Xyl)	11.04 ± 1.19	11.51 ± 0.25
Rha/GalA	0.02 ± 0.01	0.02 ± 0.01
(Ara + Gal)/Rha	4.19 ± 0.13	4.72 ± 0.47

The neutral sugar content was determined for the commercial high methylesterified citrus pectin (CP95) as well as for an enzymatically demethylesterified pectin sample with low DM (P13). The results are presented in **Table 2.2** and revealed no significant differences in neutral sugar content between these two samples. This suggests that no change in sugar composition and concentration occurred during the enzymatic demethylesterification of the pectin. GalA was the most abundant pectin monosaccharide (approximately 70%) compared to neutral sugars which accounted

for only 6%. From the neutral sugar content, it can be concluded that both CP95 and P13 mainly consisted of the linear pectin backbone (HG), evidenced by a high ratio of GalA content to the sum of the concentrations of Fuc, Rha, Ara, Gal and Xyl (approximately 11). This ratio indicates the linearity of the pectin chain (**Table 2.2**) (Houben et al., 2011) and is comparable to the ratio observed for demethylesterified citrus pectin by Kyomugasho et al. (2017), approximately 12. The concentration of Rha was very low compared to the GalA content (ratio of approximately 0.02), which indicates a low contribution of RGI to the pectin population (Houben et al., 2011). Moreover, the degree of branching was low, evidenced by the ratio of Ara and Gal to Rha (approximately 4.5) (Houben et al., 2011). Therefore, only minor influences (if any) of the side chains of the pectin samples on the cation-binding capacity could be hypothesized.

2.3.3 Molar mass distributions

The molar mass distributions and concentration profiles are presented in **Figure 2.1 a** for the P-pectins and in **Figure 2.1 b** for the C-pectins. The concentration profiles are similar for all pectin samples, showing a unimodal distribution, which indicates one pectin population with comparable molar mass. The recovery of the pectin samples varied between 55 and 84%.

Similar molar mass distributions were observed for all demethylesterified pectin samples, with higher molar mass polymers eluting earlier than low molar mass polymers (as seen from the dotted declining lines). The weight average molar masses of the different pectin samples are shown in **Table 2.1** and varied between 44.1 ± 0.4 and 66.2 ± 0.1 kDa. A decrease in molar mass was observed for the C-pectins with decreasing DM, indicating that depolymerization occurred to some extent during the alkaline demethylesterification reaction. However, these differences in molar mass values were generally not considered to clearly influence the cation binding capacity of the pectin samples.

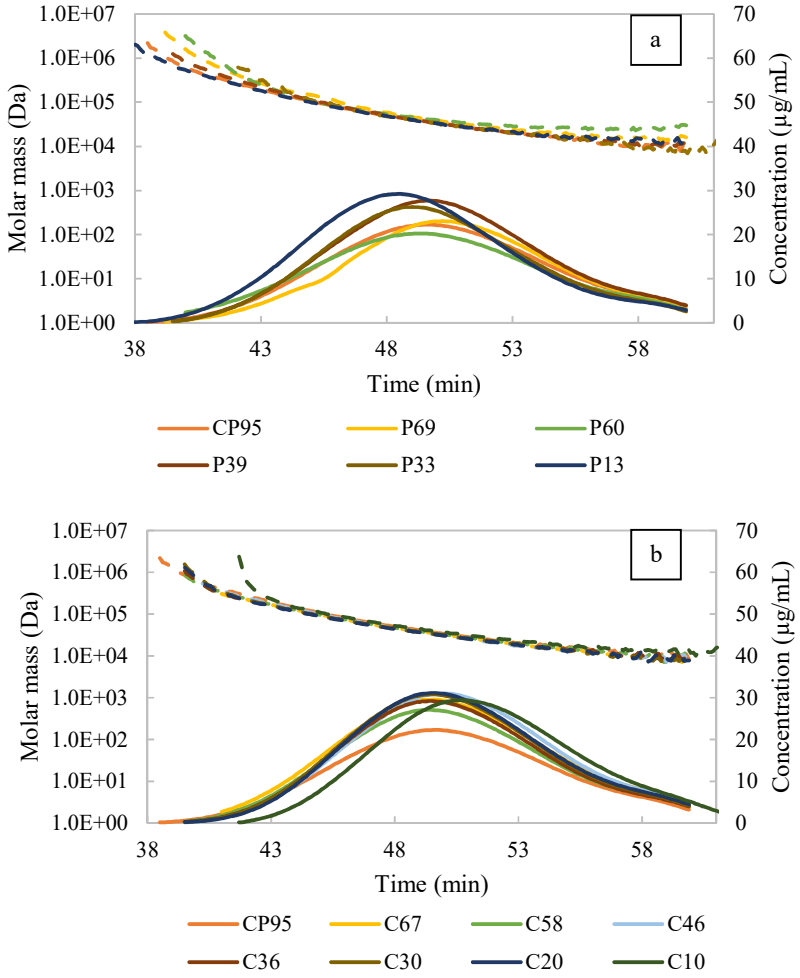

Figure 2.1: Molar mass and concentration profiles of a) enzymatically (P-pectins) and b) alkaline (C-pectins) demethylesterified pectin samples. CP95 refers to the commercial high methylesterified citrus pectin. Dotted lines represent the molar mass (Da) profiles and full lines represent concentration (µg/mL) profiles.

2.3.4 Intrinsic cation concentration of the pectin samples

The intrinsic mineral concentrations of the pectin samples are presented in **Table 2.3**. Na^+ accounts for the largest cation percentages (up to 8%) in all pectin samples, which can be attributed to residual (not removed by dialysis) sodium phosphate buffer (0.1 M) used to maintain optimal pH for enzymatic demethylesterification by PME or sodium hydroxide (0.1 M) used for alkaline demethylesterification.

Table 2.3: Intrinsic mineral content (mg/g pectin) ± standard deviation of the commercial high methylesterified citrus pectin (CP95) and demethylesterified pectin samples, with P representing enzymatically demethylesterified pectins and C the alkaline demethylesterified pectin. DB_{abs} = the estimated absolute degree of blockiness, repeated from Table 2.1. Fe content comprises the sum of Fe^{2+} and Fe^{3+}. Different letters (a-k) indicate significant ($p \leq 0.05$) differences between the pectin samples for a specific mineral (mg/g pectin).

Sample code	DB_{abs} (%)	Na^+ content (mg/g pectin)	Ca^{2+} content (mg/g pectin)	Mg^{2+} content (mg/g pectin)	Zn^{2+} content (mg/g pectin)	Fe content (mg/g pectin)
CP95	$< 0.74^{j}$	19.5 ± 0.2^{k}	2.41 ± 0.01^{de}	0.44 ± 0.01^{cd}	0.04 ± 0.01^{b}	0.02 ± 0.01^{a}
P69	20.6 ± 1.0^{g}	36.2 ± 2.7^{hi}	0.96 ± 0.04^{f}	0.17 ± 0.02^{de}	0.01 ± 0.01^{b}	0.01 ± 0.01^{a}
P60	29.0 ± 1.3^{f}	40.3 ± 1.7^{ghi}	1.15 ± 0.19^{f}	0.20 ± 0.03^{de}	0.04 ± 0.01^{b}	0.03 ± 0.01^{a}
P39	49.9 ± 1.0^{d}	51.1 ± 5.5^{ef}	0.88 ± 0.04^{f}	0.10 ± 0.01^{e}	0.01 ± 0.01^{b}	0.02 ± 0.01^{a}
P33	57.1 ± 2.5^{c}	69.5 ± 0.7^{bc}	1.49 ± 0.41^{ef}	0.22 ± 0.01^{de}	0.03 ± 0.03^{b}	0.02 ± 0.01^{a}
P13	82.4 ± 1.7^{a}	75.4 ± 4.7^{ab}	1.32 ± 0.52^{f}	0.20 ± 0.02^{de}	0.01 ± 0.01^{b}	0.02 ± 0.01^{a}
C67	5.1 ± 0.1^{ij}	25.2 ± 0.4^{jk}	5.13 ± 0.37^{a}	0.90 ± 0.33^{a}	0.02 ± 0.01^{b}	0.06 ± 0.06^{a}
C58	6.8 ± 0.3^{i}	33.9 ± 0.2^{ij}	2.72 ± 0.01^{cd}	0.56 ± 0.03^{bc}	0.02 ± 0.01^{b}	0.01 ± 0.01^{a}
C46	12.3 ± 0.3^{h}	44.3 ± 0.9^{fgh}	1.39 ± 0.20^{ef}	0.13 ± 0.02^{de}	0.03 ± 0.01^{b}	0.01 ± 0.01^{a}
C36	20.8 ± 0.8^{g}	50.4 ± 2.9^{efg}	4.10 ± 0.71^{ab}	0.71 ± 0.01^{abc}	0.03 ± 0.01^{b}	0.09 ± 0.04^{a}
C30	28.1 ± 0.4^{f}	56.4 ± 2.3^{de}	3.71 ± 0.09^{bc}	0.81 ± 0.02^{ab}	0.09 ± 0.01^{a}	0.03 ± 0.03^{a}
C20	43.9 ± 0.9^{e}	65.7 ± 2.6^{cd}	4.37 ± 0.07^{ab}	0.96 ± 0.04^{a}	0.04 ± 0.03^{b}	0.02 ± 0.01^{a}
C10	68.4 ± 3.8^{b}	78.1 ± 2.2^{a}	0.97 ± 0.12^{f}	0.14 ± 0.03^{e}	0.02 ± 0.01^{b}	0.03 ± 0.02^{a}

This difference in Na^+ concentrations possibly indicates differences in ionic strength, with low DM pectins exhibiting a higher ionic strength, given the highest residual Na^+. An increased ionic strength of a pectin solution, enriched with cations, has been reported to decrease the cation-binding capacity of pectin by screening the negative charges on the pectin polymer (Dronnet et al., 1996; Garnier et al., 1994; Renard & Jarvis, 1999). However, results obtained in this doctoral thesis suggest a limited effect of intrinsically present Na^+ on the ionic strength and thus on the cation-binding capacity, as will be clear from the results discussed later (Section 4.2.3). This suggests that the effect of monovalent cations on the binding capacity of pectin is only valid for high concentrations of monovalent cations (~ 1 M or higher).

The intrinsic Ca^{2+}, Zn^{2+}, and Fe^{2+} concentrations of the pectin samples were of particular interest with regard to the cation-binding studies in this doctoral thesis. Ca^{2+} was present in the highest concentrations, 0.88 ± 0.04 - 5.13 ± 0.37 mg Ca^{2+}/g pectin (**Table 2.3**), while Zn^{2+} and iron (sum of Fe^{2+} and Fe^{3+}) were present in clearly lower concentrations, not exceeding 0.09 ± 0.04 mg/g pectin (**Table 2.3**). The concentrations of naturally present Ca^{2+}, Zn^{2+}, and Fe^{2+} were (much) lower than the lowest amount of Ca^{2+}, Zn^{2+}, or Fe^{2+} added in the equilibrium adsorption studies (2-10 times for Ca^{2+}, 100-1000 times for Zn^{2+} and Fe^{2+}) or in the ITC experiments (15-36 times for Zn^{2+}). Therefore, no substantial contribution of the intrinsic cation concentration in the adsorption studies was expected and the observed results of pectin-cation binding capacities could therefore be attributed to the cations added.

2.4 CONCLUSION

Pectin samples with distinct DM and DB_{abs} were successfully generated by enzymatic (P-pectins) or alkaline (C-pectins) demethylesterification of commercial high methylesterified citrus pectin (CP95). In general, pectin characterization revealed similar weight average molar mass, GalA content and (pectin-related) neutral sugars for the different pectin samples, thus suggesting that during the demethylesterification reaction no other substantial structural changes occurred than lowering DM. As a consequence, P- and C-pectins with a given DM only differ in the DB_{abs} value. The pectin samples generated in this chapter were used in subsequent chapters to study the influence of pectin DM and DB_{abs} on the Zn^{2+}-, Ca^{2+}- or Fe^{2+}-binding capacity (Chapter 3, 4 and 5) and associated functionalities, specifically the role in mineral bioaccessibility (Chapter 3) and antioxidant capacity (Chapter 6 and 7).

CHAPTER 3

INFLUENCE OF PECTIN DEGREE AND PATTERN OF METHYLESTERIFICATION ON INTERACTION WITH Zn^{2+} OR Ca^{2+} AND ASSOCIATED Zn^{2+} BIOACCESSIBILITY[3]

3.1 INTRODUCTION

In order to facilitate prediction, control and optimization of pectin functionality, fundamental insight into the pectin-cation interactions as influenced by its structural properties is necessary. In this context, many studies have been performed on the effect of pectin degree and pattern of methylesterification on Ca^{2+}-binding and the associated gelling capacity (Fraeye et al., 2010a; Ngouémazong et al., 2012a; Ström et al., 2007). In addition, strong pectin-cation interactions are also reported to result in a decreased release of essential minerals in the small intestine (Bosscher et al., 2003; Kyomugasho et al., 2017). Therefore, insight into how pectin-Ca^{2+} interaction might be promoted to enhance structure build-up (if desired in some food products) without compromising the essential mineral nutritional value such as Zn^{2+} absorption is required. To the best of our knowledge, there is only one study fundamentally exploring the influence of pectin DM on the maximum Zn^{2+}-binding capacity and interaction energy (Khotimchenko et al., 2008). However, this study did not include

[3] This chapter is based on following paper:
Celus, M., Kyomugasho, C., Salvia-Trujillo, L., Van Audenhove, J., Van Loey, A., Grauwet, T., and Hendrickx, M. (2018). Interactions between citrus pectin and Zn^{2+} or Ca^{2+} and associated *in vitro* Zn^{2+} bioaccessibility as affected by degree of methylesterification and blockiness. *Food Hydrocolloids,* 79: 319-330

the pattern of methylesterification of pectin and associated *in vitro* Zn^{2+} bioaccessibilities. Moreover, scarce information is available on the role of the pectin properties in the interaction with other divalent cations, despite the hypothesized ability of pectin to bind these divalent cations, yielding specific functionalities. Therefore, an in-depth study of the maximum binding capacity and interaction energy of pectins with distinct DMs and DB_{abs} values and Zn^{2+} or Ca^{2+} and its relation with the Zn^{2+} bioaccessibility was strived for in this chapter. Zn^{2+} was chosen as a topic for the bioaccessibility study as it is reported to be an essential mineral which is associated with highly prevalent deficiencies. The objective of this study was achieved by exploration of the adsorption of Zn^{2+}- and Ca^{2+} -ions to targeted modified citrus pectins, with distinct degree and pattern of methylesterification as produced in Chapter 2. The Zn^{2+}- and Ca^{2+}-binding was studied by spectrophotometric determination of the equilibrium adsorption isotherm. Subsequently, the associated *in vitro* Zn^{2+} bioaccessibilities were explored which were then linked with the cation-binding capacity of the pectins.

3.2 MATERIALS AND METHODS

3.2.1 Materials

The pectin samples with different degrees and patterns of methylesterification, as produced and structurally characterized in Chapter 2, were used to study the interaction with Zn^{2+} or Ca^{2+} and associated role in mineral bioaccessibility. Particularly, commercial high methylesterified citrus pectin (CP95), enzymatically demethylesterified (P69, P60, P39, P33, and P13) and alkaline demethylesterified (C67, C58, C46, C36, C30, and C20) pectin samples were used for determination of the adsorption isotherms, while CP95, P60, P33, and C36 were included in the bioaccessibility study. All chemicals used were of analytical grade. Ultrapure water (organic free, 18.2 MΩ cm resistance) used for the adsorption as well as analytical experiments was supplied by a Simplicity™ water purification system (Millipore, Burlington, MA, USA).

3.2.2 Determination of adsorption isotherms of pectin for Zn^{2+} and Ca^{2+}

Adsorption isotherms of Zn^{2+} or Ca^{2+} to pectin with distinct DM and DB_{abs} values were determined to assess the effect of these structural properties on the cation-binding capacity pectin. The adsorption equilibrium studies with Zn^{2+} or Ca^{2+} were performed based on the method of Debon and Tester (2001). Therefore, 10 mL of a 0.1% (w/v) pectin solution, enriched with 0-200 mg/L of Zn^{2+} ($ZnSO_4.7H_2O$) or Ca^{2+} ($CaCl_2.2H_2O$), was transferred into rinsed dialysis membranes (Spectra/Por®, MWCO

= 3.5 kDa) and subsequently dialyzed against 50 mL of ultrapure water for 48 h at 15 °C until equilibration of the non-bound cations inside and outside the membrane. The concentration of 0.1% (w/v) pectin was selected as this is a concentration at which pectin exhibits a certain cation binding capacity without substantially increasing the viscosity of the solution. The period of 48 h was determined in a series of preliminary experiments analyzing the cation concentration as a function of time. The pH of the pectins solutions was at least one log unit above the pKa value of pectin (2.9-4.1). Afterwards, the concentration of cations in the solution outside the membrane was measured spectrophotometrically. On the one hand, Zn^{2+} determination was performed as described by Platte and Marcy (1959) with some minor modifications. A 0.2 mL aliquot of the solution outside the membrane was mixed with 0.1 mL of 0.5 M borate buffer (pH 9) followed by addition of 0.06 mL of 0.0028 M zincon and the volume was adjusted to 1 mL with ultrapure water. After 5 min, the absorbance was measured at 620 nm (1800 UV spectrophotometer, Shimadzu, Kyoto, Japan). On the other hand, the Ca^{2+} concentration of the solution outside the membrane was measured using a Spectroquant® Calcium Test (Merck KGaA, Darmstadt, Germany). To a 1 mL aliquot of the solution outside the membrane, 0.1 mL of 8-hydroxyquinoline was added to prevent interferences by Mg^{2+} or Fe^{2+}, followed by 0.1 mL of color reagent (a phthalein derivative) and the absorbance was measured at 565 nm after a 5 min reaction period (1800 UV spectrophotometer, Shimadzu, Kyoto, Japan). For both Zn^{2+} and Ca^{2+}, the analyses were performed in triplicate and the cation concentration was quantified using a standard curve of $ZnSO_4.7H_2O$ (0-20 mg Zn^{2+}/L) or $CaCl_2.2H_2O$ (0-4 mg Ca^{2+}/L), respectively. The binding capacity (q_e) of the pectin samples for the different cations was then estimated based on the difference between the initial cation concentration and the cation concentration measured after equilibrium and calculated as follows (Khotimchenko et al., 2008):

$$q_e = \frac{C_0 \cdot V_{in} - C_e \cdot (V_{in} + V_{out})}{M_w \cdot n_{GalA}} \quad [3.1]$$

In this equation, q_e (mol Zn^{2+} or Ca^{2+}/mol GalA) is the equilibrium binding capacity of the pectin sample, which can also be expressed as mol cation/mol COO^-, by taking into account the DM of the pectin sample. C_0 is the initial cation concentration (g/L), C_e, the cation concentration at equilibrium (g/L), V_{in} and V_{out}, the volume inside (0.01 L) and outside (0.05 L) the dialysis membrane, respectively while M_w and n_{GalA} represent the cation atomic weight (65.38 g/mol for Zn^{2+} and 40.078 g/mol for Ca^{2+}) and absolute amount of GalA units in the pectin sample (mol), respectively.

By plotting q_e as a function of the cation concentration at equilibrium (C_e), adsorption isotherms of the pectin samples were obtained, which can be quantitatively described by several empirical models such as the Langmuir, Freundlich, Brunauer-Emmett-Teller (BET), BiLangmuir, or Redlich-Peterson adsorption isotherm (Foo & Hameed, 2010; Ho, Huang, & Huang, 2002; Khotimchenko et al., 2008; Zhao, Repo, Yin, & Sillanpää, 2013). Such isotherms are typically characterized by certain parameters, which indicate surface properties of the adsorbent and the adsorption affinity (Ho et al., 2002). The Langmuir isotherm is the most widely used adsorption isotherm (Limousin et al., 2007) and has been successfully used before to describe the interaction between pectin and Zn^{2+} (Khotimchenko et al., 2008). The Langmuir isotherm assumes monolayer adsorption at homogenous and finite binding sites within the pectin chain and is represented as (Foo & Hameed, 2010; Ho et al., 2002; Khotimchenko et al., 2008; Zhao et al., 2013):

$$q_e = \frac{q_{max} \cdot K_L \cdot C_e}{1+K_L \cdot C_e} \quad [3.2]$$

with q_{max} (mol cation/mol GalA or mol cation/mol COO^-), the maximum binding capacity at the monolayer, q_e, the binding capacity of a GalA or COO^- unit (mol cation/mol GalA or mol cation/mol COO^-) at a certain cation equilibrium concentration, K_L, the Langmuir constant (L/mmol cation), which is a measure of the interaction energy and C_e, the cation equilibrium concentration (mmol cation/L).

The modeling of the experimental data of the pectin samples by the Langmuir adsorption model was carried out with a non-linear one step regression (SAS version 9.4, Cary, NC, USA).

3.2.3 *In vitro* simulated digestion of Zn^{2+}-enriched pectin samples

To study the effect of pectin DM and DB_{abs} (and associated cation-binding capacities and interaction energies) on Zn^{2+} bioaccessibility, a simplified standardized static *in vitro* digestion method was performed. The method involved simulations of the gastric and small intestinal phase (Minekus et al., 2014). First, a 0.4% (w/v) pectin solution was adjusted to pH 3 using 2 M HCl followed by enrichment with different amounts of a 0.6 M $ZnSO_4$ stock solution to obtain a 0.1% (w/v) pectin concentration and 0.3 mM, 1 mM or 3 mM Zn^{2+} in the final digest. These Zn^{2+} concentrations were selected to represent different phases of the adsorption curves. The gastric and the small intestinal phase were subsequently simulated according to the procedure of Minekus et al. (2014) with some modifications and without the use of simulated gastric or intestinal fluids, in order to avoid contributions of the minerals present in such fluids

to the Zn^{2+}-binding capacity of pectin. The gastric phase (pH 3) consisted of addition of pepsin (2000 U/mL), followed by end-over-end rotation at 37 °C for 2 h. During the small intestinal phase, the pH was increased to 7 with 1 M NaOH, bile salts (10 mM) and pancreatin (2000 U/mL) were added and the mixture was rotated end-over-end for 2 h at 37 °C. The *in vitro* digestion of the Zn^{2+}-enriched pectin solutions was performed in presence (final concentrations of 0.3375 mM Ca^{2+}) and absence of $CaCl_2$ during digestion to study the possible competition between Zn^{2+} and Ca^{2+} for binding to pectin.

After the intestinal phase, the final digest (10 mL) was transferred into rinsed dialysis membranes (Spectra/Por®, MWCO = 3.5 kDa) and dialyzed against ultrapure water (1:5 v/v) for 64 h followed by spectrophotometric determination of the Zn^{2+} concentration in the dialysis water as described in Section 3.2.2. The bioaccessibility was established as the percentage ratio of amount of free Zn^{2+} to the total initial amount of Zn^{2+} added to the pectin sample (Grundy et al., 2016; Kyomugasho et al., 2017; Parada & Aguilera, 2007).

3.2.4 Statistical data analysis

The experimental data were statistically analyzed with the software JMP (JMP 13, SAS Institute Inc., Cary, NC, USA). A one-way analysis of variance (ANOVA) and a Tukey HSD test were carried out to analyze significant differences with a 95% confidence interval ($p \leq 0.05$) between the experimental data.

3.3 RESULTS AND DISCUSSION

3.3.1 Adsorption isotherms of pectin samples for Zn^{2+} or Ca^{2+} in general

To study the influence of pectin DM and DB_{abs} on Zn^{2+}- or Ca^{2+}-binding capacities, adsorption isotherms of these cations to P- and C-pectins were generated. The adsorption isotherms display the pectin binding capacity q_e (mol cation/mol GalA) as a function of the equilibrium cation concentration C_e (mmol cation/L) (**Figure 3.1**). During the adsorption experiments, the pH was at least one log unit higher than pKa of pectin (2.9-4.1) in order to facilitate ionization of the carboxyl groups of non-methylesterified GalA units, thereby promoting the electrostatic interactions with divalent cations.

For both Zn^{2+} and Ca^{2+}, the experimental data of the pectin binding capacities were well described by the Langmuir adsorption model ($R^2_{adjusted} > 0.98$, results not shown), implying an increase in binding capacity with increasing equilibrium cation concentration until a plateau was reached. As the Langmuir adsorption model was successfully used to fit the experimental data, samples can be considered to contain a limited number of homogeneous binding sites, with pectin-cation interactions occurring via monolayer adsorption with a constant adsorption energy distribution (Foo & Hameed, 2010).

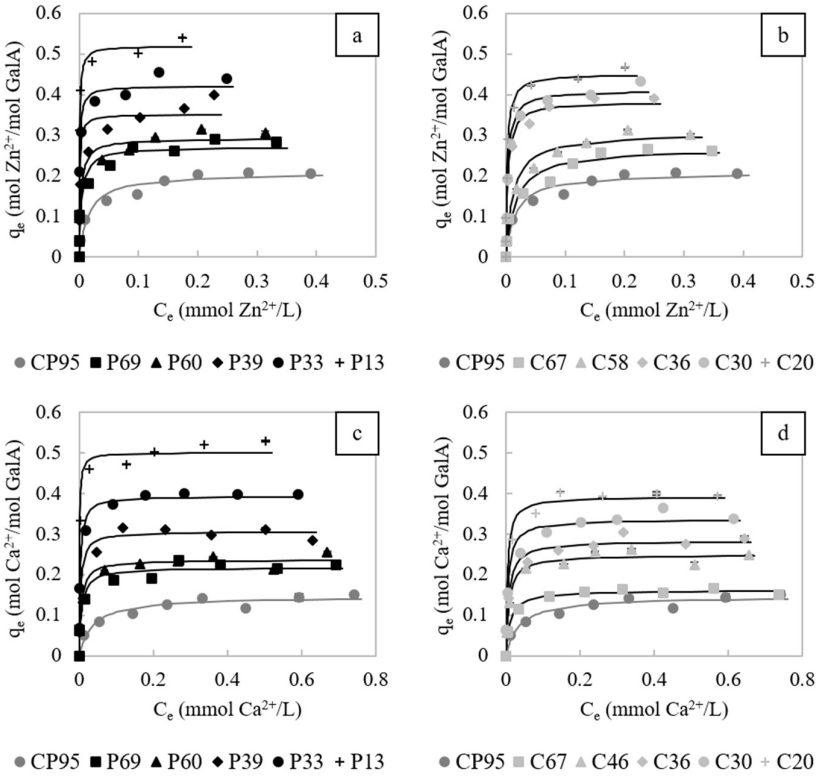

Figure 3.1: Adsorption isotherms representing the equilibrium cation binding capacity, q_e (mol cation/mol GalA) as a function of the cation equilibrium concentration, C_e (mmol/L), for a) Zn^{2+} to P-pectins, b) Zn^{2+} to C-pectins , c) Ca^{2+} to P-pectins, and d) Ca^{2+} to C-pectins. P-pectins represent enzymatically demethylesterified pectins (black symbols), C-pectins the alkaline demethylesterified pectins (grey symbols) while CP95 refers to the commercial high methylesterified citrus pectin (dark grey symbols). Symbols indicate the experimental data with standard deviation. Black and dark grey curves are modeled Langmuir adsorption isotherms.

The Langmuir adsorption model is typically characterized by two parameters; the maximum binding capacity, q_{max}, which is represented by the plateau of the adsorption isotherm and the Langmuir constant, K_L (L/mmol cation), which is a measure for the pectin-cation interaction energy (Khotimchenko et al., 2008). On the one hand, when the maximum binding capacity of pectin is reached, the binding sites are saturated and no further binding occurs (Foo & Hameed, 2010). In the present study, the maximum binding capacity is expressed as mol cation/mol GalA or as mol cation/mol COO^-, indicated as q^G_{max} or q^C_{max}, respectively. On the other hand, an increase of the K_L value is related with a steeper ascending part of the adsorption isotherm, indicating stronger pectin-cation interaction (Zhao et al., 2013). These estimated parameters (q^G_{max}, q^C_{max} and K_L) are shown in **Table 3.1** for each pectin sample and for both Zn^{2+}- and Ca^{2+}-binding.

3.3.2 Influence of pectin DM and DB_{abs} on the maximum Zn^{2+}- or Ca^{2+}-binding capacity

3.3.2.1 q^G_{max} values

To obtain better insight into the extent to which DM and DB_{abs} influence the pectin-cation interactions, the q^G_{max} values (mol cation/mol GalA) of the P- and C-pectins in **Table 3.1** are plotted as a function of the DM (%) and estimated DB_{abs} (%) of pectin, with **Figure 3.2 a** and **b** showing Zn^{2+}-binding and **Figure 3.2 c** and **d** Ca^{2+}-binding. As presented in **Figure 3.2** and **Table 3.1**, the maximum binding capacities (mol cation/mol GalA, q^G_{max}) of both P- and C-pectins for Zn^{2+} and Ca^{2+}, increased with decreasing DM as well as increasing DB_{abs}. This implies that a higher maximum amount of cations was bound to the pectin sample as the number of negatively chargeable carboxyl groups increased (decreasing DM) or when more blockwise distributions of carboxyl groups were present (increasing DB_{abs}) within the pectin HG chain. For instance, the commercial high methylesterified citrus pectin sample (which exhibited the highest DM, CP95) was shown to bind 0.208 ± 0.005 mol Zn^{2+}/mol GalA or 0.147 ± 0.004 mol Ca^{2+}/mol GalA whereas pectin samples with the lowest DMs, P13 and C20, bound 0.520 ± 0.015 and 0.450 ± 0.012 mol Zn^{2+}/mol GalA or 0.501 ± 0.007 and 0.393 ± 0.005 mol Ca^{2+}/mol GalA, respectively. Furthermore, q^G_{max} values increased with increasing DB_{abs} up to the highest DB_{abs} explored in this study (82.4 ± 1.7%) (**Figure 3.2**), which can be attributed to the presence of a higher number or longer blocks of successive negatively chargeable GalA units.

Table 3.1: Parameter estimates ± standard deviation for Langmuir adsorption model-based isotherms of Zn^{2+}- or Ca^{2+}-binding to the commercial high methylesterified citrus pectin (CP95) and demethylesterified pectin samples, with P representing enzymatically demethylesterified pectins and C the alkaline demethylesterified pectins. DB_{abs} (%) is the estimated absolute degree of blockiness repeated from Table 2.1, q^{G}_{max} and q^{C}_{max} are the maximum cation-binding capacities, expressed as mol cation/mol GalA and mol cation/mol COO^-, respectively, and K_L (L/mmol cation) represents the interaction energy. Different capital letters (A-B) indicate significant differences ($p \leq 0.05$) in q^{G}_{max}, q^{C}_{max} or K_L values between $Zn^{2+}$and Ca^{2+} of the same pectin sample. Different lower case letters (a-i) indicate significant differences ($p \leq 0.05$) in DB_{abs} and q^{G}_{max}, q^{C}_{max} or K_L between different pectin samples for a particular cation (Zn^{2+}- or Ca^{2+}-binding). nd. = not determined.

Sample code	DB_{abs} (%)	q^{G}_{max} (mol Zn^{2+}/mol GalA)	q^{C}_{max} (mol Zn^{2+}/mol COO^-)	K_L (L/mmol Zn^{2+})	q^{G}_{max} (mol Ca^{2+}/mol GalA)	q^{C}_{max} (mol Ca^{2+}/mol COO^-)	K_L (L/mmol Ca^{2+})
CP95	$< 0.74^{i}$	0.208 ± 0.005^{Ah}	4.238 ± 0.111^{Aa}	63 ± 10^{Ac}	0.147 ± 0.004^{Bi}	2.990 ± 0.087^{Ba}	28 ± 5^{Bf}
P69	20.6 ± 1.0^{f}	0.271 ± 0.007^{Afg}	0.886 ± 0.023^{Ab}	251 ± 53^{Ab}	0.218 ± 0.005^{Bg}	0.712 ± 0.015^{Bb}	156 ± 32^{Acde}
P60	29.0 ± 1.3^{e}	0.292 ± 0.007^{Afg}	0.726 ± 0.017^{Bd}	336 ± 59^{Ab}	0.237 ± 0.004^{Bf}	0.589 ± 0.010^{Bc}	186 ± 30^{Acd}
P39	49.9 ± 1.0^{c}	0.351 ± 0.011^{Ae}	0.578 ± 0.019^{Ae}	1125 ± 240^{Aa}	0.307 ± 0.004^{Bd}	0.505 ± 0.007^{Bd}	263 ± 28^{Bbc}
P33	57.1 ± 2.5^{b}	0.420 ± 0.013^{Abcd}	0.627 ± 0.020^{Ae}	1058 ± 201^{Aa}	0.394 ± 0.005^{Ab}	0.588 ± 0.008^{Ac}	348 ± 35^{Bb}
P13	82.4 ± 1.7^{a}	0.520 ± 0.015^{Aa}	0.597 ± 0.018^{Ae}	1329 ± 174^{Aa}	0.501 ± 0.007^{Aa}	0.576 ± 0.008^{Ac}	1035 ± 110^{Aa}
C67	5.1 ± 0.1^{h}	0.268 ± 0.008^{Ag}	0.813 ± 0.025^{Abc}	62 ± 11^{Ac}	0.162 ± 0.002^{Bh}	0.493 ± 0.005^{Bd}	91 ± 8^{Ae}
C58	6.8 ± 0.3^{h}	0.305 ± 0.010^{f}	0.731 ± 0.023^{cd}	85 ± 16^{c}	nd.	nd.	nd.
C46	12.3 ± 0.3^{g}	nd.	nd.	nd.	0.249 ± 0.004^{f}	0.461 ± 0.008^{ef}	126 ± 17^{de}
C36	20.8 ± 0.8^{f}	0.382 ± 0.007^{Ade}	0.596 ± 0.011^{Ae}	314 ± 33^{Ab}	0.284 ± 0.005^{Be}	0.443 ± 0.008^{Bf}	135 ± 19^{Bde}
C30	28.1 ± 0.4^{e}	0.410 ± 0.006^{Ac}	0.585 ± 0.008^{Ae}	341 ± 26^{Ab}	0.337 ± 0.006^{Bc}	0.480 ± 0.008^{Bde}	183 ± 26^{Bcd}
C20	43.9 ± 0.9^{d}	0.450 ± 0.012^{Ab}	0.567 ± 0.015^{Ae}	481 ± 62^{Ab}	0.393 ± 0.005^{Bb}	0.494 ± 0.007^{Bd}	247 ± 25^{Bbc}

Similarly, other researchers reported an increased binding capacity for Zn^{2+} as the DM of citrus pectin decreased (Khotimchenko et al., 2008). In addition, comparable Zn^{2+}-binding capacities were established for demethylesterified citrus pectins of a given DM, based on the results of Khotimchenko et al. (2008). For instance, the reported maximum binding capacities in this study of 0.31, 0.38 and 0.45 mol Zn^{2+}/mol GalA for alkaline demethylesterified citrus pectins with DMs of 58, 36 and 20%, respectively, are in line with the results of Khotimchenko et al. (2008), being 0.26, 0.30 and 0.43 mol Zn^{2+}/mol GalA for alkaline demethylesterified citrus pectins with DMs of 60, 40 and 19%, respectively (**Table 1.2**). In the case of Ca^{2+}, a comparable maximum Ca^{2+}-binding capacity (~ 0.4 mol Ca^{2+}/mol GalA) for enzymatically demethylesterified citrus pectin with a DM around 33% has for instance been reported by Kyomugasho et al. (2018) as shown in **Table 1.2**.

From **Figure 3.2 a** and **Table 3.1**, it can be seen that P- and C-pectins with a similar DM exhibited comparable q^G_{max} values for Zn^{2+}, as for instance P69 and C67 were shown to maximally bind 0.271 ± 0.007 and 0.268 ± 0.008 mol Zn^{2+}/mol GalA, respectively. Given that no significant differences ($p > 0.05$) in maximum Zn^{2+}-binding capacities were generally observed between P- and C- pectins of a given DM, it was concluded that the maximum amount of Zn^{2+} bound to pectin is largely determined by the number of methylesterified GalA units (DM) rather than their distribution along the HG chain (DB_{abs}). With regard to Ca^{2+}-binding, significant ($p \leq 0.05$) differences in q^G_{max} values were observed between P- and C-pectins with similar DMs (**Figure 3.2 c** and **Table 3.1**), with P-pectins showing higher values, which could be attributed to their higher DB_{abs} values at a given DM. As such, in the case of Ca^{2+}, both DM and DB_{abs} influenced the maximum binding capacity. Nevertheless, smaller differences in q^G_{max} values were observed between samples with a similar DM (**Figure 3.2 c)** compared to samples with a similar DB_{abs} (**Figure 3.2 d**). For instance P60 and C30, which exhibited comparable estimated DB_{abs} values of 29.0 ± 1.3% and 28.1 ± 0.4%, respectively, bound 0.237 ± 0.004 and 0.337 ± 0.006 mol Ca^{2+}/mol GalA. The higher q^G_{max} values observed for the C-pectins compared to P-pectins with similar DB_{abs} could be related to the lower DM of the former, as more negative charges of the C-pectins (more non-methylesterified carboxyl groups) could attract more Ca^{2+}. It can therefore be concluded that for both Zn^{2+}- and Ca^{2+}-binding, the maximum binding capacity (q^G_{max}) is mainly influenced by the number of non-methylesterified GalA units (DM) and to a lesser extent by their distribution pattern (DB_{abs}).

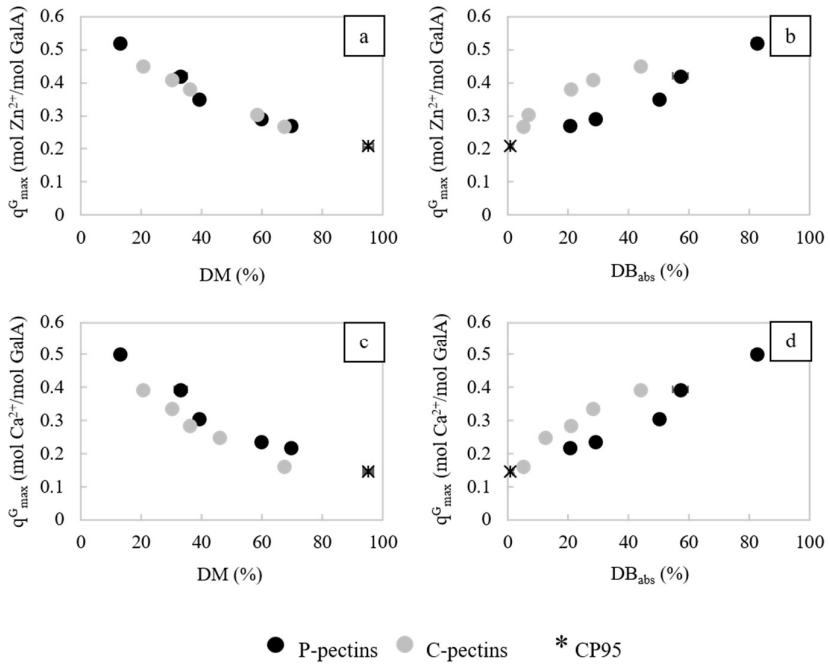

Figure 3.2: Estimated maximum binding capacity, q^G_{max} (mol cation/mol GalA) with standard deviation as a function of DM (%) and estimated DB_{abs} (%) with standard deviation of enzymatically (P-pectins, black) and alkaline (C-pectins, grey) demethylesterified pectins, and commercial high methylesterified citrus pectin (CP95, black asterisk) for Zn^{2+}-binding (a and b) and for Ca^{2+}-binding (c and d) as determined by equilibrium adsorption experiments.

3.3.2.2 q^C_{max} values

To obtain more information on the role of the non-methylesterified groups in cation binding, the estimated maximum binding capacities were expressed as mol cation/mol COO^- (q^C_{max}) (**Table 3.1**), which is a measure of the number of moles of a specific cation bound to each mole of negatively charged carboxyl group (COO^-). Contrary to q^G_{max} (mol cation/mol GalA), the former takes into account the DM of the pectin sample. The q^C_{max} values of P- and C-pectins for Zn^{2+}- or Ca^{2+}-binding are displayed in **Figure 3.3** as a function of the DM (%) and estimated DB_{abs} (%). The commercial high methylesterified citrus pectin (CP95) exhibited exceptional high values of 4.238 ± 0.111 mol Zn^{2+}/mol COO^- and 2.990 ± 0.087 mol Ca^{2+}/mol COO^-, which can be attributed to binding of cations to other functional groups of pectin (e.g., OH^-) in addition to COO^- (which are only 5% of the GalA in the case of CP95). Although the other pectin samples (lower DMs) also contain these functional groups (such as OH^-), the COO^- groups probably showed a higher affinity for ionic interactions,

forming stronger interactions and destabilizing the weaker ones (for instance with OH^-). The q^C_{max} values of CP95 are removed from **Figure 3.3** to better visualize the differences between P- and C-pectins for Zn^{2+} or Ca^{2+}.

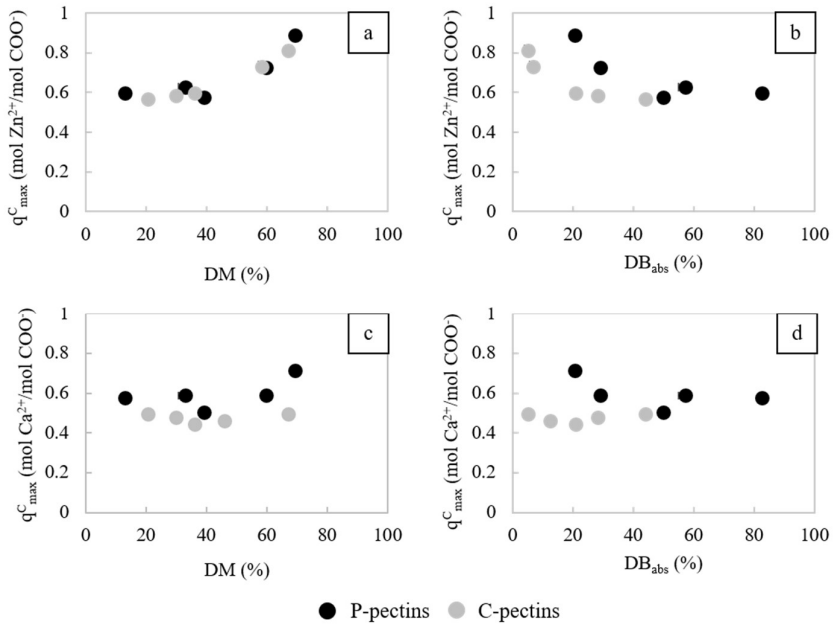

Figure 3.3: Estimated maximum binding capacity, q^C_{max} (mol cation/mol COO^-) with standard deviation as a function of DM (%) and estimated DB_{abs} (%) with standard deviation of enzymatically (P-pectins, black) and alkaline (C-pectins, grey) demethylesterified pectins for Zn^{2+}-binding (a and b) and for Ca^{2+}-binding (c and d) as determined by equilibrium adsorption experiments.

The interaction between Zn^{2+} and P- or C-pectins of a given DM resulted in similar q^C_{max} values as illustrated in **Figure 3.3 a**, indicating that the distributions of non-methylesterified GalA units did not influence the amount of Zn^{2+} bound. For a given DB_{abs} value, P-pectins showed significantly ($p \leq 0.05$) higher q^C_{max} values compared to C-pectins (**Figure 3.3 b**) with for instance P69 (DB_{abs} = 20.6 ± 1.0%) bound 0.886 ± 0.023 mol Zn^{2+}/mol COO^-, while C36 (DB_{abs} = 20.8 ± 0.8%) bound 0.596 ± 0.11. This can be explained by the lower number of negatively charged carboxyl groups in the P-pectins compared to C-pectins with a similar DB_{abs}, resulting in higher q^C_{max} values. Furthermore, the q^C_{max} values of both P- and C- pectins decreased with decreasing DM or increasing DB_{abs} (**Figure 3.3 a** and **b**), approaching 0.5 mol Zn^{2+}/mol COO^- for DMs < 40%. This observation indicates that pectins with a DM higher than 40% were probably mainly interacting with Zn^{2+} via monocomplexation (through COO^-) as well

as through other functional groups, such as hydroxyl groups as proposed by Assifaoui et al. (2015). In an ideal situation of dimerization that assumes the egg-box of cation binding, the q^{C}_{max} should be approximately between 0.25 and 0.55 mol cation/mol COO^- for complete neutralization of the pectin carboxylate groups (Fang et al., 2009; Ngouémazong, Jolie, et al., 2012). It can therefore be concluded that as the DM decreased below 40%, the mechanism of Zn^{2+}-binding to pectin probably approached the egg-box model binding as described for Ca^{2+} (Grant et al., 1973), implying more dominant binding between carboxylate groups and Zn^{2+} and possibly destabilization of the weaker interactions (e.g., cation-OH^- interactions).

Interaction between pectin and Ca^{2+} showed significantly lower q^{C}_{max} values for both P- and C-pectins compared to Zn^{2+}-binding (**Table 3.1** and **Figure 3.3 c** and **d**). This observation is in accordance with the findings of Dronnet et al. (1996) who also reported that the carboxylate groups of an alkaline demethylesterified citrus pectin of DM 54% bound lower amounts of Ca^{2+} than Zn^{2+}, with values of approximately 0.5 mol Ca^{2+}/mol COO^- compared to 0.8 mol Zn^{2+}/mol COO^-. In the current study, the lower q^{C}_{max} values for Ca^{2+} compared to Zn^{2+} were more pronounced for C-pectins, which exhibited comparable q^{C}_{max} values, approximating 0.5 mol Ca^{2+}/mol COO^-, while 0.576-0.712 mol Ca^{2+}/mol COO^- were observed for P-pectins (**Table 3.1**). As such, the q^{C}_{max} values of P-pectins for Ca^{2+} were significantly higher than those of C-pectins, suggesting that Ca^{2+} interaction with C-pectins was mainly restricted to binding via COO^-. In analogy with Zn^{2+}-binding, P-pectins exhibited decreasing q^{C}_{max} values for Ca^{2+}-binding with decreasing DM (**Figure 3.3 c**) or increasing DB_{abs} (**Figure 3.3 d**). This possibly implies Ca^{2+}-binding to P-pectins via monocomplexation (with COO^-) as well as via other functional groups such as hydroxyl groups for pectins with high DM (> 40%) while for low DM pectin (< 40%), binding becomes restricted to COO^- groups (dimerization). Considering that in general decreasing DM (or increasing DB_{abs}) led to dimerization of the pectin chains in presence of Zn^{2+} or Ca^{2+} ions, it can be concluded that a certain DB_{abs} is required for binding via the egg-box model. Moreover, the hydrated atomic radii of both cations are comparable (0.40-0.43 and 0.41-0.42 nm for Zn^{2+} and Ca^{2+}, respectively) (Tansel, 2012), assuming that both cations could fit into the fixed size of the egg-box model.

3.3.3 Influence of pectin DM and DB_{abs} on interaction energy between pectin and Zn^{2+} or Ca^{2+}

The interaction energy between the pectin samples and Zn^{2+} or Ca^{2+} is expressed as K_L, the Langmuir constant (L/mmol cation) as presented in **Table 3.1** and **Figure 3.4**. Increasing K_L values are related to stronger pectin-cation interactions. For both Zn^{2+} (**Figure 3.4 a** and **b**) and Ca^{2+} (**Figure 3.4 c** and **d**), K_L increased with decreasing DM and increasing estimated DB_{abs}, with the latter showing a larger influence. This evidences stronger pectin-cation interactions when a higher number of negatively chargeable carboxyl groups (decreasing DM) as well as more consecutive non-methylesterified GalA units (increasing DB_{abs}) were present within the pectin HG chain. For Zn^{2+} (**Figure 3.4 a**), an increase in K_L values was observed for P-pectins until a DB_{abs} of 49.9% was reached, after which no further significant increase occurred. The same trend was observed for the C-pectins, with an increase until a DB_{abs} of 20.8%, where after K_L did not increase significantly (**Table 3.1**). However, clearly lower absolute K_L values were found compared to P-pectins. In analogy, for Ca^{2+} (**Figure 3.4 d**) a sharp increase in K_L occurred for the P-pectins beyond a DB_{abs} of 57.1%. For C-pectins, K_L increased up to the highest DB_{abs} (43.9%) without a sharp increase as described for the P-pectins. Nevertheless, the binding of Ca^{2+} (and Zn^{2+}) to C-pectins was not explored beyond a DB_{abs} 44% and it is hypothesized that beyond a DB_{abs} of 57.1%, the C-pectins might exhibit a similar trend as the P-pectins. This observation indicates that gradually stronger interactions between pectin and Zn^{2+} or Ca^{2+} were exhibited with increasing DB_{abs} until a certain DB_{abs} value was reached, after which no significantly stronger interactions occurred. This observation is in accordance with the anti-cooperative binding between pectin in water (ion-free) and cations such as Zn^{2+} and Ca^{2+} as described by Garnier et al. (1994) and Dronnet et al. (1996), respectively. Anti-cooperativity between pectin (with only one type of binding sites as assumed by the Langmuir model) and a cation implies a decreased affinity of the cation for pectin as the binding proceeds (Garnier et al., 1994; Renard & Jarvis, 1999). The pectin-cation interaction decreases the electrostatic potential, resulting in less and less favorable interaction.

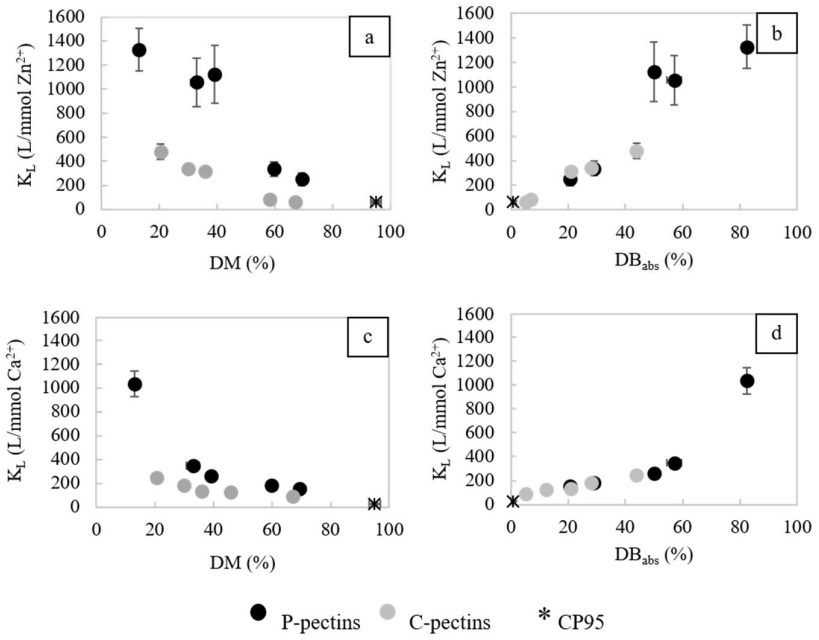

Figure 3.4: Estimated interaction energy, K_L (L/mmol cation) with standard deviation as a function of DM (%) and estimated DB_{abs} (%) with standard deviation of enzymatically (P-pectins, black) and alkaline (C-pectins, grey) demethylesterified pectins, and commercial high methylesterified citrus pectin (CP95, black asterisk) for Zn^{2+}-binding (a and b) and Ca^{2+}-binding (c and d) as determined by equilibrium adsorption experiments.

For both Zn^{2+}- and Ca^{2+}-binding, no significant ($p > 0.05$) differences in interaction energies were observed between P- and C-pectins with a similar DB_{abs} (**Figure 3.4 b** and **d,** and **Table 3.1**). For instance, at a given DB_{abs}, P69 (DB_{abs} of 20.6 ± 1.0%) and C36 (DB_{abs} of 20.8 ± 0.8%) exhibited comparable K_L values of 251 ± 53 and 314 ± 33 L/mmol Zn^{2+} or 156 ± 32 and 135 ± 19 L/mmol Ca^{2+}, respectively. By contrast, at a given DM, P-pectins showed significantly ($p \leq 0.05$) higher K_L values compared to C-pectins, with for instance P60 and C58 possessing K_L values of 336 ± 59 and 85 ± 16 L/mmol Zn^{2+}, respectively. This could be related to the higher DB_{abs} values of P-pectins, implying stronger pectin-cation interactions for pectins with a higher number or longer blocks of successive negatively chargeable groups, as mentioned earlier. In conclusion, the absolute degree of blockiness largely influenced the interaction energy, due to formation of more stable cross-links as suggested by Ngouémazong et al. (2012c). At a given DB_{abs} value, the degree of methylesterification (DM) did not play a significant role in determining the pectin-cation interaction energy.

3.3.4 Influence of cation type (Zn^{2+} or Ca^{2+}) on interactions with pectin

This section describes the differences between pectin-Zn^{2+} and pectin-Ca^{2+} interactions based on the estimated parameters of the adsorption isotherms, as presented in **Table 3.1**. For the majority of the pectin samples, the maximum binding capacities (q^G_{max}) of pectin for Zn^{2+} were significantly ($p \leq 0.05$) higher than for Ca^{2+}. This may be explained by the ability of Zn^{2+} to bind to OH^- groups, in addition to COO^- groups of the pectin HG chain, whereas Ca^{2+} is reported to only interact via carboxylate groups (Assifaoui et al., 2015). Nevertheless, the interaction between Zn^{2+} and COO^- groups are believed to be stronger compared to binding to OH^- groups. However, no significant differences were observed between the q^G_{max} of the very low DM or high DB_{abs} P-pectin samples (P33 and P13) for Zn^{2+} and Ca^{2+}. Values of 0.420 ± 0.013 mol Zn^{2+}/mol GalA and 0.394 ± 0.005 mol Ca^{2+}/mol GalA were exhibited by P33 while P13 showed 0.520 ± 0.015 and 0.501 ± 0.007, indicating that beyond a certain DB_{abs} (57.1%), there is no significant difference in moles of Zn^{2+} or Ca^{2+} bound to pectin.

With regard to the interaction energy, significantly ($p \leq 0.05$) higher K_L values were observed for Zn^{2+}- than Ca^{2+}-binding to the majority of the pectin samples. These differences were also clearly visible in **Figure 3.4 a** and **b** compared to **Figure 3.4 c** and **d**, indicating stronger interactions between pectin and Zn^{2+} than pectin and Ca^{2+}. This observation is in agreement with the findings of Dronnet et al. (1996) and Assifaoui et al. (2015), who reported higher affinities of citrus pectin for Zn^{2+} than Ca^{2+}. Since the hydrated atomic radii of Zn^{2+} and Ca^{2+} are comparable (0.40-0.43 nm and 0.41-0.42 nm, respectively) (Tansel, 2012), the higher interaction energy between citrus pectin and Zn^{2+} might be attributed to the higher electronegativity of Zn^{2+} (~1.65) compared to Ca^{2+} (~1.00) (Allred, 1961), resulting in a more readily and stronger attraction of electrons, hence stronger interactions (Kyomugasho et al., 2017).

3.3.5 In vitro bioaccessibility of Zn^{2+}

A simulated *in vitro* digestion was performed to study the influence of pectin degree and pattern of methylesterification on the bioaccessibility of Zn^{2+} and its relation with the cation-binding capacity and interaction energy. Results of the Zn^{2+} bioaccessibility for three different Zn^{2+} concentrations are presented in **Figure 3.5** (**a, b** and **c**). The three Zn^{2+} levels correspond to different positions of the adsorption isotherms (see **Figure 3.1 a** and **b**); beginning of the ascending part where all pectin samples contain enough binding sites to bind all Zn^{2+} (represented by 0.3 mM), middle of the

ascending part where only CP95 theoretically does not contain enough binding sites (1 mM) and above the plateau value of the isotherm where an excess of Zn^{2+} was added for all pectins (3 mM). A blank, containing water instead of pectin solution, spiked with Zn^{2+} was also included. It can be observed from **Figure 3.5** that the bioaccessibility of Zn^{2+} was influenced by pectin DM, DB_{abs} and Zn^{2+} concentration (0.3, 1 and 3 mM).

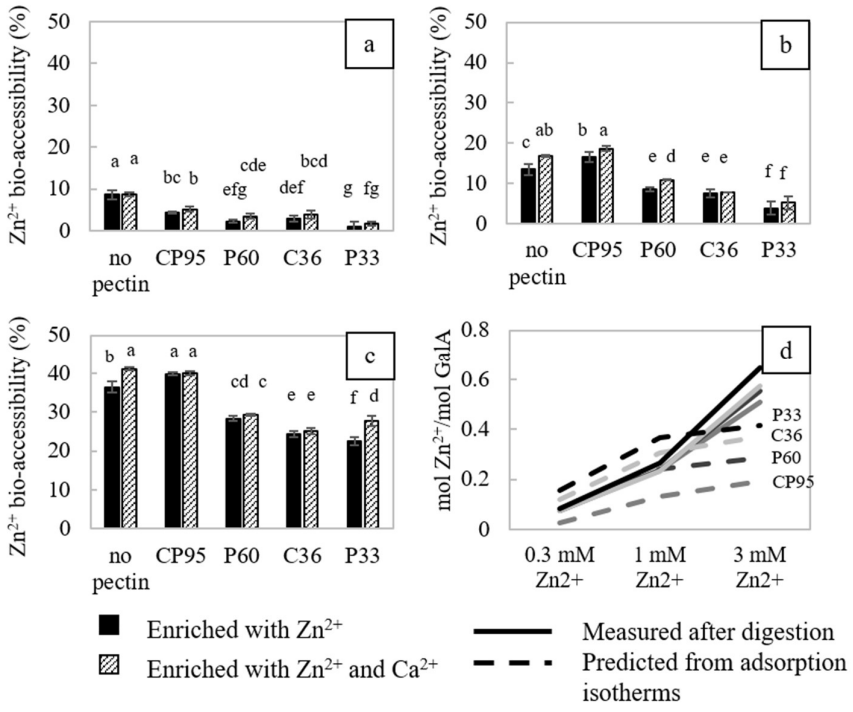

Figure 3.5: The *in vitro* Zn^{2+} bioaccessibility (%) with standard deviation of digests without and with 0.1% enzymatically or alkaline demethylesterified pectins (P-pectins or C-pectins, respectively), and commercial high methylesterified citrus pectin (CP95), enriched with a) 0.3 mM, b) 1 mM and c) 3 mM Zn^{2+}- ions. Filled and striped bars represent digests enriched with only Zn^{2+} and enriched with Zn^{2+} and Ca^{2+} (approximately 0.33 mM), respectively. Different letters (a-g) indicate significant ($p \leq 0.05$) differences between the *in vitro* Zn^{2+} bioaccessibilities. d) The amount of Zn^{2+} bound to enzymatically and alkaline demethylesterified pectins (P-pectins and C-pectin, respectively) and the commercial high methylesterified citrus pectin (CP95) (mol Zn^{2+}/mol GalA) for the three enriched Zn^{2+}concentrations (0.3, 1 and 3 mM) measured after digestion (solid lines) or predicted from the adsorption isotherms (dotted lines).

In absence of pectin (blank), the bioaccessibility of Zn^{2+} increased from 8.6 ± 1.1% to 13.5 ± 1.7% and to 36.4 ± 1.3% with increasing Zn^{2+} concentrations from 0.3 (**Figure 3.5 a**) to 1 mM (**Figure 3.5 b**) to 3 mM (**Figure 3.5 c**). This logically evidences a higher amount of free Zn^{2+} at higher Zn^{2+} concentrations. Nevertheless, in absence of pectin, the Zn^{2+} bioaccessibility was expected to approximate 100%, implying that all Zn^{2+} added would be free and available for absorption after digestion. The fact that decreased Zn^{2+} bioaccessibilities were observed in the samples without pectin suggests the binding of Zn^{2+} to other components added during digestion, such as pepsin or pancreatin as well as bile salts. Nevertheless, further research is needed to confirm this hypothesis.

Regarding the pectin solutions enriched with only Zn^{2+}, the Zn^{2+} bioaccessibilities increased in all samples, irrespective of the DM or DB_{abs}, with increasing Zn^{2+} enrichment concentrations (**Figure 3.5 a, b** and **c**). This is in accordance to the blank samples (no pectin), in which a higher Zn^{2+} concentration resulted in a higher amount of free Zn^{2+}. In samples enriched with low Zn^{2+} concentration (0.3 mM, **Figure 3.5 a**), the Zn^{2+} bioaccessibility decreased with increasing DB_{abs}: CP95 > C36 > P60 > P33. Pectins containing a higher number or longer blocks of successive carboxylate groups could bind a higher amount or stronger with Zn^{2+}, as shown previously (Section 3.3.2 and 3.3.3), leading to less free Zn^{2+} during the intestinal phase. At low cation concentrations, pectin is less sensitive to cation interactions and consequently the DB_{abs} is mainly determining the pectin-cation interactions. By contrast, the bioaccessibility of the samples at high Zn^{2+} concentrations (1 and 3 mM, **Figure 3.5 b** and **c**) decreased significantly ($p \leq 0.05$) with decreasing DM. For instance, the Zn^{2+} bioaccessibility in the samples enriched with 3 mM Zn^{2+} decreased from 39.8 ± 1.4% for CP95 to 22.5 ± 0.6% for P33. Given the pH of 7 during the intestinal phase of the *in vitro* digestion, which was above the pKa of pectin (2.9-4.1), non-methylesterified carboxyl groups were completely ionized, resulting in higher Zn^{2+}-binding capacities as well as stronger interactions for low DM pectins, such that only a limited amount of cations was free and bioaccessible. The observation that both DM and DB_{abs} determined the Zn^{2+} bioaccessibilities depending on the initial Zn^{2+} concentration can be explained by the previously discussed results (Section 3.3.2 and 3.3.3). Indeed, the DB_{abs} mainly influenced the interaction-energy, which is related with low cation concentrations on the adsorption isotherms (ascending part), whereas the DM determined the maximum binding capacity, which is associated with higher Zn^{2+} concentrations on the adsorption isotherms (plateau).

Examining the bioaccessibility results at 0.3 and 1 mM in comparison to the maximally adsorbed amounts as determined in Section 3.2. (**Figure 3.5 d**), a higher amount of Zn^{2+} was bound after digestion than estimated for CP95. In contrast, for the other pectin samples (P60, C36 and P33) less Zn^{2+} was bound after digestion than estimated and this difference increased with decreasing DM. At high Zn^{2+} concentration (3 mM Zn^{2+}) an excess was added for all pectins and theoretically 75%, 62%, 50%, and 50% of the Zn^{2+} added should be free and bioaccessible in CP95, P60, C36 and P33, respectively. Nevertheless, the observed bioaccessibilities were clearly lower, being 39.8 ± 1.4%, 28.3 ± 0.5%, 24.3 ± 0.8% and 22.5 ± 0.6% for CP95, P60, C36, and P33, respectively. This, as depicted in **Figure 3.5 d**, indicates that substantially higher amounts of Zn^{2+} were bound after digestion than estimated in the maximum binding capacity study (Section 3.3.2., **Table 3.1**). The binding of Zn^{2+} to bile salts or enzymes, as suggested based on the samples without pectin (blank), could explain the higher amount of Zn^{2+} bound after digestion compared to the expected amount as predicted based on the maximum cation-binding capacity of pectin. Moreover, given that at a specific level of Zn^{2+} enrichment the Zn^{2+} bioaccessibility in water was comparable to that in CP95 pectin solutions, shows that CP95 in general is not able to bind substantial amounts of Zn^{2+} or more strongly due to its low amount of carboxylate groups.

Finally, results of Zn^{2+} bioaccessibility in presence of Ca^{2+} (from $CaCl_2$ added during digestion) are presented in **Figure 3.5** to explore the influence of Ca^{2+} on the Zn^{2+} bioaccessibility. Pectin solutions enriched with Zn^{2+} and Ca^{2+} exhibited slightly higher Zn^{2+} bioaccessibilities (**Figure 3.5 a, b** and **c**), suggesting binding of Ca^{2+} to pectin, releasing more free Zn^{2+} ions. However, the bioaccessibilities were not significantly ($p > 0.05$) higher for the majority of the samples, compared to the samples without Ca^{2+}. As previously discussed (Section 3.3.4) that all pectin samples exhibited significantly higher binding capacity (q_{max}) and stronger (K_L) interaction with Zn^{2+} than with Ca^{2+}, it is not surprising that addition of the latter (particularly in low amounts) did not readily compromise the pectin-Zn^{2+} interaction.

3.4 CONCLUSION

This chapter investigated the influence of citrus pectin degree and pattern of methylesterification, represented by DM and estimated absolute degree of blockiness (DB_{abs}), respectively, on the binding of Zn^{2+} as well as Ca^{2+} and associated Zn^{2+} bioaccessibility. Adsorption isotherms of both Zn^{2+} and Ca^{2+} were obtained through equilibrium adsorption experiments and were well fitted by the Langmuir adsorption model, resulting in quantification of pectin maximum binding capacity and pectin-cation interaction energy. Binding of Zn^{2+} or Ca^{2+} to pectin was promoted by decreasing DM (pectins with a high number of negatively chargeable GalA units) and increasing DB_{abs} (high number of successive non-methylesterified GalA units). Whereas the DM was mainly determining the maximum binding capacity of pectin for Zn^{2+} or Ca^{2+}, the interaction energy (pectin-Zn^{2+}/Ca^{2+}) was mainly determined by the DB_{abs}. Besides the pectin properties, the type of cation influenced the pectin-cation interaction. Higher binding capacities and stronger interactions energies were observed for Zn^{2+} compared to Ca^{2+}, possibly due to binding of the former to other functional groups (such as OH^-) in addition to carboxylate groups and due to its higher electronegativity. Finally, results of the *in vitro* bioaccessibility study revealed that decreasing DM or increasing DB_{abs}, resulted in lower Zn^{2+} bioaccessibilities, due to higher Zn^{2+}-binding capacities. Moreover, while a low Ca^{2+} concentration was shown not to influence Zn^{2+} bioaccessibility, binding of Zn^{2+} to components other than pectin, such as enzymes and bile salts added during digestion was shown to further impair Zn^{2+} bioaccessibility. The results of this work suggest that targeted modification of citrus pectin, in terms of DM and DB_{abs}, can be applied to direct its binding with Zn^{2+} or Ca^{2+} and therefore its associated functionalities. To this extent, an optimized cation-binding capacity can for instance be obtained to promote the pectin-cation interactions for structure build-up in food products without compromising the mineral nutrition value.

CHAPTER 4

ISOTHERMAL TITRATION CALORIMETRY FOR ASSESSING THE Zn^{2+}-BINDING CAPACITY OF PECTIN[4]

4.1 INTRODUCTION

Equilibrium adsorption studies on the Zn^{2+}-binding of demethylesterified pectin samples in Chapter 3 revealed that both the degree and pattern of methylesterification influence the pectin-Zn^{2+} interaction: decreasing DM or increasing DB_{abs} resulted in both a higher amount of Zn^{2+} bound and stronger pectin-Zn^{2+} interactions. Besides the use of equilibrium adsorption studies, the interaction between a ligand and an adsorbent can be studied using isothermal titration calorimetry (ITC). The advantage of this technique over an equilibrium adsorption study is that, in addition to the binding stoichiometry and binding constant, ITC provides insight into the thermodynamics of biopolymer binding interactions such as enthalpy change (ΔH) or entropy change (ΔS) (Freire, Schön, & Velazquez-Campoy, 2009). The interaction between pectin and Zn^{2+} using ITC has been scarcely described in literature. According to Assifaoui et al. (2015), the binding process between low methylesterified citrus pectin and Zn^{2+} is comparable to Ca^{2+}, being via monocomplexation or point-like cross-links at low molar ratios (< 0.3), which was associated with an endothermic process. At higher cation concentrations (molar ratio

[4] This chapter is based on following paper:
Celus, M., Kyomugasho, C., Lombardo, S., Thielemans, W., and Hendrickx, M. (2018). Isothermal titration calorimetry to study the influence of citrus pectin degree and pattern of methylesterification on Zn^{2+} interaction. *Carbohydrate Polymers*, 197: 460-468

> 0.3), the endothermic process is followed by an exothermic process, indicating the formation of an ordered structure such as dimerization (Assifaoui et al., 2015). However, thermodynamic insights into the interaction between pectin with distinct degrees and patterns of methylesterification and Zn^{2+} have not yet been explored. These insights are of importance in understanding the role of pectin structural properties, and in particular its DM and DB, in Zn^{2+}-binding and the associated pectin-Zn^{2+} related functionalities, e.g., Zn^{2+} bioaccessibility during digestion (Kyomugasho et al., 2017; Raes et al., 2014). This chapter aims to explore the interactions between pectin with distinct DMs and DB_{abs} values and Zn^{2+} using ITC in order to gain a more in-depth understanding into the thermodynamic properties of this interaction.

4.2 MATERIALS AND METHODS

4.2.1 Materials

The pectin samples with different degrees and patterns of methylesterification that have been produced and structurally characterized in Chapter 2 were studied for their Zn^{2+} interaction by isothermal titration calorimetry. Particularly, commercial high methylesterified citrus pectin (CP95), enzymatically demethylesterified (P69, P60, P39, P33, and P13) and alkaline demethylesterified (C67, C46, C36, C30, C20, and C10) pectin samples were used. All chemicals used were of analytical grade. Ultrapure water (organic free, 18.2 MΩ cm resistance) was used for the isothermal titration calorimetry as well as analytical experiments and was supplied by a Simplicity™ water purification system (Millipore, Burlington, MA, USA).

4.2.2 Isothermal titration calorimetry

Isothermal titration calorimetry (ITC) measurements were conducted using a TAM III isothermal calorimeter (TA Instruments, New Castle, DE, USA) based on the procedure as described by Lombardo et al. (2017). Pectin was dissolved and diluted with ultrapure water in order to obtain GalA concentrations varying from 1.81 to 14.05 mM. These concentrations were chosen in order to obtain a detectable heat change from which the thermodynamic parameters could be estimated. The pH values of the pectin solutions were at least one log unit above the pKa value of pectin (2.9-4.1), thus facilitating almost complete ionization of the carboxyl groups. Prior to the experiments, pectin and Zn^{2+} solutions were thoroughly degassed by sonication for 15 min under vacuum. Titrations were performed at 25 °C (in duplicate) by adding twenty injections of 10 µL of 6.67 mM $ZnSO_4.7H_2O$ solution into a calorimeter sample cell (1 mL) containing 800 µL pectin solution, which was continuously stirred at 120 rpm. The intervals between successive injections varied between 1200 and

2400 s to make sure the signal trace fully returned to the baseline after each injection. A blank experiment was also performed by identical injections of 6.67 mM $ZnSO_4.7H_2O$ into ultrapure water at 25 °C. Binding isotherms were obtained by integration of each injection peak using the NanoAnalyze data analysis software (TA Instruments, New Castle, DE, USA), from which the blank was subtracted in order to correct for the heat of dilution for the ligand. Thermodynamic parameters, particularly the stoichiometric ratio (n), the binding constant (K_a) and the enthalpy change (ΔH), were estimated by non-linear regression (via iterative fitting) of a model of independent binding sites to the binding isotherm using NanoAnalyze data analysis software (TA Instruments, New Castle, DE, USA). The model is based on the equilibrium constant (**Equation 4.1**) and mass balance (**Equation 4.2**) equations as described by Freyer and Lewis (2008):

$$\Theta_j = \frac{[L].K_j}{1+[L].K_j} \quad [4.1]$$

$$L_t = [L] + P_t \sum_{j=1}^{k}(n_j.\Theta_j) \quad [4.2]$$

In these equations, Θ_j is the fraction of site *j* occupied by the ligand, *[L]* is the free ligand concentration, L_t is the total ligand concentration, K_j is the binding constant for process *j*, P_t is the total macromolecule concentration and n_j is the total stoichiometric ratio for process *j*. By substituting *[L]* in **Equation 4.1**, the fraction of occupied binding sites *j* can be calculated. The total heat produced can subsequently be calculated by **Equation 4.3**:

$$Q = P_t.V_0 \sum_{j=1}^{k}(n_j.\Theta_j.\Delta H_j) \quad [4.3]$$

With V_0 the initial volume of the sample cell and ΔH_j the molar enthalpy change for process *j*. The differential heat is defined by **Equation 4.4**:

$$\Delta Q = Q(i) - Q(i-1) \quad [4.4]$$

The Gibbs free energy change (ΔG) can be calculated from the binding constant (K_a) using **Equation 4.5** and the entropy change (ΔS) using **Equation 4.6**, with *T* the temperature in Kelvin and R the gas constant (8.31 J/K.mol):

$$\Delta G = -RT.\ln(K_a) \quad [4.5]$$

$$\Delta G = \Delta H - T\Delta S \quad [4.6]$$

4.2.3 Statistical data analysis

The experimental data were statistically analyzed with the software JMP (JMP 13, SAS Institute Inc., Cary, NC, USA). A one-way analysis of variance (ANOVA) and a Tukey HSD test were carried out to analyze significant differences with a 95% confidence interval ($p \leq 0.05$) between the experimental data.

4.3 RESULTS AND DISCUSSION

4.3.1 Isothermal titration calorimetry in general

The influence of pectin DM and DB_{abs} on the interaction with Zn^{2+} was studied using isothermal titration calorimetry (ITC). **Figure 4.1** is an example of an ITC thermogram, illustrating the corrected heat rate (µJ/s) as a function of time (min), from the addition of 6.67 mM Zn^{2+} into a pectin solution (3.97 mM GalA of P60) and into ultrapure water (blank). Negative values of the calorimetric peaks indicate endothermic binding between pectin and Zn^{2+} and the areas of the peaks decrease until the peaks become exothermic. This transition indicates saturation of the pectin sample for Zn^{2+}-binding, as from this point on, the calorimetric traces of the sample equal the traces of the blank, which implies dilution of Zn^{2+} into ultrapure water. The thermogram in **Figure 4.1** is representative for all the other ITC measurements.

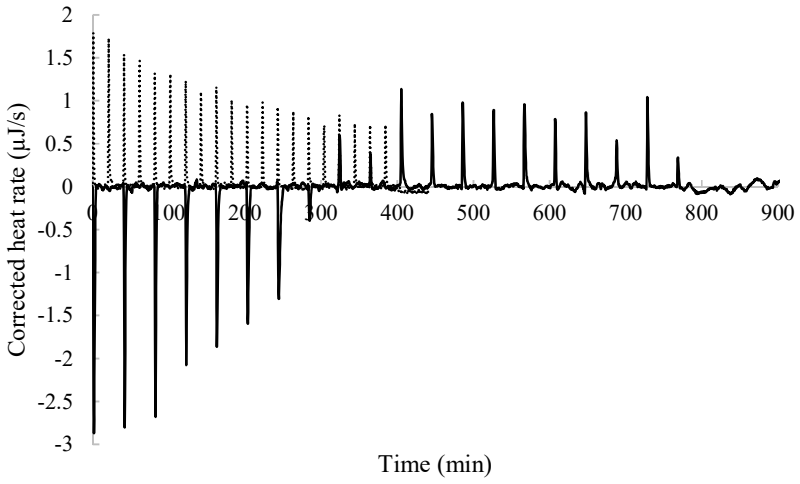

Figure 4.1: ITC thermogram representing the corrected heat rate (µJ/s) as a function of time (min), obtained from the titration of 6.67 mM Zn^{2+} to a solution containing 3.97 mM GalA units of an enzymatically demethylesterified citrus pectin sample with DM of 59.8 ± 1.4% (P60) (solid black line), and from the dilution of Zn^{2+} into ultrapure water (dotted black line).

The transition between this endothermic and exothermic process in **Figure 4.1** also suggests a two-step binding mechanism between pectin and Zn^{2+} during titration with Zn^{2+}. The endothermic binding can be attributed to the formation of monocomplexes and point-like cross-links between pectin and Zn^{2+}, while the exothermic process corresponds to dimerization as a second step. This observation is in agreement with the observations of Assifaoui et al. (2015). In accordance with Fang et al. (2008), the results of these ITC measurements do not evidence the lateral association of pectin dimers (multimerization). This might be explained by the strong interaction between Zn^{2+} and carboxylate groups (Huynh et al., 2016), implying a lower probability for the pectin chains to rearrange and form lateral associations between dimers.

By integrating the peaks, the raw data of the thermogram can be converted to a binding isotherm, which indicates the heat absorbed after each addition of Zn^{2+} (belonging to a corresponding peak) as a function of the molar ratio (mol Zn^{2+}/mol GalA). The binding isotherms are presented for each pectin sample in **Figure 4.2** and **4.3** for P- and C-pectins, respectively. From **Figure 4.2** it can be seen that with decreasing DM, the binding isotherms of the P-pectins show a sharper decrease and that the inflection point occurs at higher molar ratios. This indicates a stronger and promoted Zn^{2+}-binding for low DM pectins when compared to pectins samples with higher DM. For C-pectins (**Figure 4.3**), the binding isotherms are not changing tremendously with decreasing DM, except from C10, which exhibits a clearly sharper decrease of the curve. Despite the steeper curve for this low DM sample, the inflection point for all C-pectins appears at a comparable molar ratio. Moreover, the binding isotherms of the C-pectins are less steep in comparison to P-pectins for a comparable DM. This difference can be explained by the higher number or longer blocks of negatively charged GalA units for the P-pectins compared to C-pectins, promoting the cation interaction. Additionally, it is visible from **Figure 4.2** and **4.3** that a sudden increase in the steepness of the curves occurred for P-pectins from a DM of 39% (P39) and for C-pectins from a DM of 10% (C10). With decreasing DM, the pectin samples become more sensitive to gelling in the presence of divalent cations and it is reported that pectin with a blockwise distribution gels at higher DM than pectin with a random distribution of non-methylesterified GalA units (Fraeye et al., 2009; Ngouémazong et al., 2012a; Ström et al., 2007). Despite all pectin-Zn^{2+} solutions being rather viscous and turbid, only the ITC experiments with low DM pectins or high DB_{abs} were probably influenced by gelling, which might have interfered with the stability of the calorimetric baseline. This may also explain the higher standard errors observed between the repeated measurements for low DM pectins.

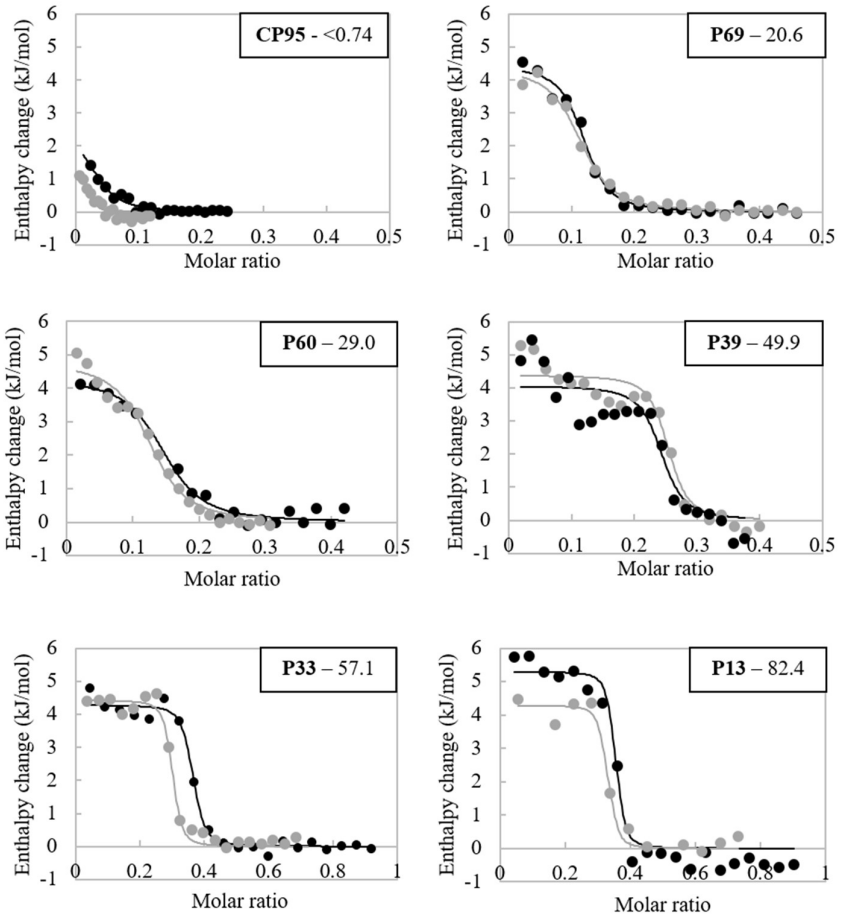

Figure 4.2: Binding isotherms representing the enthalpy change (kJ/mol) as a function of the molar ratio (mol Zn^{2+}/mol GalA) of enzymatically demethylesterified pectins (P-pectins) with different DMs (%) (with estimated DB_{abs} value indicated after the hyphen) and the commercial high methylesterified citrus pectin (CP95). Dots indicate the heat adsorbed after every addition of Zn^{2+} solution to the pectin solution, determined from the integral of the corresponding peak. The lines represent the fitted curve. Black and grey represent duplicates.

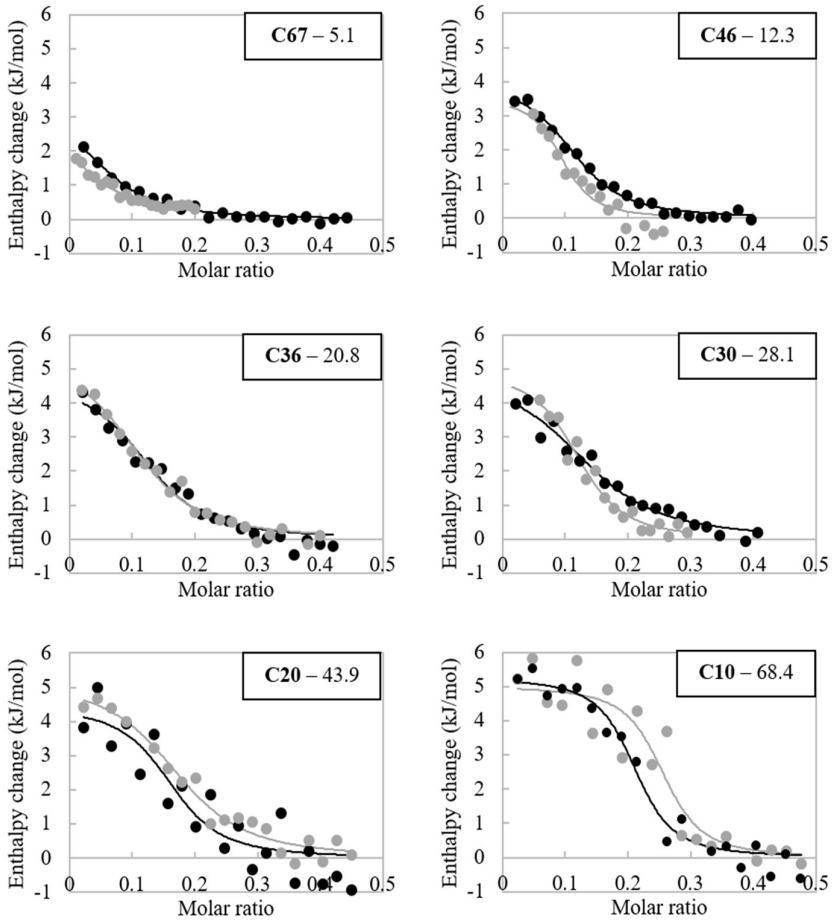

Figure 4.3: Binding isotherms representing the enthalpy change (kJ/mol) as a function of the molar ratio (mol Zn^{2+}/mol GalA) of alkaline demethylesterified pectins (C-pectins) with different DMs (%) (with estimated DB_{abs} value indicated after the hyphen). Dots indicate the heat adsorbed after every addition of Zn^{2+} solution to the pectin solution, determined from the integral of the corresponding peak. The lines represent the fitted curve. Black and grey represent duplicates.

4.3.2 Influence of pectin DM and DB_{abs} on Zn^{2+}-binding capacity

Modeling of the binding isotherms facilitated estimation of binding stoichiometry values (n), in this doctoral thesis referred to as the binding capacities (mol Zn^{2+}/mol GalA) and presented in **Table 4.1** and **Figure 4.4** as a function of DM or estimated DB_{abs}. For both P- and C-pectins, the binding capacity increased (not always significant, $p > 0.05$) with decreasing DM (**Figure 4.4 a**) or increasing DB_{abs} (**Figure 4.4 b**), implying an increased amount of Zn^{2+} bound to pectin when a higher number of negatively charged GalA units or longer blocks of these groups are present within the pectin chain, respectively. Despite the higher Na^{+} content in the low DM pectin samples compared to high DM pectins (**Table 2.3**), and thus probably a higher ionic strength in these low DM pectins, a higher Zn^{2+}-binding capacity was observed. This suggests a minor influence of the intrinsically present Na^{+} on the ionic strength and on the cation-binding capacity.

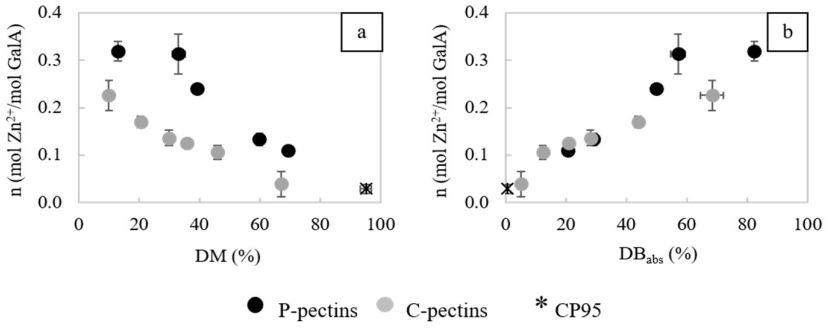

Figure 4.4: Estimated binding capacity, n (mol Zn^{2+}/mol GalA) with standard deviation as a function of a) DM (%) with standard deviation or b) estimated DB_{abs} (%) with standard deviation of enzymatically (P-pectins, black) and alkaline demethylesterified (C-pectins, grey) pectins, and commercial high methylesterified citrus pectin (CP95, black asterisk) as determined by ITC.

P-pectins exhibit significant ($p \leq 0.05$) higher binding capacity values compared to C-pectins for a given DM, which can be attributed to the more blockwise distribution pattern of negatively chargeable carboxyl groups for a given DM in comparison with C-pectins. From **Figure 4.4 b** it can be seen that the distribution pattern of non-methylesterified GalA units is indeed an important parameter in determining the pectin-Zn^{2+} interaction. For a given DB_{abs}, the Zn^{2+}-binding capacity is comparable between P- and C-pectins. Moreover, from a DB_{abs} of 44%, a sharper increase of the binding capacity is observed, suggesting that a certain number of blocks or longer blocks of non-methylesterified GalA units are required to enhance the sensitivity for Zn^{2+}-binding.

Table 4.1: Parameters estimates ± standard deviation for a model of independent binding sites as determined by ITC for Zn^{2+}-binding to commercial high methylesterified citrus pectin (CP95) and demethylesterified pectin samples, with P representing enzymatically demethylesterified pectins and C the alkaline demethylesterified pectins. DB_{abs} (%) is the estimated absolute degree of blockiness repeated from Table 2.1, n (mol Zn^{2+}/mol GalA or mol Zn^{2+}/mol COO^-) is the binding capacity and K_a (mM^{-1}) represents the binding constant. Different letters (a-k) indicate significant ($p \leq 0.05$) differences between the pectin samples for an estimated parameter.

Sample code	DB_{abs} (%)	n (mol Zn^{2+}/mol GalA)	n (mol Zn^{2+}/mol COO^-)	K_a (mM^{-1})
CP95	$< 0.74^{i}$	0.029 ± 0.010^{e}	0.592 ± 0.202^{a}	28 ± 23^{cd}
P69	20.6 ± 1.0^{g}	0.111 ± 0.002^{cd}	0.361 ± 0.007^{abcd}	61 ± 23^{cd}
P60	29.0 ± 1.3^{f}	0.134 ± 0.013^{c}	0.333 ± 0.032^{abcd}	35 ± 7^{cd}
P39	49.9 ± 1.0^{d}	0.241 ± 0.006^{ab}	0.396 ± 0.010^{abc}	224 ± 62^{c}
P33	57.1 ± 2.5^{c}	0.314 ± 0.042^{a}	0.468 ± 0.062^{ab}	805 ± 32^{b}
P13	82.4 ± 1.7^{a}	0.319 ± 0.021^{a}	0.366 ± 0.024^{abc}	1298 ± 190^{a}
C67	5.1 ± 0.1^{i}	0.040 ± 0.027^{de}	0.121 ± 0.082^{d}	11 ± 11^{d}
C46	12.3 ± 0.3^{h}	0.107 ± 0.015^{cde}	0.197 ± 0.027^{cd}	18 ± 4^{cd}
C36	20.8 ± 0.8^{g}	0.125 ± 0.008^{c}	0.195 ± 0.013^{cd}	11 ± 2^{cd}
C30	28.1 ± 0.4^{f}	0.137 ± 0.016^{c}	0.195 ± 0.023^{cd}	12 ± 5^{cd}
C20	43.9 ± 0.9^{e}	0.170 ± 0.011^{bc}	0.214 ± 0.014^{bcd}	19 ± 8^{cd}
C10	68.4 ± 3.8^{b}	0.226 ± 0.031^{b}	0.251 ± 0.035^{bcd}	69 ± 9^{cd}

The Zn^{2+}-binding capacities for citrus pectin observed in this study are higher than observed by Assifaoui et al. (2015) using ITC. These authors reported a binding capacity of 0.07 ± 0.04 mol Zn^{2+}/mol GalA for a citrus pectin sample with DM of 30% (unknown method of demethylesterification), whereas in the present study binding capacities of 0.31 ± 0.04 molZn^{2+}/mol GalA for P33 or 0.14 ± 0.02 mol Zn^{2+}/mol GalA for C30 were found. Moreover, the observations in this chapter are somewhat in contrast with Zn^{2+}-binding capacities of the same pectin samples determined in Chapter 3. Although exactly the same pectin samples and materials were used in the two studies, no difference in maximum Zn^{2+}-binding capacity between the P- and C-

pectins at a given DM was observed in Chapter 3. In addition, significantly higher binding capacities were observed for C-pectins compared to P-pectins for a given DB_{abs}. The discrepancy between the two chapters might be explained by the difference in properties measured. While the study in Chapter 3 was based on the spectrophotometric measurement of the free Zn^{2+} concentration after equilibrium of Zn^{2+}-enriched pectin solutions, the present study measured the heat absorbed at every injection of Zn^{2+} into a pectin solution. Therefore, using the latter technique, a heat is measured when an interaction between pectin and Zn^{2+} occurs. By contrast, in the spectrophotometric technique, it is assumed that Zn^{2+} can be entrapped in a pectin network, without being necessarily bound to pectin, thus not being able to dialyze out of the membrane, which can influence the concentration measured. Moreover, the concentrations used in the previous chapter differed from those in the present study, as ITC experiments required specific pectin/Zn^{2+} ratios in order to optimize the calorimetric traces. It might be assumed that the pectin concentration influenced the cation binding, however, this effect is considered to be of minor importance since the binding capacities are expressed as mole cation bound per mole GalA units. In addition, the absolute values of binding capacity determined by ITC were slightly lower than the values measured spectrophotometrically. This was also observed by Lombardo et al. (2017), who studied the interaction between cellulose nanocrystals with different degrees of substitution of pyridinium grafts and *bovine serum albumin*. It can be concluded that different techniques in measuring the binding capacity can lead to different results as distinct methods are applied. Therefore careful interpretation of the results is necessary, taking into account the properties measured. However, in general, decreasing DM or increasing DB_{abs} promoted the pectin-Zn^{2+} interaction in both studies.

With regard to the cation binding capacity expressed as mol Zn^{2+}/mol COO^-, no significant differences ($p > 0.05$) were found between the different P-pectins (0.33-0.47 mol Zn^{2+}/mol COO^-) or between distinct C-pectins (0.12-0.25 mol Zn^{2+}/mol COO^-) (**Table 4.1**). These values correspond to the threshold molar ratios indicating the transition between monocomplexes and point-like cross-links to dimerization, as explained in Section 1.3 and **Table 1.1**. The binding capacities of the P-pectins are higher than those from the C-pectins, which can be explained by their higher DB_{abs} value for a given DM. Moreover, the high value for CP95 can be attributed to the binding of Zn^{2+} to other functional groups than COO^-, such as hydroxyl groups, in analogy to the results from Chapter 3 (Section 3.3.2.2).

4.3.3 Influence of pectin DM and DB_{abs} on binding constant of pectin-Zn^{2+} interaction

The estimated binding constant values (K_a) of the interaction between Zn^{2+} and the pectin samples are presented as a function of DM (**Figure 4.5 a**) or DB_{abs} (**Figure 4.5 b**) and in **Table 4.1**.

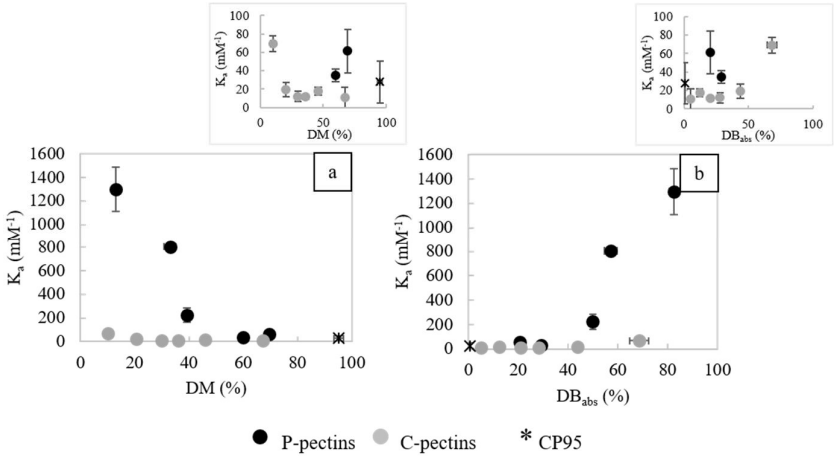

Figure 4.5: Estimated binding constant, K_a (mM^{-1}) with standard deviation as a function of a) DM (%) with standard deviation or b) estimated DB_{abs} (%) with standard deviation of enzymatically (P-pectins, black) and alkaline demethylesterified (C-pectins, grey) pectins, and commercial high methylesterified citrus pectin (CP95, black asterisk) as determined by ITC. Small figures on top are magnifications of the low K_a (mM^{-1}) values (< 100) with standard deviation as a function of DM (%) and estimated DB_{abs} (%) with standard deviation.

With regard to P-pectins, decreasing DM or increasing DB_{abs} resulted generally in significant ($p \leq 0.05$) higher binding constants. This implies stronger interactions between Zn^{2+} and pectin when a higher number or longer blocks of negatively charged carboxyl groups are present in the pectin chain. Moreover, it can be seen in **Figure 4.5** that from a DB_{abs} of 50% (P39) a sharp increase in binding constant occurred. However, it should be noted that for the low DM samples (P13 and P33), microgel particles were formed during the ITC experiment as a consequence of the Zn^{2+} interaction with this low DM pectin samples, resulting in less reliable and reproducible results. For the C-pectins, the binding constant values did not increase significantly between C67 and C20 with values varying between 11 and 19 mM^{-1}, while an increase from 19 to 69 mM^{-1} was observed between C20 and C10. This can be attributed to the low DB_{abs} for the samples C67 to C20, given the randomly demethylesterification for the C-pectins. Sample C10 exhibits a substantially higher

DB_{abs}, resulting in a stronger interaction with Zn^{2+}. From **Figure 4.5 a** it is clear that the enzymatically demethylesterified pectin samples (P-pectins) exhibited significantly higher K_a values than C-pectins for a comparable DM. For instance P69 showed a binding constant of 61 mM^{-1}, while C67 exhibited 11 mM^{-1}. This implies clearly stronger interactions between Zn^{2+} and P-pectins compared to C-pectins, which is attributed to the higher number or longer blocks of non-methylesterified GalA units for P-pectins for a given DM. As such a higher number and stronger junctions zones can be formed.

Assifaoui et al. (2015) found a similar binding constant for the interaction between citrus pectin with DM of 30% and Zn^{2+} (21.5 ± 7.6 mM^{-1}) as our C30 sample (12 ± 5 mM^{-1}). The results of the binding constants from the present study are also in accordance with the previously measured binding constants in Chapter 3, although using a different measuring technique (equilibrium adsorption study versus ITC). Indeed, we also found stronger interaction energies for the binding of Zn^{2+} to P-pectins compared to C-pectins. Moreover, a sharp increase in binding constant was observed in both studies between a DB_{abs} of 29% and 50% in the previous chapter, whereas between 50 and 57% in the present study. The absolute values observed with ITC measurements are generally also comparable to the values obtained by spectrophotometric measurements. Additionally, a stronger interaction between blocky pectins (P-pectins) and cations compared to pectins with a random pattern of negatively charged GalA units (C-pectins) but comparable DM, as observed in the present study, was also reported by Fraeye et al. (2009) and Ngouémazong et al. (2012a) in terms of gel stiffness.

4.3.4 Influence of pectin DM and DB_{abs} on entropy and enthalpy change for pectin-Zn^{2+} interaction

In addition to the binding capacity and binding constant, ITC measurements allow estimation of additional thermodynamic parameters, being the enthalpy change (ΔH) and the Gibbs free energy change (ΔG) (**Table 4.2**). From these estimated parameters, the entropy change (TΔS) (**Table 4.2**) is calculated using following equation: $\Delta G = \Delta H - T\Delta S$, with T the temperature in Kelvin (298 K). From **Table 4.2** it can be observed that the positive entropy change contributes to a higher extent to the Gibbs free energy change than the unfavorable positive enthalpy change, resulting in a negative Gibbs free energy change for all the pectin samples and thus a spontaneous Zn^{2+}-binding to pectin. Therefore, it can be concluded that the binding process between the pectin samples and Zn^{2+} is entropy driven.

Table 4.2: Parameters estimates ± standard deviation for a model of independent binding sites as determined by ITC for Zn^{2+}-binding to commercial high methylesterified citrus pectin (CP95) and demethylesterified pectin samples, with P representing enzymatically demethylesterified pectins and C the alkaline demethylesterified pectins. DB_{abs} (%) is the estimated absolute degree of blockiness repeated from Table 2.1, ΔH is the enthalpy change (kJ/mol), ΔS is the entropy change (kJ/mol.K), ΔG, the Gibbs free energy (kJ/mol) and T the temperature in Kelvin (298 K). Different letters (a-k) indicate significant ($p \leq 0.05$) differences between the pectin samples for an estimated parameter.

Sample code	DB_{abs} (%)	ΔH (kJ/mol)	TΔS (kJ/mol)	ΔG (kJ/mol)
CP95	$< 0.74^{i}$	1.83 ± 0.95^{c}	26.7 ± 1.4^{fg}	-24.8 ± 2.3^{ab}
P69	20.6 ± 1.0^{g}	4.40 ± 0.04^{ab}	31.6 ± 1.0^{cd}	-27.2 ± 1.0^{abc}
P60	29.0 ± 1.3^{f}	4.52 ± 0.34^{ab}	30.4 ± 0.2^{cde}	-25.9 ± 0.5^{ab}
P39	49.9 ± 1.0^{d}	4.22 ± 0.22^{ab}	34.7 ± 0.9^{b}	$-30.5 \pm 0.7b^{cd}$
P33	57.1 ± 2.5^{c}	4.36 ± 0.10^{ab}	38.1 ± 0.2^{a}	-33.7 ± 0.1^{cd}
P13	82.4 ± 1.7^{a}	4.79 ± 0.71^{a}	39.6 ± 1.1^{a}	-34.9 ± 0.4^{d}
C67	5.1 ± 0.1^{i}	2.57 ± 1.2^{bc}	26.1 ± 0.6^{g}	-21.5 ± 3.8^{a}
C46	12.3 ± 0.3^{h}	3.79 ± 0.36^{abc}	28.0 ± 0.2^{efg}	-24.2 ± 0.6^{ab}
C36	20.8 ± 0.8^{g}	5.07 ± 0.52^{a}	28.2 ± 0.1^{efg}	-23.1 ± 0.5^{a}
C30	28.1 ± 0.4^{f}	4.89 ± 0.04^{a}	28.0 ± 1.2^{efg}	-23.1 ± 1.2^{a}
C20	43.9 ± 0.9^{e}	4.83 ± 0.53^{a}	29.2 ± 0.5^{def}	-24.4 ± 0.7^{ab}
C10	68.4 ± 3.8^{b}	5.13 ± 0.17^{a}	32.7 ± 0.1^{bc}	-27.6 ± 0.3^{abc}

The positive entropy change indicates an increase in disorder of the system (Chodera & Mobley, 2014), which is suggested to be attributed to the loss of polar interactions between the GalA units and water (dehydration), resulting in a possible collapse of the structure of water molecules surrounding the pectin chain (Assifaoui et al., 2015; Lombardo et al., 2017; Privalov & Gill, 1989). This dehydration is probably associated with the interaction between pectin and Zn^{2+}, thereby releasing bound water molecules from the pectin chain. The observation that low DM pectin samples interacted stronger and with a higher amount of Zn^{2+} compared to high DM pectins, probably explains the slight increase (although not always significantly, $p > 0.05$) in entropy change with decreasing DM, from 26.7 ± 1.4 to 39.6 ± 1.1 kJ/mol for P-pectins and to 32.7 ± 0.1 kJ/mol for C-pectins. As can be seen in **Table 4.2**, the entropy

change is significantly ($p \leq 0.05$) higher for P-pectins compared to C-pectins for a given DM or DB_{abs} (except for P60), indicating a higher degree of disorder in the suspensions containing P-pectins compared to suspensions with C-pectins for a given DM or DB_{abs}. As mentioned above, the higher degree of disorder for P-pectins can be associated with a higher release of bound water molecules from the pectin chain as a consequence of an increased amount of Zn^{2+} bound to P-pectins and stronger interactions with Zn^{2+} for P-pectins compared to C-pectins.

The positive enthalpy change in **Table 4.2** indicates an endothermic reaction between the pectin samples and Zn^{2+}. The values increased significantly ($p \leq 0.05$) as a function of DB_{abs} until a DB_{abs} of 20% (C36 or P69), implying a more endothermic reaction, after which no significant ($p > 0.05$) increase was observed (**Table 4.2**). Since a certain DB_{abs} is required for cation binding according to the egg-box model, this result suggests that beyond a DB_{abs} of 20%, stronger electrostatic interactions occurred (accompanied by dimerization) in comparison to samples with DB_{abs} values below 20%. Presumably, all pectin samples characterized by DB_{abs} values higher than 20% could form dimers due to the interaction with Zn^{2+}, resulting in a constant enthalpy change. Dimerization between pectin chains is mostly preceded by the formation of point-like cross-links or monocomplexation between pectins and cations, which are less strong electrostatic interactions (Assifaoui et al., 2015; Fang et al., 2008; Huynh et al., 2016). This possibly explains the initial increase in enthalpy change before a DB_{abs} of 20% is reached.

4.4 CONCLUSION

Isothermal titration calorimetry (ITC) was used as a tool to study the effect of citrus pectin degree (DM) and pattern (DB_{abs}) of methylesterification on the interaction with Zn^{2+}. ITC proved to be a more informative technique compared to equilibrium adsorption experiments to obtain insights into the pectin-cation interactions, as it provides more thermodynamic information about the binding between Zn^{2+} and pectin. Based on the results obtained, that pectin with a higher number or longer blocks of negatively charged galacturonic acid units interacts stronger (higher binding constant) and with a higher amount of Zn^{2+} (higher binding capacity), this technique can form a basis for optimized pectin-Zn^{2+} related functionalities. For instance, by directing the pectin DM and DB_{abs}, thus controlling the cation-binding capacity of pectin, an improved (for structure-build up) or reduced (for enhanced mineral absorption) Zn^{2+}-binding capacity can be intended. Moreover, this study can be extended to other divalent cations as a base to understand other pectin-cation-associated functionalities such as its antioxidant capacity (due to Fe^{2+}-binding). However, it is advised to carefully select the sample and cation concentrations for ITC experiments as low DM pectin samples are sensitive to gelling, which possibly influences the ITC measurements.

CHAPTER 5

INFLUENCE OF PECTIN DEGREE AND PATTERN OF METHYLESTERIFICATION ON Fe^{2+} INTERACTION[5]

5.1 INTRODUCTION

Although pectin DM and DB are extensively explored in the context of gelation with Ca^{2+}, pectin has also been a subject of adsorption studies with cations other than Ca^{2+}. Few studies have explored the interaction between pectin and Fe^{2+}, mainly in the context of bioaccessibility (Debon & Tester, 2001; Kim, 1998; Kyomugasho et al., 2017; Miyada, Nakajima, & Ebihara, 2012). This is interesting given that Fe^{2+} can promote lipid oxidation in a variety of lipid-based food products and that Fe^{2+}-binding by pectin might effectively reduce lipid oxidation (Chen, McClements, & Decker, 2010; Huang, Lu, Wang, & Wu, 2011). Fundamental insight into the adsorption of Fe^{2+} by pectin could contribute to this innovative aspect. However, to the best of our knowledge, no quantitative analysis has been performed on the influence of pectin most studied structural properties, DM and DB_{abs}, on the Fe^{2+}-binding by using adsorption isotherms. Therefore, the objective of this chapter is to investigate the role and extent to which the DM and DB_{abs} influence the Fe^{2+}-binding capacity of pectin, which is hypothesized to be analogous to the Zn^{2+}- or Ca^{2+}-binding in Chapter 3. Therefore, targeted modification of pectin DM and DB_{abs}, followed by determination

[5] This chapter is based on following paper:
Celus, M., Kyomugasho, C., Jamsazzadeh Kermani, Z., Roggen, K., Van Loey, A., Grauwet, T., and Hendrickx, M. (2017). Fe^{2+} adsorption on citrus pectin is influenced by the degree and pattern of methylesterification. *Food Hydrocolloids*, 73: 101-109

of the adsorption isotherms could be of great importance in exploring its Fe^{2+}-binding capacity and related pectin functionalities. A better understanding of the influence of these structural factors on the Fe^{2+}-binding could provide more insight into the optimization of pectin-Fe^{2+} interactions in view of its functionalities, particularly its lipid antioxidant capacity in oil-in-water emulsions.

5.2 MATERIALS AND METHODS

5.2.1 Materials

The pectin samples with different degrees and patterns of methylesterification, as produced and structurally characterized in Chapter 2, were used to study the interaction with Fe^{2+}. Particularly, commercial high methylesterified citrus pectin (CP95), enzymatically demethylesterified (P69, P60, P39, P33, and P13) and alkaline demethylesterified (C67, C46, C36, C30, and C20) pectin samples were used. All chemicals used were of analytical grade. Ultrapure water (organic free, 18.2 MΩ cm resistance) was supplied by a Simplicity™ water purification system (Millipore, Burlington, MA, USA) and used for the adsorption as well as analytical experiments.

5.2.2 Determination of adsorption isotherms of pectin for Fe^{2+}

In order to determine the Fe^{2+}-binding capacity of pectin and specifically the relation between the Fe^{2+}-binding capacity and pectin DM and DB_{abs}, an adsorption equilibrium study was performed as previously described in Chapter 3 for pectin-Zn^{2+} or -Ca^{2+} interaction studies. Briefly, deaerated aqueous solutions (10 mL) of the pectin samples (0.1% w/v) were enriched with 0 to 200 mg/L Fe^{2+} ($FeSO_4.7H_2O$) and subsequently transferred to previously rinsed dialysis membranes (Spectra/Por®, MWCO = 3.5 kDa). These membranes were equilibrated in closed jars containing 50 mL deaerated ultrapure water, which was constantly stirred. The jars were placed in a pharmaceutical refrigerator (MPR-311D (H), Sanyo Electric Biomedical Co., Tokyo, Japan) at 15 °C for 48 h until an equilibrium between non-bound Fe^{2+} inside and outside the membrane was achieved. In addition to the use of deaerated water, the experiment was performed in a nitrogen atmosphere using a pyramid portable glove bag (Erlab, Val de Reuil, France), installed in the refrigerator to avoid an oxygen-rich atmosphere, hence Fe^{2+} oxidation. After equilibration, the Fe^{2+} concentration of the outside solution was measured spectrophotometrically according to Viollier, Inglett, Hunter, Roychoudhury, and Van Capellen (2000) with some minor modifications. An aliquot of the outside solution (1 mL) was transferred into a cuvette with the addition of 100 µL of 0.01 M ferrozine (3-(2-pyridyl)-5,6-diphenyl-1,2,4-triazine-*p*,*p*'-disulfonic acid monosodium salt hydrate) and 50 µL of 5 M ammonium acetate buffer

(pH 9.5). After 5 min, the absorbance was measured at 562 nm (1800 UV spectrophotometer, Shimadzu, Kyoto, Japan). The analysis was performed in triplicate and the Fe^{2+} concentration was determined using a standard curve of $FeSO_4.7H_2O$ solutions (0-6 mg Fe^{2+}/L). The Fe^{2+}-binding capacity (q_e) of pectin was estimated based on the difference between the initial Fe^{2+}concentration and the concentration measured after equilibrium and calculated as follows (Khotimchenko et al., 2008):

$$q_e = \frac{C_0 \cdot V_{in} - C_e \cdot (V_{in} + V_{out})}{M_w \cdot n_{GalA}} \quad [5.1]$$

with C_0, the initial Fe^{2+} concentration (g/L), C_e, the Fe^{2+} concentration at equilibrium (g/L), V_{in} and V_{out}, the volume inside (0.01 L) and outside (0.05 L) the dialysis membrane, respectively. M_w and n_{GalA} represent the atomic weight of Fe^{2+} (55.85 g/mol) and the absolute amount of GalA units in the pectin sample (mol), respectively. q_e is the equilibrium binding capacity of the pectin sample, expressed as mol Fe^{2+}/mol GalA. Taking into account the DM of the pectin sample, q_e can be expressed as mol Fe^{2+}/mol COO^- as well.

Since the adsorption equilibrium studies were performed at a constant temperature, adsorption isotherms indicating the amount of Fe^{2+} bound to each GalA or COO^- unit (q_e) as a function of the Fe^{2+} concentration at equilibrium (C_e) were obtained. The adsorption isotherms of the pectin samples were subsequently modeled by the Langmuir adsorption model (Ho et al., 2002; Khotimchenko et al., 2008; Zhao et al., 2013). The Langmuir isotherm, which is the most widely used adsorption isotherm, assumes monolayer adsorption at homogenous and finite binding sites within the pectin chain (Foo & Hameed, 2010):

$$q_e = \frac{q_{max} \cdot K_L \cdot C_e}{1 + K_L \cdot C_e} \quad [5.2]$$

with q_{max} as the maximum binding capacity at the monolayer (mol Fe^{2+}/mol GalA or mol Fe^{2+}/mol COO^-), q_e, the binding capacity of a GalA or COO^- unit (mol Fe^{2+}/mol GalA or mol Fe^{2+}/mol COO^-) belonging to an Fe^{2+} equilibrium concentration, K_L, the Langmuir constant (L/mmol Fe^{2+}), which is a measure of the interaction energy and C_e, the Fe^{2+} equilibrium concentration (mmol Fe^{2+}/L).

Modeling of the experimental data of the pectin samples by the Langmuir adsorption isotherm was performed using non-linear one step regression (SAS version 9.4, Cary, NC, USA).

5.2.3 Statistical data analysis

Differences in experimental data were analyzed using the statistical software JMP (JMP 13, SAS Institute Inc., Cary, NC, USA) and the Tukey's studentized range post-hoc test was carried out to analyze significant differences with a 95% confidence interval ($p \leq 0.05$) between the experimental data.

5.3 RESULTS AND DISCUSSION

5.3.1 Adsorption isotherms of pectin samples for Fe^{2+} in general

Adsorption isotherms of the differently demethylesterified citrus pectin samples were obtained to determine their binding capacity of Fe^{2+} and the relation between this Fe^{2+}-binding capacity and pectin DM as well as DB_{abs} (**Figure 5.1**).

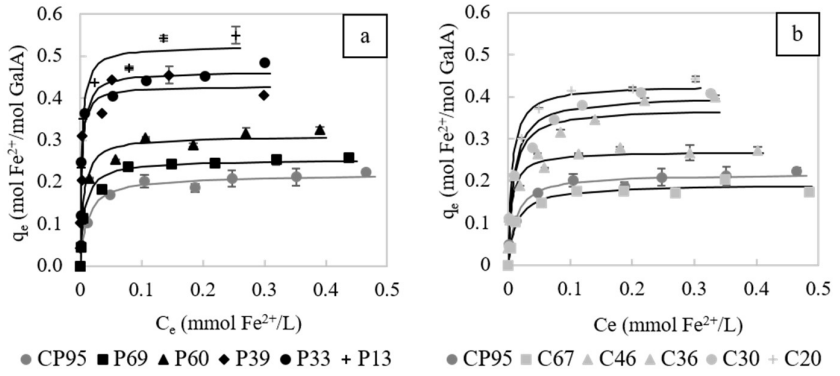

Figure 5.1: Adsorption isotherms representing the equilibrium cation binding capacity, q_e (mol Fe^{2+}/mol GalA) as a function of the cation equilibrium concentration, C_e (mmol/L), for a) Fe^{2+} to P-pectins and b) Fe^{2+} to C-pectins. P-pectins represent enzymatically demethylesterified pectins (black symbols), C-pectins the alkaline demethylesterified pectins (grey symbols) while CP95 refers to the commercial high methylesterified citrus pectin (dark grey symbols). Symbols indicate the experimental data with standard deviation. Black and dark grey curves are modeled Langmuir adsorption isotherms.

From the adsorption isotherms of the P- and C-pectins shown in **Figure 5.1**, it can be observed that the equilibrium binding capacity (mol Fe^{2+}/mol GalA) of all samples increased with increasing equilibrium Fe^{2+}concentration until a maximum was reached. This plateau indicates saturation and represents the maximum amount of Fe^{2+} that can be bound to the pectin sample (q_{max}) (Schmuhl et al., 2001; Zhao et al., 2013). The experimental data of the pectin samples were well described by the Langmuir adsorption model, with $R^2_{adjusted}$ values ≥ 0.98 (results not shown). The use of the Langmuir adsorption isotherm implies that demethylesterified citrus pectin contains a

limited number of homogeneous binding sites and Fe^{2+}-binding occurred via monolayer adsorption with a constant adsorption energy distribution (Foo & Hameed, 2010; Schmuhl et al., 2001; Zhao et al., 2013). The estimated parameters of the Langmuir adsorption isotherm are shown in **Table 5.1**, in which the maximum Fe^{2+}-binding capacity expressed as mol Fe^{2+}/mol GalA is indicated as q^G_{max} while the maximum amount of Fe^{2+} bound to each mole of COO^- is represented as q^C_{max}.

Table 5.1: Parameter estimates ± standard deviation for Langmuir adsorption model-based isotherms of Fe^{2+}-binding to the commercial high methylesterified citrus pectin (CP95) and demethylesterified pectin samples, with P representing enzymatically demethylesterified pectins and C the alkaline demethylesterified pectins. DB_{abs} (%) is the estimated absolute degree of blockiness repeated from Table 2.1, q^G_{max} and q^C_{max} are the maximum Fe^{2+}-binding capacities, expressed as mol Fe^{2+}/mol GalA and mol Fe^{2+}/mol COO^-, respectively, and K_L (L/mmol Fe^{2+}) represents the interaction energy. Different letters (a-h) indicate significant differences ($p \leq 0.05$) in estimated parameter between different pectin samples.

Sample code	DB_{abs} (%)	q^G_{max} (mol Fe^{2+}/mol GalA)	q^C_{max} (mol Fe^{2+}/mol COO^-)	K_L (L/mmol Fe^{2+})
CP95	$< 0.74^{i}$	0.217 ± 0.005^{g}	4.427 ± 0.110^{a}	85 ± 15^{de}
P69	20.6 ± 1.0^{g}	0.253 ± 0.004^{f}	0.826 ± 0.013^{b}	146 ± 16^{cd}
P60	29.0 ± 1.3^{f}	0.309 ± 0.006^{e}	0.768 ± 0.013^{cd}	190 ± 26^{c}
P39	49.9 ± 1.0^{d}	0.429 ± 0.015^{bc}	0.705 ± 0.025^{de}	474 ± 104^{ab}
P33	57.1 ± 2.5^{c}	0.463 ± 0.011^{b}	0.692 ± 0.017^{e}	351 ± 43^{a}
P13	82.4 ± 1.7^{a}	0.523 ± 0.010^{a}	0.602 ± 0.012^{f}	399 ± 41^{a}
C67	5.1 ± 0.1^{i}	0.191 ± 0.004^{h}	0.582 ± 0.012^{fg}	79 ± 10^{e}
C46	12.3 ± 0.3^{h}	0.270 ± 0.005^{f}	0.499 ± 0.010^{h}	195 ± 31^{bc}
C36	20.8 ± 0.8^{g}	0.372 ± 0.011^{d}	0.580 ± 0.017^{fg}	129 ± 23^{cde}
C30	28.1 ± 0.4^{f}	0.401 ± 0.010^{cd}	0.572 ± 0.014^{fg}	119 ± 18^{cde}
C20	43.9 ± 0.9^{e}	0.427 ± 0.009^{bc}	0.537 ± 0.011^{gh}	180 ± 22^{c}

5.3.2 Influence of pectin DM and DB_{abs} on the maximum Fe^{2+}-binding capacity

As presented in **Table 5.1** and **Figure 5.2 a** and **b**, presenting the q^{G}_{max} values as a function of the DM (%) and estimated DB_{abs} (%), the DM had a clear influence on the Fe^{2+}-binding capacity of both P- and C-pectins. In general, the maximum binding capacities, expressed in mol Fe^{2+}/mol GalA (q^{G}_{max}), of both P- and C-pectins increased significantly ($p \leq 0.05$) with decreasing DM. For instance, commercial high methylesterified citrus pectin CP95, could bind 0.217 ± 0.005 mol Fe^{2+}/mol GalA, while P13 and C20 revealed q^{G}_{max} values of 0.523 ± 0.010 and 0.427 ± 0.009 mol Fe^{2+}/mol GalA, respectively. This observation can be attributed to the higher number of negatively chargeable carboxyl groups in pectin samples with lower DM. The results of this study are in agreement with the findings of Chapter 3 and Khotimchenko et al. (2008), that decreasing the DM of citrus pectin promoted the Zn^{2+}- or Ca^{2+}-binding capacity. The data of the aforementioned researchers were also modeled by the Langmuir adsorption isotherm. In the case of C-pectins of the present study, one exception was observed where C67 bound significantly less Fe^{2+} than CP95, with 0.191 ± 0.004 compared to 0.217 ± 0.005 mol Fe^{2+}/mol GalA, respectively (**Table 5.1** and **Figure 5.2 a**). Despite exhibiting a lower DM value, the random demethylesterification did not necessarily increase the sensitivity of C67 to Fe^{2+} due to the limited blocks of chargeable non-methylesterified GalA residues. Consequently, C67 and CP95 exhibited comparable and low DB_{abs} values, which probably explains the comparable maximum binding capacities. Moreover, it evidences that a certain number of blocks (DB_{abs} > 5.1 ± 0.1%, **Table 5.1**) has to be achieved before pectin-Fe^{2+} interactions occurred. This observation is in comparison with reported pectin-Ca^{2+} interactions, where in general at least six to ten consecutive non-methylesterified GalA units are required along the pectin chain for formation of stable junction zones with Ca^{2+} (Luzio & Cameron, 2008; Ngouémazong et al., 2012c; Thakur et al., 1997; Voragen et al., 2009).

More insight into the role of pectin DM and DB_{abs} in the Fe^{2+}-binding capacity was obtained by comparing the q^{G}_{max} values of P- and C- pectins among each other. From **Figure 5.2**, it is clear that q^{G}_{max} values increased with decreasing DM or increasing DB_{abs} for both P- and C-pectins. This implies that pectin with both a higher number and more consecutive negatively chargeable non-methylesterified GalA units bound a higher amount of Fe^{2+}. However, from a DB_{abs} of approximately 44%, only little further increase in the maximum binding capacity occurred. Irani, Owen, Mercadante,

and Williams (2017) also observed that maximum 40% of the galacturonic acid residues, present in blocks, was bound to counter ions. This observation contrasts with a previous study in Chapter 3 on pectin-Zn^{2+} or -Ca^{2+} interactions, in which the amount of Zn^{2+} or Ca^{2+} bound to pectin increased with increasing DB_{abs} until the highest DB_{abs} explored (82.4 ± 1.7%). This implies that the electrostatic interaction between pectin and Zn^{2+} or Ca^{2+} was continuously promoted by an increase in the number or length of blocks of consecutive negatively chargeable GalA units, while an increase in blocks of negatively chargeable carboxyl groups beyond 44% did not necessarily lead to more Fe^{2+}-binding.

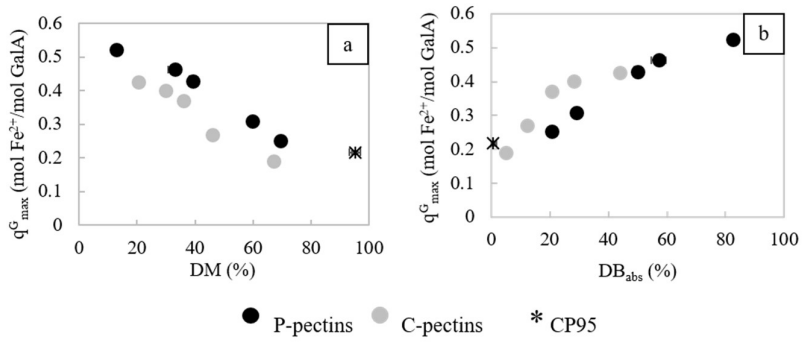

Figure 5.2: Estimated maximum binding capacity, q^G_{max} (mol Fe^{2+}/mol GalA) with standard deviation as a function of a) DM (%) with standard deviation and b) estimated DB_{abs} (%) with standard deviation of enzymatically (P-pectins, black) and alkaline (C-pectins, grey) demethylesterified pectins, and commercial high methylesterified citrus pectin (CP95, black asterisk) as determined by an equilibrium adsorption experiment.

For a given DM, the P-pectins showed generally significantly ($p \leq 0.05$) higher q^G_{max} values than the C-pectins, which is illustrated in **Figure 5.2 a**. For instance, for P39 and C36, both pectin samples with similar DM, q^G_{max} values of 0.429 ± 0.015 and 0.372 ± 0.011 mol Fe^{2+}/mol GalA, respectively, were observed. This difference in q^G_{max} between the P- and C-pectins for a given DM could be largely attributed to the higher DB_{abs} of the P-pectins. In addition, higher maximum binding capacities were observed for C-pectins compared to P-pectins of the same DB_{abs} (**Figure 5.2 b**), with 0.309 ± 0.006 mol Fe^{2+}/mol GalA for P60 (DB_{abs} of 29.0 ± 1.3%) and 0.372 ± 0.011 mol Fe^{2+}/mol GalA for C36 (DB_{abs} of 28.1 ± 0.4%), which is explained by the lower DM for the C-pectins. Although both structural parameters (DM and DB_{abs}) influenced the Fe^{2+}-binding capacity of pectin, it can be concluded that the DM is more determining the maximum Fe^{2+}-binding capacity of pectin than the DB_{abs}. Samples with a similar DM exhibited smaller differences in q^G_{max} value (**Figure 5.2 a**) than samples with a

similar DB_{abs} (**Figure 5.2 b**). In other words, the number of negative charges had a larger influence on the amount of Fe^{2+} that can be bound compared to the consecutiveness of these negative charges. The conclusions of the present study that both the DM and DB_{abs} influenced the Fe^{2+}-binding capacity are in accordance with the results of the Zn^{2+}- or Ca^{2+}-binding study as reported in Chapter 3.

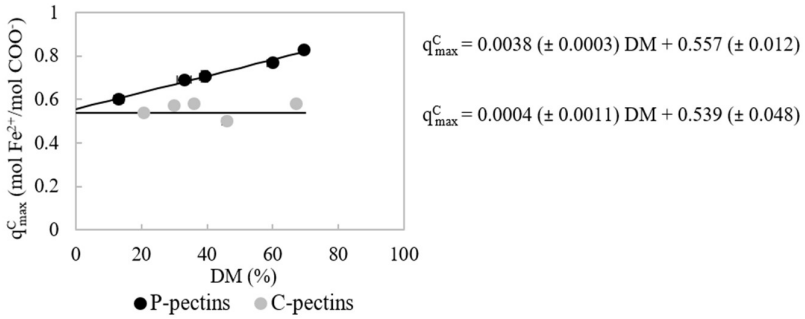

Figure 5.3: Estimated maximum binding capacity, q^C_{max} (mol Fe^{2+}/mol COO^-) with standard deviation as a function of DM (%) with standard deviation of enzymatically (P-pectins, black) and alkaline (C-pectins, grey) demethylesterified pectins as determined by an equilibrium adsorption experiment. Symbols indicate the estimated q^C_{max} values. Black curves represent linear models with associated equations.

Finally, in **Table 5.1** the moles of Fe^{2+} bound to each mole of COO^- for the different pectin samples are shown (q^C_{max}). The commercial high methylesterified citrus pectin (CP95) revealed an exceptionally high value, which probably implies binding of Fe^{2+} to functional groups of pectin, other than COO^-, such as hydroxyl groups as proposed for Zn^{2+} (Assifaoui et al., 2015). Nevertheless, low DM pectins also contain hydroxyl groups but probably showed higher sensitivity for ionic interaction via negatively chargeable carboxyl groups. **Figure 5.3** shows the q^C_{max} values (mol Fe^{2+}/mol COO^-) as a function of the DM (%), fitted by a linear equation (q^C_{max} = a.DM + b). The q^C_{max} value of CP95 is removed to clearly visualize the differences between the P- and C-pectins. The q^C_{max} values exhibited by the C-pectins were not significantly different ($p > 0.05$) and were characterized by a linear curve with a slope not significantly different ($p > 0.05$) from zero. In addition, the q^C_{max} values of the C-pectins were approximately 0.5 mol Fe^{2+}/mol COO^-, which implies an ionic interaction of two moles of COO^- with one mole of Fe^{2+} and suggests egg-box model binding as described for Ca^{2+} (Grant et al., 1973). The P-pectins exhibited an increase in binding capacity with increasing DM, with a slope significantly ($p \leq 0.05$) higher than that of the C-pectins. For a given DM, this implies that significantly higher amounts of Fe^{2+} were bound to negatively charged carboxyl groups of pectin with a higher DB_{abs} (P-pectins compared to C-

pectins) or that other interactions than via COO^- were possible. Moreover, it indicates monocomplexation as described for Zn^{2+} and Ca^{2+} for pectins with DM > 40%. It is noteworthy that the estimated parameters of the intercept of both P- and C-pectins are not significantly different, indicating that the amount of Fe^{2+} bound to each mole of COO^- is similar at very low DM or in other words, when DB_{abs} is comparable between the P- and C-pectins.

5.3.3 Influence of pectin DM and DB_{abs} on interaction energy between pectin and Fe^{2+}

The estimated Langmuir constant (K_L) is related to the affinity between pectin and Fe^{2+} and is considered as a measure of the interaction energy (Khotimchenko et al., 2008). The K_L value (L/mmol Fe^{2+}) increased proportionally with decreasing DM and increasing estimated DB_{abs} for both P- and C-pectins, which can be seen in **Table 5.1** and **Figure 5.4 a** and **b**. This observation indicates stronger pectin-Fe^{2+} interactions with an increasing number of (consecutive) negative charges. A sharp increase of K_L was observed between pectin samples with a DB_{abs} of 43.9 ± 0.9% (C20) and 49.9± 1.0% (P39), which evidences that the pectin-Fe^{2+} interaction was clearly stronger when pectin exhibited a higher number or longer blocks of successive negatively chargeable GalA units (DB_{abs} > 44%) (**Figure 5.4 b**). However, beyond this increase, particularly for DB_{abs} values higher than 49%, no significant ($p > 0.05$) increase in K_L value was observed (**Figure 5.4 b**), indicating that a further increment of the DB_{abs} did not lead to stronger pectin-Fe^{2+} interactions.

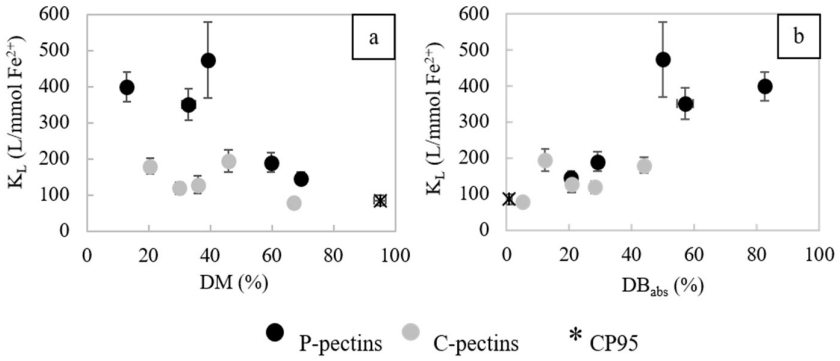

Figure 5.4: Estimated interaction energy, K_L (L/mmol Fe^{2+}) with standard deviation as a function of a) DM (%) with standard deviation and b) estimated DB_{abs} (%) with standard deviation of enzymatically (P-pectins, black) and alkaline (C-pectins, grey) demethylesterified pectins, and commercial high methylesterified citrus pectin (CP95, black asterisk) as determined by an equilibrium adsorption experiment.

Figure 5.4 a also illustrates significant ($p \leq 0.05$) differences in K_L values between the P- and C-pectins with similar DMs, which might be explained by the higher estimated DB_{abs} values for P-pectins compared to C-pectins as P39 (DB_{abs} of 49.9 ± 1.0 %) exhibited a value of 474 ± 104 L/mmol Fe^{2+}, whereas C36 (DB_{abs} of 20.8 ± 0.8 %) showed a K_L value of 129 ± 23 L/mmol Fe^{2+}. Therefore, pectin with a given DM and higher DB_{abs} value interacted stronger with Fe^{2+}, which is in analogy with the reported studies of pectin-Ca^{2+} interactions (Fraeye et al., 2009; Löfgren, Guillotin, Evenbratt, Schols, & Hermansson, 2005; Ralet et al., 2001). In contrast, no clear differences in K_L values were observed between P- and C-pectins of a given DB_{abs} (**Figure 5.4 b**). As a result, it can be concluded that the pectin-Fe^{2+} interaction energy is determined by the DB_{abs}. The DM did not largely influence the Fe^{2+} affinity for pectin with a given DB_{abs}. The findings of this chapter, that the maximum binding capacity and pectin-cation interaction energy were mainly influenced by pectin DM and DB_{abs}, respectively, are in accordance with the results of our previous study on pectin-Zn^{2+} or Ca^{2+} interaction (Chapter 3).

5.4 CONCLUSION

This research explored the relation between the structural properties of citrus pectin, in particular the DM and DB_{abs}, and its Fe^{2+}-binding capacity. The adsorption isotherms obtained were well described by the Langmuir adsorption model. Analogous to the results of Chapter 3 regarding the Zn^{2+}- and Ca^{2+}-binding, the results of this chapter revealed a dependence of the Fe^{2+}-binding of citrus pectin on both pectin DM and DB_{abs}. A high Fe^{2+}-binding capacity was exhibited by low DM pectin due to the presence of a higher number of negatively chargeable carboxyl groups, and by a higher number of blocks of successive non-methylesterified GalA units (high DB_{abs}). In addition, the maximum binding capacity was mainly determined by the DM while the pectin-Fe^{2+} interaction energy was predominantly influenced by the DB_{abs} of citrus pectin. Comparison of the results of this chapter with the Zn^{2+}- and Ca^{2+}-binding from Chapter 3 revealed the highest maximum binding capacity and interaction energy for Zn^{2+} compared to Ca^{2+} and Fe^{2+}. This could be explained by possible binding of Zn^{2+} to other functional groups (such as OH^-) in addition to carboxylate groups or by the fact that Zn^{2+} exhibits the highest electronegative value. The results from this chapter suggest that targeted modification of pectin DM and DB_{abs} can be applied to derive desired functionality, particularly cation-binding capacity. For instance, pectin structural properties can be directed to obtain high Fe^{2+}-binding capacities for use as antioxidant in emulsion-based food products, as Fe^{2+} is considered to be a pro-oxidative metal ion. Moreover, the results of this chapter could form the basis for exploring pectin *in situ* for its cation-binding capacity. By targeted processing of fruits and vegetables, pectin can be structurally modified to obtain desired cation-binding properties, without addition of externally modified pectin as an additive.

CHAPTER 6

INFLUENCE OF PECTIN DEGREE AND PATTERN OF METHYLESTERIFICATION ON PHYSICAL AND OXIDATIVE STABILITY OF OIL-IN-WATER EMULSIONS[6]

6.1 INTRODUCTION

Oil-in-water emulsions (o/w), rich in poly-unsaturated fatty acids (PUFAs), especially ω-3 PUFAs, are susceptible to lipid oxidation, which negatively affects the quality and shelf-life of the food product (McClements et al., 2000). The autoxidation of PUFAs, which are located at the oil droplet surface, is typically accelerated in o/w emulsions by Fe^{2+}, located in the aqueous phase (Jacobsen, Let, Nielsen, & Meyer, 2008; McClements & Decker, 2000; Mei et al., 1998). Consequently, chelation of this pro-oxidative metal ion, to remove it from the vicinity of the oil-water interface, is a common strategy to retard lipid oxidation (Chen, McClements, & Decker, 2010; Hu et al., 2004; McClements et al., 2000). Currently, ethylenediaminetetraacetic acid (EDTA) is widely used as a commercial antioxidant as it has been shown to effectively reduce lipid oxidation in several o/w emulsions due to its high chelating capacity (Haahr & Jacobsen, 2008; Hu et al., 2004; Mei et al., 1998). A ratio EDTA:Fe^{2+} of higher than one, i.e. excess of EDTA, has been reported to effectively reduce the Fe^{2+}-mediated lipid oxidation (Hu et al., 2004; Mozuraityte, Kristinova, Rustad, & Storrø,

[6] This chapter is based on following paper:
Celus, M., Salvia Trujillo, L., Kyomugasho, C., Maes, I., Van Loey, A., Grauwet, T., and Hendrickx, M. (2018). Structurally modified pectin for targeted lipid antioxidant capacity in linseed/sunflower oil-in-water emulsions. *Food Chemistry*, 241: 86-96

2016). However, the use of such synthetic additives is associated with a negative perception of the consumer because of its reported cytotoxic and genotoxic effects (Lanigan & Yamarik, 2002). Particular interest consists on reducing synthetic antioxidants by using natural alternatives, for instance pectin, to chelate Fe^{2+} in lipid-based food products, which are more appealing to consumers (McClements et al., 2000; Shahidi, 2000). To date, only a few studies explored the antioxidant capacity of pectin (Chen et al., 2010; Huang et al., 2011; Qiu et al., 2015; Shimada et al., 1996; Xu et al., 2017). However, most of these authors did not study the effect of pectin structural properties on the antioxidant capacity. Only Chen et al. (2010) and Huang et al. (2011) included different pectin DMs but they did not report the pectin source or the method of demethylesterification. In general, these studies did not investigate the effect of pectin structural properties on the lipid antioxidant capacity by systematically modifying the pectin structural properties, in terms of DM and DB_{abs}. In this sense, process-induced changes of pectin structural properties are hypothesized to alter its cation-binding capacity and subsequently its antioxidant capacity. The addition of pectin to food emulsions as an antioxidant can contribute to more natural food products and to multiple functionalities, as pectin is already used as a functional additive in food emulsions. However, fundamental insights into the influence of pectin addition on emulsion stability are necessary for desired food formulation. On the one hand, pectin has been reported to stabilize emulsions due to its ability to increase the viscosity of the aqueous phase in o/w emulsions (Dickinson, 2003). On the other hand, the addition of sufficiently high concentrations of polysaccharides (> *critical flocculation concentration*) to the aqueous phase of emulsions, stabilized with previously adsorbed surfactants, might cause physical instability by either depletion or bridging flocculation (Dickinson, 2003). In addition to the (de)stabilizing effect of polysaccharides, an increased viscosity of the aqueous phase in o/w emulsions is hypothesized to influence the oxidative stability by restricting the movement of metal ions or oxygen through the aqueous phase towards the oil droplet (Shimada et al., 1996). Therefore, this chapter aims to investigate the role of targeted citrus pectin modification, in particular the degree of methylesterification and blockiness, in the oxidative and physical stability of linseed/sunflower o/w emulsions. This goal is achieved by addition of enzymatically or alkaline demethylesterified pectin structures in the aqueous phase of linseed/sunflower o/w emulsions. In addition, the lipid antioxidant capacity of the demethylesterified citrus pectins will be compared with the antioxidant capacity of EDTA.

6.2 MATERIALS AND METHODS

6.2.1 Materials

The pectin samples with different degrees and patterns of methylesterification, as generated and structurally characterized in Chapter 2, were used to study the lipid antioxidant capacity in oil-in-water emulsions. Particularly, commercial high methylesterified citrus pectin (CP95), enzymatically demethylesterified (P60, P33, and P13) and alkaline demethylesterified (C58 and C10) pectins were used. A blend of linseed/sunflower oil (30/70%) was kindly donated by Vandemoortele (Izegem, Belgium) and was used as it contained a high amount of poly-unsaturated fatty acids in order to study the lipid oxidation. Ethylenediaminetetraacetic acid (EDTA) disodium salt hydrate was obtained from Acros organics (Geel, Belgium), while $FeSO_4$, $FeCl_3$, $BaCl_2$, Tween 80, iso-octane, methanol, and ammonium thiocyanate were obtained from Sigma-Aldrich Belgium. 2-propanol was purchased from VWR Chemicals (Leuven, Belgium). Ultrapure water (organic free, 18.2 MΩ cm resistance) was supplied by a Simplicity™ water purification system (Millipore, Burlington, MA, USA) and used for emulsion and sample preparation as well as for analytical experiments. All chemicals used were of analytical grade.

6.2.2 Emulsion preparation

Stock o/w emulsion

First, a coarse o/w emulsion was prepared by blending 20% (w/v) linseed/sunflower oil (LSSO) and 2% (w/v) Tween 80 with 78% (w/v) of ultrapure water at 9500 rpm for 10 min using an Ultra-Turrax (T25, IKA, Staufen, Germany). This o/w emulsion was further stabilized by high-pressure homogenization at 100 MPa for one pass (Pressure Cell Homogenizer, Stansted Fluid Power LTD., Harlow, UK) and is referred as the stock emulsion.

o/w emulsions with pectin or EDTA addition

Stock pectin solutions of 1.7% (w/v) were prepared for addition to the stock emulsion by dissolving pectin samples in ultrapure water overnight to ensure complete dissolution. In addition, stock EDTA solutions (3 mM) were freshly prepared before addition to the stock emulsion. Subsequently, the pectin solutions or EDTA solutions were mixed with the stock emulsion by stirring for 10 min to obtain a final concentration of 5% (w/v) LSSO, 0.5% (w/v) Tween 80 and different pectin (0.1 and 1% w/v) or EDTA (0.05 and 0.1 mM) concentrations. In the emulsion without pectin or EDTA (control), the stock emulsion was mixed with equal amounts of ultrapure water. Fe^{2+} was added to explore the influence of Fe^{2+} on both lipid oxidation and

emulsion physical stability. For this, a stock Fe^{2+} solution of 0.5 M was freshly prepared by dissolving $FeSO_4.7H_2O$ into ultrapure water and added to the emulsions to obtain a final concentration of 0.1 mM Fe^{2+} (based on preliminary experiments, results not shown). For the physical stability study, emulsions were prepared both with and without Fe^{2+}, whereas for the oxidation study all samples contained 0.1 mM Fe^{2+}. Given that the 0.1% pectin concentration was chosen as for this concentration some polysaccharides have been reported to exhibit a significant antioxidant capacity (Chen et al., 2010; Salvia-Trujillo et al., 2016) while concentrations higher than 1% could increase the viscosity substantially thus possibly affecting the lipid oxidation results, the COO^-:Fe^{2+} ratios varied between 1.75 and 32 or between 17.5 and 320 for 0.1% and 1% (w/v) pectin concentrations, respectively. This indicates that even at the low pectin concentration (0.1% w/v) an excess of free carboxyl groups was present to bind all Fe^{2+} added. EDTA concentrations of 0.05 and 0.1 mM were chosen to obtain EDTA:Fe^{2+} ratios of 1:2 and 1:1, respectively. EDTA has been shown to effectively reduce the Fe^{2+}-mediated lipid oxidation when present in ratios of 1:1 or higher (Hu et al., 2004; Mozuraityte et al., 2016).

For the physical stability study, emulsions without or with high (CP95), intermediate (P60) and low (P13) DM pectin (enzymatically demethylesterified) and without or with Fe^{2+} addition were evaluated. Samples were divided into small glass tubes containing 5 mL aliquots. On the one hand, tubes were stored for creaming index measurements, so that they remained undisturbed, and on the other hand for particle size distribution, particle electrical charge, pH, and microscopic measurements. Emulsions were stored in the dark at 25 °C. For the oxidative stability study, same pectin samples were used as described above and additionally alkaline (C58 and C10) and enzymatically (P33) demethylesterified pectin samples were incorporated. Emulsions were stored in the dark at 35 °C for approximately 21 days and the peroxide formation was determined.

6.2.3 Physical characterization of emulsion stability

The physical stability of all LSSO emulsions was determined by measuring the particle electrical charge, creaming index, particle size distribution and the microstructure.

6.2.3.1 Particle electrical charge

The electrical charge (ζ-potential) of the oil droplets in all LSSO emulsions and of the pectin solutions was determined by phase-analysis light scattering using an automated capillary electrophoresis equipment (Zetasizer NanoZS, Malvern Instruments,

Worcestershire, UK). Before each measurement, samples were diluted 1:100 (v/v) with ultrapure water and subsequently transferred into a capillary cell equipped with two electrodes. During the measurement, a potential was applied and the electrophoretic mobility was determined based on the particle velocity through the sample. The electrophoretic mobility is converted into ζ-potential values by the instrument's software, using the equation of Henry. The ζ-potentials of the emulsions and pectin samples were determined immediately after being produced. The sample preparation and analysis were performed in duplicate.

6.2.3.2 Creaming index

The creaming index of all LSSO emulsions, with and without Fe^{2+} and/or pectin addition, was measured after two weeks of storage. The capped glass tubes, filled with the emulsion, were not shaken or opened during storage time. The total height of the emulsion (H_e) and the height of the cream layer (H_c) were measured using a caliper (Mitutoyo Belgium, Kruibeke, Belgium). The creaming index (%) is expressed as follows (Guerra-Rosas, Morales-Castro, Ochoa-Martínez, Salvia-Trujillo, & Martín-Belloso, 2016):

$$\text{Creaming index (\%)} = \left(\frac{H_c}{H_e}\right).100 \qquad [6.1]$$

6.2.3.3 Particle size distribution

The particle size distributions of all LSSO emulsions, with and without Fe^{2+} and/or pectin addition, were measured using a laser diffraction equipment (Beckman Coulter Inc., LS 13 320, Miami, FL, USA). The measurement was performed in duplicate and at day 0, 7 and 14 of storage. Emulsions were agitated prior to particle size measurements and a small amount was poured into a stirring tank which was filled with demineralized water. The sample was pumped into the measurement cell were the laser light, with the wavelength of the main illumination source 750 nm and wavelengths of halogen light for Polarization Intensity Differential Scattering (PIDS) 450 nm, 600 nm, and 900 nm, is scattered by the particles. The intensity of the scattered laser light is detected and analyzed by the Fraunhofer model. The particle sizes of the emulsions are reported as the d_{43} or d_{32} value, which define the volume-weighted or surface-weighted mean particle size, respectively.

6.2.3.4 Microstructure

The microstructure of representative LSSO emulsions mixed with 1% (w/v) pectin solutions and Fe^{2+} (0.1 mM) was determined at day 0, 7 and 14 of storage. Emulsions were gently agitated before placing a drop on a microscope slide. Visualization of the

microstructure was performed at different magnifications with an optical microscope (Olympus BX41, Olympus Corporation, Tokyo, Japan) equipped with a digital camera (Olympus BX51, Olympus Optical Co. LTD., Tokyo, Japan).

6.2.4 Determination of emulsion oxidative stability

The oxidative stability of LSSO emulsions was studied as a function of storage time by assessing the formation of peroxides spectrophotometrically as a measure for primary oxidation products. The procedure is based on the method described by Shantha and Decker (1994) with some modifications. A 0.3 mL aliquot of the agitated emulsion was added to 1.5 mL iso-octane/2-propanol (3:1 v/v) in glass tubes and vortexed three times for 10 s. The tubes were then centrifuged (Sigma 4-16KS centrifuge, swing-out rotor, Osterode am Harz, Germany) at 1000 g for 2 min at 20 °C and 0.2 mL of the upper organic layer was after centrifugation added to 2.8 mL of a methanol-2-propanol (2:1 v/v) solution. Subsequently, 15 µL of a 3.94 M ammonium thiocyanate solution and 15 µL of a 0.0072 M Fe^{2+} solution were added and the mixture was vortexed. After 20 min in absence of light, the absorbance of the mixture was measured at 510 nm (Ultropec 2100 Pro, Amersham Bioscience, Little Chalfont, UK). The analysis was performed in triplicate and the Fe^{3+}concentration in the emulsion was determined from a standard curve of $FeCl_3$ solutions (0-2.7 µM). The peroxide concentration, expressed in mEq peroxide/L emulsion, was calculated by dividing the concentration of Fe^{3+} in the emulsion (µg/mL) by 55.845 g/mol, the atomic weight of Fe^{3+}, and by two to express the peroxide value as mEq of peroxide instead of mEq of oxygen as explained by Shantha and Decker (1994).

6.2.5 Statistical data analysis

Statistical analysis of the experimental data was carried out with the statistical software JMP (JMP 13, SAS Institute Inc., Cary, NC, USA). A one-way analysis of variance (ANOVA) and a Tukey HSD test were carried out to analyze significant differences with a 95% confidence interval ($p \leq 0.05$) between the experimental data.

6.3 RESULTS AND DISCUSSION

6.3.1 Emulsion physical stability

The influence of pectin DM, pectin concentration, and Fe^{2+} addition on the physical stability of LSSO emulsions was studied by measuring the particle electrical charge, creaming index, particle size distribution, and the microstructure during storage time. LSSO emulsions were prepared with and without the addition of 0.1 mM Fe^{2+} and/or pectin with different DMs at two different concentrations (0.1 and 1% w/v).

6.3.1.1 Particle electrical charge measurements

ζ-potential measurements were assessed to determine the electrical charge of the oil droplets at the oil-water interface, which indicates the species that are adsorbed at the interface and therefore could help to understand the possible destabilization phenomena. The electrical charges (ζ-potential) of the 0.1 and 1% (w/v) pectin solutions as such were also measured and presented in **Figure 6.1 a, b**, and **c**.

Pectin with decreasing DM showed a more negative ζ-potential in comparison with high DM pectin due to their higher number of negatively chargeable non-methylesterified GalA units. For instance, the ζ-potential of CP95 pectin solution at 0.1 % (w/v) was -16.3 ± 1.9 mV whereas the one of P13 was -41.5 ± 6.9 mV at the same concentration. In addition, pectin solutions at a higher concentration revealed a more negative ζ-potential, related to a higher number negatively chargeable particles.

The electrical charges of the LSSO emulsions are also shown in **Figure 6.1 d, e**, and **f** and reveal that all emulsions were characterized by anionic charged oil droplets, despite the use of a non-ionic surfactant (Tween 80). Since Tween 80 is not expected to provide a negative charge to the oil droplets, these results can be explained by the presence of impurities, such as free fatty acids, from the surfactant or from the oil (McClements, 2016). Indeed, the pH values of the emulsions were above the pKa value of fatty acids (4.8-5) (Spector, 1975), leading to ionization of their carboxyl groups, which could contribute to the negative charge of the oil droplets. Of secondary importance in explaining the negative charges of the oil droplets is the orientation of OH^- ions of the aqueous phase in the vicinity of the oil droplets (McClements, 2016). Besides, it cannot be excluded from the results of this study that pectin is partly adsorbing on the oil droplets via its methylesters groups (Verkempinck et al., 2018) and thus partly contributing to the negative ζ-potentials via its negatively charged non-methylesterified carboxyl groups. Nevertheless, the highly negative ζ-potential value of the emulsion without pectin (black filled bar) suggests that other compounds than pectin are causing the negative ζ-potential. As negative ζ-potentials are observed in the emulsions, it can be assumed for this study that pectin would be most probably present in the aqueous phase rather than adsorbing at the oil droplet, since i) the possible electrostatic repulsion between the negatively charged oil droplet surfaces and anionic pectin molecules and ii) Tween 80 is known to be a strong amphiphilic emulsifier that provides steric stabilization at oil-water interfaces.

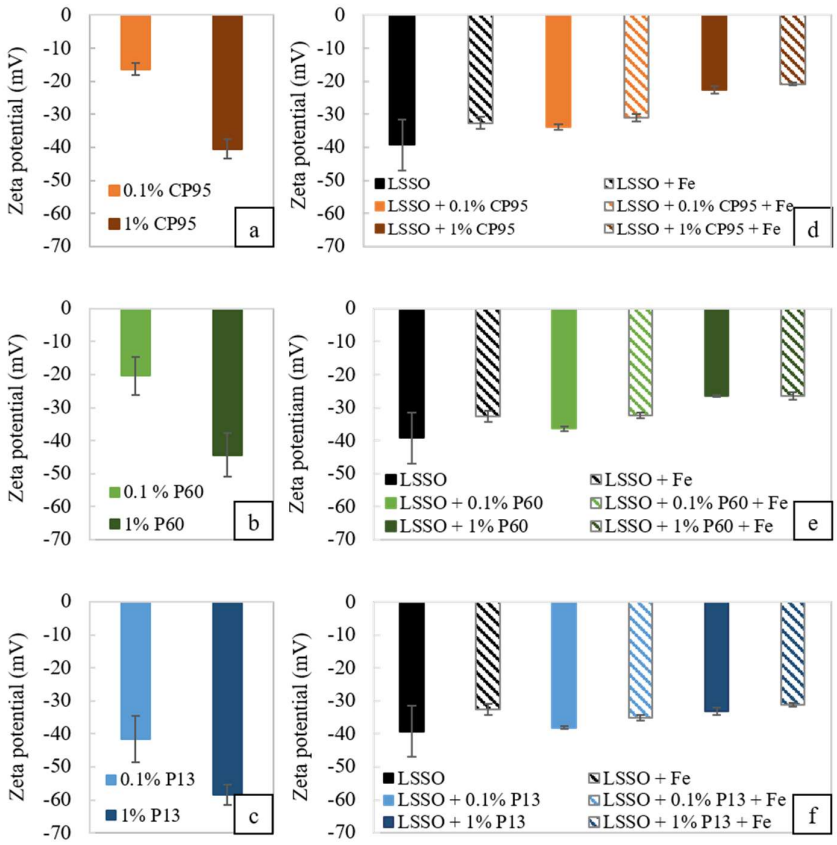

Figure 6.1: Zeta (ζ)-potential (mV) with standard deviation at day 0 of storage of the pectin solutions (a-c) and linseed/sunflower oil (LSSO) emulsions (d-f) with (0.1 and 1% w/v) and without commercial high methylesterified citrus pectin (CP95) and enzymatically demethylesterified pectin samples (P-pectins), with and without 0.1 mM Fe^{2+} (striped and filled bars, respectively).

The addition of pectin to the LSSO emulsions led to less negative ζ-potential values (**Figure 6.1 d, e**, and **f**), which was only significant ($p \leq 0.05$) in the 1% (w/v) pectin containing emulsions. For instance, the ζ-potential of the LSSO emulsion without Fe^{2+} changed from -39.2 ± 7.7 mV to -22.6 ± 1.1 mV, -26.4 ± 0.3 mV and -33.1 ± 1.1 mV with addition of 1% (w/v) CP95, P60 and P13, respectively. The ζ-potential is determined by measurement of the Brownian motion of particles through a path when a voltage is applied, which means that the higher the absolute electrical charge of particles, the higher their electrophoretic mobility. Therefore, the less negative ζ-potential values observed when pectin is added to the emulsions, can be attributed to two possible hypotheses. Firstly, if anionic polymers, such as pectin, are located in

the aqueous phase, the difference in potential between the oil droplet surface and aqueous phase will be reduced, resulting in a less negative net charge. This implies a slower movement of particles and thus a less negative ζ-potential value. Secondly, the electrophoretic mobility of the particles might be influenced by the particle size, being that smaller particles have a higher mobility than larger particles. In this regard, the addition of pectin to the emulsions led to an increase in volume-weighted mean particle sizes (d_{43}) (**Table 6.1**, for discussion see Section 6.3.1.2), increasing from 0.91 ± 0.05 µm to 1.78 ± 0.06 µm, which might have resulted in a slower movement of the particles, explaining the less negative ζ-potential observed in the emulsions with pectin in comparison with the non-pectin containing emulsions. Both hypotheses also explain the observation that higher pectin concentration (1% w/v) led to less negative ζ-potential values compared to lower concentration (0.1% w/v).

The ζ-potential was also slightly less negative with increasing pectin DM, as for example -33.8 ± 0.8 mV for 0.1% (w/v) CP95, -36.4 ± 0.8 mV for 0.1% (w/v) P60 and -38.1 ± 0.4 mV for 0.1% (w/v) P13. This observation is in contrast with the abovementioned explanation about the reduced potential difference. The location of pectin, being in the aqueous phase or on the oil-water interface, is however not really clear from these results, leading to several possible hypotheses explaining the results observed in this particle electrical charge study. In this specific case, i.e., the more negative ζ-potential with decreasing DM, might be explained by interference of the pectin negative charges with the measurement of the oil droplet charges. Low DM pectin contains more negatively chargeable carboxyl groups, resulting in a more negative ζ-potential. Surh, Decker, and McClements (2006) reported that pectin is expected to be present in the aqueous phase when oil droplets exhibit a negative ζ-potential. However, they did not observe an increase in ζ-potential if 0.25 wt% pectin was added to sodium caseinate stabilized o/w emulsions, which might be explained by the lower pectin concentration compared to the present study. In addition, they did not observe differences between low and high DM pectin. As a result, the influence of pectin on the ζ-potential of o/w emulsions might be mainly concentration dependent, since in this study only significant differences in ζ-potentials were observed in LSSO emulsions containing 1% (w/v) pectin.

The addition of Fe^{2+} (0.1 mM) to the LSSO emulsions did not significantly influence the electrical charge of the oil droplets, except for the emulsion without pectin (**Figure 6.1**). In the latter, Fe^{2+} might absorb onto the negatively charged oil droplets and lead to less negative ζ-potential values. Ogawa, Decker, and McClements (2003) also observed less negative ζ-potential values when adding Ca^{2+} ions to lecithin stabilized

o/w emulsions and attributed this to adsorption of Ca^{2+} ions on the negatively charged oil droplet surfaces. In the LSSO emulsions containing pectin, Fe^{2+} is probably bound to pectin, which is located in the aqueous phase, thus not being able to increase the electrical charge of the oil droplets.

6.3.1.2 Emulsion particle size, creaming index and microstructure

The presence of hydrocolloids in emulsions may compromise emulsion stability (Dickinson, 2003). Therefore, the emulsions particle size distribution and creaming index (%) were measured to detect possible destabilization phenomena occurring during two weeks of storage at 25 ºC. The volume-weighted (d_{43}) and surface-weighted (d_{32}) mean particle sizes are presented in **Table 6.1** for each LSSO emulsion as a function of storage time (day 0, 7 and 14), together with the creaming index (%), measured at day 14. Both the d_{43} and d_{32} values of the samples showed the same trend. However, the discussion will mainly focus on the volume-weighted mean particle size, as it is more sensitive to particle size growth. Representative micrographs of LSSO emulsions with pectin (1% w/v) and Fe^{2+} addition and its changes during storage time are shown in **Figure 6.2**. No clear differences were observed between the micrographs of the emulsions with and without Fe^{2+}.

The LSSO emulsion presented an initial mean particle size of 0.91 ± 0.05 µm which remained constant during 14 days of storage, without evidences of creaming (**Table 6.1**). Moreover, after the addition of Fe^{2+} (0.1 mM) to the LSSO emulsion at day 0, its particle size remained unchanged. During storage time, LSSO emulsion with Fe^{2+} exhibited a significant larger particle size compared to the emulsion without Fe^{2+}. Nonetheless, no creaming could be detected after 14 days of storage in both the LSSO emulsion and the Fe^{2+}-containing LSSO emulsion. This evidenced that, despite the addition of a positively charged entity to the system (Fe^{2+}), the strong steric stabilization provided to the oil droplets by the surfactant (Tween 80) was not compromised at this Fe^{2+} concentration (0.1 mM), which was also confirmed by the microscopic images (**Figure 6.2 a, b**, and **c**). Nevertheless, preliminary studies (data not shown) revealed that the addition of an increased Fe^{2+} concentration to LSSO emulsions, up to 2 mM, lead to strong emulsion instability, which was already noticeable at day 0. This implies that Fe^{2+} at high concentrations may substantially absorb at the oil droplet surface, resulting in a decrease of the electrostatic repulsion between the oil droplets and inducing emulsion instability. These results might be important regarding the formulation of emulsion-based food products with a high Fe^{2+} content.

Table 6.1: Volume-weighted (d_{43}) and surface-weighted (d_{32}) mean particle sizes (µm) ± standard deviation, measured at storage day 0, 7, 14 and the creaming index (%) ± standard deviation at storage day 14 of linseed/sunflower oil (LSSO) emulsions without and with (0.1 and 1% w/v) commercial high methylesterified citrus pectin (CP95) and enzymatically demethylesterified pectin samples, with or without 0.1 mM Fe^{2+}. Different capital (A-C) and lower case letters (a-g) indicate significant differences ($p \leq 0.05$) in d_{43} or d_{32} between storage times of the same sample or between different samples at the same storage day, respectively.

Emulsion	Day 0		Day 7		Day 14		Creaming index (%)
	d_{43} (µm)	d_{32} (µm)	d_{43} (µm)	d_{32} (µm)	d_{43} (µm)	d_{32} (µm)	Day 14
LSSO	0.91 ± 0.05^{Af}	0.52 ± 0.01^{Ae}	0.88 ± 0.01^{Af}	0.51 ± 0.04^{Ae}	1.19 ± 0.48^{Acd}	0.45 ± 0.01^{Ag}	0
LSSO + Fe	0.90 ± 0.04^{Cf}	0.51 ± 0.01^{Ae}	5.37 ± 0.07^{Bb}	0.49 ± 0.01^{Ae}	3.60 ± 0.05^{Acd}	0.52 ± 0.04^{Ag}	0
LSSO + 0.1% CP95	1.20 ± 0.01^{Ae}	0.87 ± 0.01^{Acd}	1.20 ± 0.02^{Af}	0.87 ± 0.01^{Ad}	1.13 ± 0.02^{Bd}	0.85 ± 0.01^{Bf}	20.0
LSSO + 0.1% CP95 + Fe	1.17 ± 0.01^{Be}	0.86 ± 0.01^{Bd}	1.20 ± 0.03^{ABf}	0.86 ± 0.01^{Bd}	1.25 ± 0.05^{Ad}	0.88 ± 0.01^{Af}	14.0
LSSO + 1% CP95	1.76 ± 0.10^{Cbc}	1.18 ± 0.07^{Cb}	2.20 ± 0.03^{Be}	1.44 ± 0.03^{Bc}	3.81 ± 0.23^{Acd}	1.83 ± 0.07^{Ae}	28.4
LSSO + 1% CP95 + Fe	1.62 ± 0.02^{Bc}	1.13 ± 0.01^{Cb}	2.25 ± 0.20^{Be}	1.47 ± 0.09^{Bc}	21.45 ± 0.68^{Aa}	2.28 ± 0.02^{Ac}	22.5
LSSO + 0.1% P60	1.14 ± 0.04^{Ae}	0.85 ± 0.01^{Ad}	1.11 ± 0.03^{Af}	0.84 ± 0.01^{Ad}	1.18 ± 0.05^{Ad}	0.87 ± 0.02^{Af}	19.4
LSSO + 0.1% P60 + Fe	1.08 ± 0.04^{Ae}	0.83 ± 0.01^{Ad}	1.12 ± 0.02^{Af}	0.84 ± 0.01^{Ad}	1.05 ± 0.06^{Ad}	0.83 ± 0.02^{Af}	12.7
LSSO + 1% P60	1.78 ± 0.06^{Bab}	1.16 ± 0.03^{Cb}	3.07 ± 0.49^{Bd}	1.72 ± 0.11^{Bb}	15.20 ± 2.33^{Ab}	2.88 ± 0.13^{Ab}	23.8
LSSO + 1% P60 + Fe	1.92 ± 0.05^{Ba}	1.26 ± 0.02^{Ca}	7.38 ± 0.11^{Ba}	1.92 ± 0.09^{Ba}	24.73 ± 5.34^{Aa}	3.34 ± 0.27^{Aa}	21.6
LSSO + 0.1% P13	1.14 ± 0.04^{Ae}	0.88 ± 0.02^{Acd}	1.07 ± 0.03^{Bf}	0.84 ± 0.01^{Bd}	1.08 ± 0.01^{Bd}	0.85 ± 0.01^{Bf}	18.4
LSSO + 0.1% P13 + Fe	1.09 ± 0.06^{Ae}	0.86 ± 0.02^{Ad}	1.09 ± 0.07^{Af}	0.87 ± 0.01^{Ad}	1.11 ± 0.03^{Acd}	0.86 ± 0.01^{Af}	15.1
LSSO + 1% P13	1.14 ± 0.08^{Ce}	0.83 ± 0.01^{Cd}	3.25 ± 0.06^{Bd}	1.72 ± 0.01^{Bb}	5.84 ± 0.59^{Ac}	2.02 ± 0.04^{Ade}	16.0
LSSO + 1% P13 + Fe	1.39 ± 0.09^{Cd}	0.93 ± 0.03^{Cc}	3.73 ± 0.12^{Bc}	1.87 ± 0.02^{Ba}	4.13 ± 0.13^{Acd}	2.07 ± 0.02^{Acd}	18.3

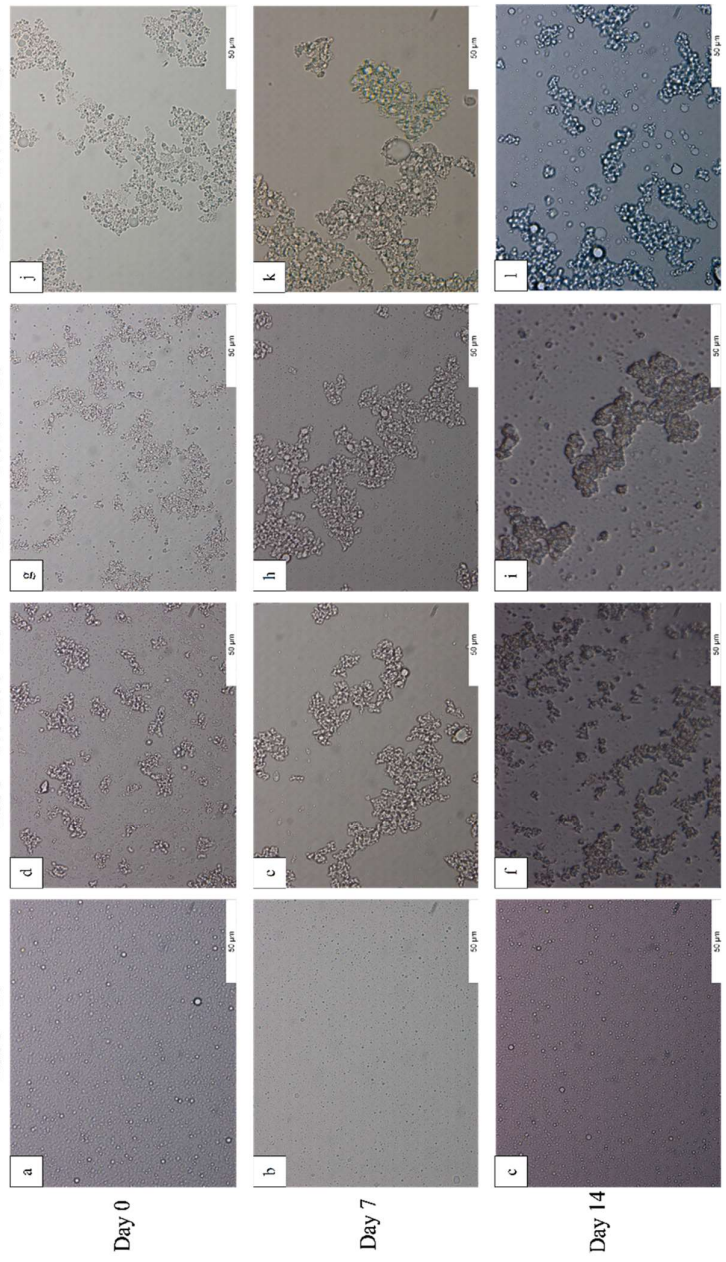

Figure 6.2: Micrographs at day 0, 7, and 14 of storage of the linseed/sunflower oil (LSSO) emulsions without (a-c) and with (1% w/v) (d-l) commercial high methylesterified citrus pectin (CP95) and enzymatically demethylesterified pectin samples (P-pectins), with 0.1 mM Fe^{2+}. Scale bar represents 50 µm.

The addition of pectin solutions to the LSSO emulsion led to an immediate (day 0) significant ($p \leq 0.05$) increase in their particle sizes, varying from 1.08 ± 0.04 to 1.92 ± 0.05 μm (**Table 6.1**), regardless the molecular characteristics of the pectin samples. Nevertheless, this increase was in general more pronounced at higher pectin concentrations (1% w/v) in comparison with lower pectin concentrations (0.1% w/v). The increase in particle size was probably caused by droplet flocculation, which was clearly visible in the microscopy images of LSSO emulsions immediately after being mixed with pectin solutions (day 0) (**Figure 6.2 d, g**, and **j**). Pectin is generally considered to act as a stabilizing agent in emulsions due to the viscosity increase of the aqueous phase, resulting in the hindrance of oil droplets movement (Dickinson, 2003). However, when emulsions are stabilized with strong amphiphilic emulsifiers, such as Tween 80, pectin tend to be mainly located in the bulk aqueous phase. Moreover, due to electrostatic repulsion between the negatively charged oil droplets and the anionic pectin, pectin is assumed in this study to be mainly present in the aqueous phase, despite some of the pectin molecules might be adsorbed onto the oil droplets as well. In this situation, pectin molecules in the aqueous phase are excluded from the vicinity of the oil droplets, thus leading to a pectin concentration depleted zone. The pectin concentration difference between the surroundings of the oil droplets and the bulk aqueous phase creates an osmotic driving force caused by the movement of water to the bulk aqueous phase, resulting in the attraction of oil droplets together. In addition to the depletion flocculation, pectin is reported to cause bridging flocculation which also may contribute to the abovementioned droplet flocculation (Dickinson, 2003). Similar results were obtained by Surh et al. (2006), who observed that the presence of pectin increased the volume-weighted mean diameter of the particle sizes substantially in emulsions exhibiting a negative ζ-potential.

During storage time, the mean particle sizes of the LSSO emulsions containing 0.1% (w/v) pectin (with or without Fe^{2+}) did not significantly change. However, at higher pectin concentrations (1% w/v), the particle size became gradually larger during the two weeks of storage time (**Table 6.1**). Namely, the oil droplet size of the emulsions with 1% (w/v) CP95, P60, and P13 increased from 1.76 ± 0.10 to 3.81 ± 0.23 μm, from 1.78 ± 0.06 to 15.20 ± 2.33 μm and from 1.14 ± 0.08 to 5.84 ± 0.59 μm, respectively. Despite that the oil droplet size remained constant during storage after the addition of 0.1% (w/v) pectin solution, a noticeable emulsion creaming was observed at both pectin concentrations as reflected by the creaming index values (**Table 6.1**). This evidences that the flocs formed immediately after mixing the LSSO emulsion with pectin solutions, led to eventually gravitational separation and

ultimately to the creaming of the oil droplets. Moreover, at a high pectin concentration (1% w/v), the flocculation and creaming led to the coalescence of oil droplets, thus explaining the increase in particle size during storage time. In fact, the coalescence phenomena, with visible larger oil droplets, was also observed in the microscopy images (**Figure 6.2 f, i**, and **l**). During the measurement of the particle size by light scattering technique, samples were diluted in a stirring tank filled with distilled water, thus causing the decrease in pectin concentration and disrupting the flocs formed. However, when the flocculation led to coalescence, this is reflected by an increase in the oil droplet size (Salvia-Trujillo et al., 2016). In addition, the higher instability of LSSO emulsions containing 1% (w/v) pectin was confirmed by the reported creaming indices, which were generally higher than those from the 0.1% (w/v) pectin containing emulsions (**Table 6.1**). These results are in agreement with the findings of Guerra-Rosas et al. (2016), who observed a substantial increase in average particle size as a function of storage time (up to 56 days) in oregano and thyme nanoemulsions containing 1% (w/v) high methylesterified pectin.

In general, the DM of the pectin samples had only little influence on the emulsion destabilization observed. For all pectin types, depletion flocculation and coalescence were observed in LSSO emulsions containing 0.1 and 1% (w/v) pectin, respectively. According to Surh et al. (2006), this may be explained by similar driving forces for depletion flocculation for each pectin sample due to their similar observed molar masses (**Table 2.1**). Emulsions with 1% (w/v) P60 exhibited higher particle sizes during storage time (**Table 6.1**). However, no clear differences were observed by visualization of the microstructure compared to the other DMs (**Figure 6.2**). At lower DMs, slightly lower creaming indices were observed, which can be related to more compact creaming layers (**Table 6.1**).

In bulk oils and emulsions, lipid oxidation occurs at very low rate, therefore Fe^{2+} was added to the emulsions to accelerate the lipid oxidation process, thus allowing the observation of the antioxidant capacity of citrus pectin. In preliminary experiments (data not shown), high destabilization of LSSO emulsions (without pectin) was observed after Fe^{2+}addition at concentrations of 0.1 mM Fe^{2+} and higher. Therefore, the influence of Fe^{2+} on both lipid oxidation and emulsion stability was studied in this doctoral thesis. The incorporation of Fe^{2+} (0.1 mM) to the LSSO emulsions containing pectin had no additional significant influence on droplet flocculation based on the measured particle sizes at day 0 (**Table 6.1**). However, a large increase in particle size was observed for samples containing 1% (w/v) CP95 or P60 as the storage time increased, which could indicate that a part of the Fe^{2+} adsorbed onto the negatively

charged oil droplet surface and decreased the electrostatic repulsion between the oil droplets, leading to larger particle sizes. In general, thinner cream layers were observed in the emulsions with Fe^{2+} in comparison with those not containing Fe^{2+}. This might be due to the screening effect that Fe^{2+} can induce to the negatively charged pectin molecules, leading to pectin molecules with less intramolecular repulsion and therefore more compact layers of pectin between oil droplets may be formed.

6.3.2 Emulsion oxidative stability

The influence of pectin DM and DB_{abs} on the Fe^{2+}-catalyzed lipid oxidation was studied in LSSO emulsions by measuring the peroxide value during storage, as a measure of the primary lipid oxidation products. LSSO emulsions were prepared with the addition of 0.1 mM Fe^{2+} as a pro-oxidant and pectin with distinct DMs and DB_{abs} at two different concentrations (0.1 and 1% w/v). Results of the peroxide measurements are shown in **Figure 6.3**. The autocatalytic lipid oxidation process can typically be described by three consecutive reactions consisting firstly of a lag phase where the formation of free radicals occurs (initiation) without a significant increase in peroxide concentration. This period is followed by the formation of lipid peroxides (propagation), during which a progressive increase in peroxides can be observed. As peroxides are decomposed to secondary oxidation products (termination), a maximum level of peroxides is observed after which the decomposition process dominates (Frankel, 1980; Manzocco, Calligaris, & Nicoli, 2010). Those three reactions were clearly observed during storage of the majority of the LSSO emulsions (**Figure 6.3**).

Pectin addition to the LSSO emulsion led, in general, to a delayed lag phase of the lipid oxidation and overall reduction of the lipid oxidation reaction depending on the concentration used and its structural characteristics (DM and DB_{abs}) (**Figure 6.3**). The addition of CP95 and C58 to the emulsions did not clearly retard the initiation phase, whereas in the emulsions with P60, P33, P13, and C10 a delayed lag phase was observed up until day 7. Thus, the addition of low or intermediate DM pectin, associated with high a DB_{abs}, to the LSSO emulsions led to a delay in the lipid oxidation reaction, even at low concentration (0.1% w/v). Moreover, in the emulsions with high pectin concentration and/or low DM (particularly with high DB_{abs}) the maximum peroxide value was substantially reduced. It should be noted that in **Figure 6.3** the highest experimentally determined peroxide value does not necessarily represent the maximum peroxide value formed during the autoxidation process. However, comparison of the experimentally determined maximum peroxide values of the different emulsions was found to be useful in this study in order to describe the effect of pectin concentration and structure on the lipid oxidation.

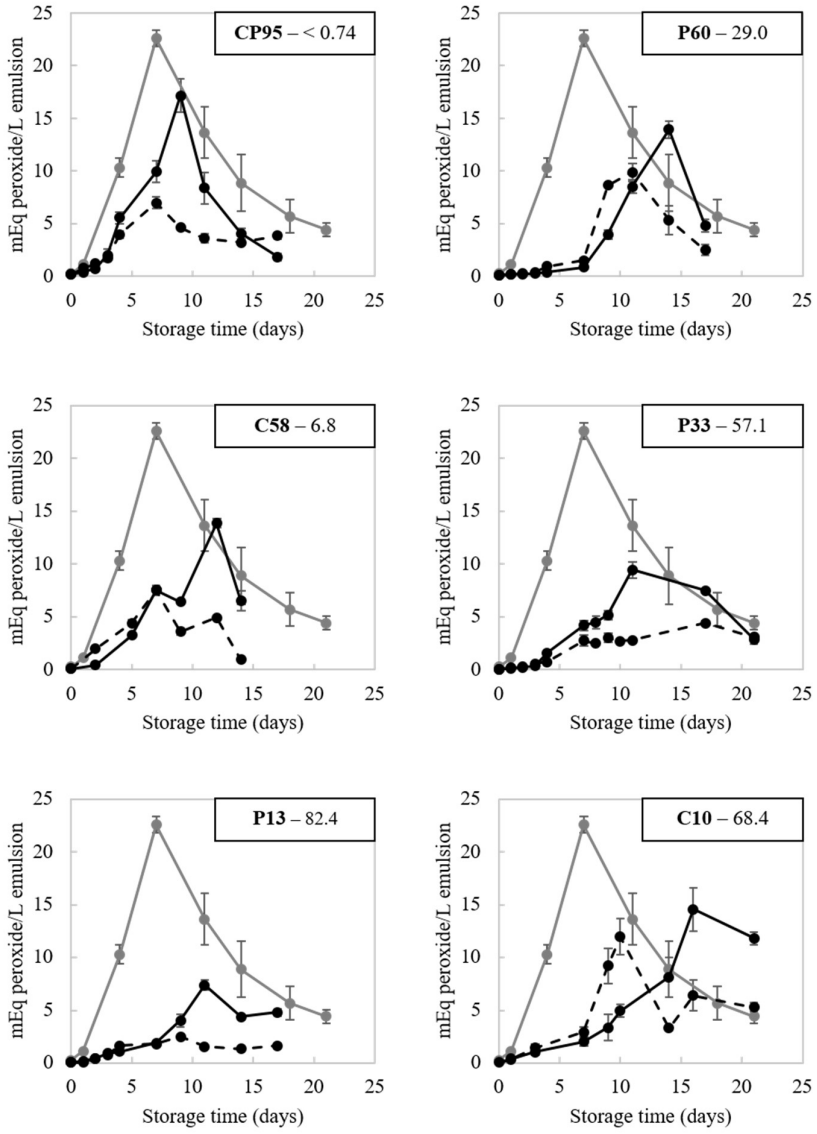

Figure 6.3: Peroxide concentration (mEq peroxide/L emulsion) with standard deviation as a function of storage time (days) of the linseed/sunflower oil (LSSO) emulsions without pectin (grey), with 0.1% (w/v) (black line), and with 1% (w/v) (black dotted line) commercial high methylesterified citrus pectin (CP95) and enzymatically or alkaline demethylesterified pectin samples (P- and C-pectins, respectively) with different DMs and DB_{abs} (%) (with estimated DB_{abs} indicated after the hyphen). All LSSO emulsions contained 0.1 mM Fe^{2+}.

On the one hand, regardless of the pectin DM, a higher pectin concentration was more effective in decreasing lipid oxidation, especially the propagation reaction. All emulsions containing 1% (w/v) pectin showed lower maximum amounts of peroxides compared to emulsions with 0.1% pectin (w/v), with a decrease up to 65% (**Figure 6.3**). For instance, at 0.1% (w/v) CP95 a maximum amount of 17.2 mEq peroxide/L emulsions was found compared to 7.0 mEq peroxide/L emulsion for 1% (w/v) CP95 and a decrease from 7.4 to 2.5 mEq peroxide/L emulsion was found for 0.1 and 1% (w/v) P13, respectively. On the other hand, and in agreement with the initial hypothesis, the DM influenced the lipid antioxidant capacity of pectin. Considering only the enzymatically demethylesterified pectin samples, high (CP95) and intermediate (P60) DM pectin showed a remarkable antioxidant capacity at 1% (w/v), but rather limited at 0.1% (w/v), except for 0.1% (w/v) P60, where a substantial delay of the lipid oxidation was observed (**Figure 6.3**). Moreover, low DM pectin (P33 and P13) exhibited an antioxidant capacity at both high (1% w/v) and low (0.1% w/v) concentration, although the capacity to slow down the lipid oxidation was more pronounced at 1% (w/v) (**Figure 6.3**). In this sense, low DM pectin was more effective in decreasing the lipid oxidation reaction compared to high or intermediate DM. In addition, the maximum amounts of peroxide values in the LSSO emulsions with low DM pectin were clearly lower than in the emulsions containing high or intermediate DM pectin, with 2.5 mEq peroxide/L emulsion for 1% (w/v) P13 compared to 9.9 mEq peroxide/L emulsion for 1% (w/v) P60 (**Figure 6.3**). With regard to the alkaline demethylesterified pectin samples (C58 and C10), decreasing DM did surprisingly not result in a clear effect on the maximum peroxide value. Nevertheless, the emulsions containing C10 (both 0.1 and 1% w/v) exhibited a longer lag phase compared to C58. These results confirm the hypothesis that non-methylesterified GalA units in pectin can bind the pro-oxidative Fe^{2+} ions, being removed from the oil droplet surface at which lipid oxidation occurs. Therefore, low DM pectin, in particular with high DB_{abs}, contains a higher number of (successive) negatively chargeable carboxyl groups, which can bind a higher amount of pro-oxidant metal ions as previously reported in Chapter 5, thus explaining the higher antioxidant capacity.

The findings of the present study are in agreement with the observations of Chen et al. (2010) and Huang et al. (2011), who reported both that low methylesterified pectin was more effective in inhibiting lipid oxidation compared to high methylesterified pectin and which effect was more pronounced at higher pectin concentration. However, in both studies, pectins with different DM were obtained without specific control in changing only the DM without changing other molecular structures, such as the molar mass, which might also determine the pectin cation-binding capacity and

therefore influence the lipid oxidation reaction. Therefore, the present study provides an insight into the antioxidant capacity of pectin with tailored molecular characteristics (DM and DB_{abs}) and similar molar masses.

The influence of pectin DB_{abs} on the lipid oxidation was studied by comparing the results of C58 to P60 and P13 to C10, samples with similar DMs but distinct estimated DB_{abs} values (**Table 2.1**). No clear differences in maximum peroxide values were observed between P60 and C58, for either 0.1 or 1% (w/v) (**Figure 6.3**). Indeed, the maximum amount of peroxides were 14.0 and 13.9 mEq peroxide/L emulsion for 0.1% (w/v) and 9.9 and 7.5 mEq peroxide/L emulsion for 1% (w/v) P60 and C58, respectively. However, it is noteworthy that the lipid oxidation in the LSSO emulsion containing P60 showed a delayed lag phase compared to C58, suggesting that the distribution pattern of the negatively chargeable carboxyl groups plays a slight role in the pectin antioxidant capacity. Nonetheless, pectin samples with those intermediate DMs presented a limited antioxidant capacity as described before. Pectin samples with a lower DM but distinct DB_{abs} could provide a clearer insight into the effect of pectin DB_{abs} on the lipid antioxidant capacity in emulsions. In this sense, comparison of the peroxide values of P13 and C10 revealed a similar lag phase of approximately 7 days, but a higher antioxidant capacity for P13 in terms of maximum peroxide value, both for 0.1 and 1% (w/v). For instance, the maximum peroxide values reached for P13 and C10 were 7.4 and 14.6 mEq peroxide/L emulsion, for 0.1% w/v, whereas 2.5 and 12.0 mEq peroxide/L emulsion for 1% (w/v), respectively. It should be noted that C10 showed a remarkably high peroxide value for both 0.1 and 1% (w/v), which is comparable to the peroxide values established in the emulsions with P60. The observation that P-pectins exhibited more reduced peroxide values compared to C-pectins with a similar DM are in accordance with the hypothesis that pectins with a higher number or longer blocks of successive negatively charged GalA units can bind a higher amount or stronger to pro-oxidant metal ions. As such, enzymatically demethylesterified pectins with low DMs are of more interest to be used as antioxidant in o/w emulsions compared to alkaline demethylesterified pectins of comparable DM.

The lipid oxidation of LSSO emulsions containing 0.1 mM Fe^{2+} and 0.05 or 0.1 mM EDTA was followed in order to compare the lipid antioxidant capacity of pectin with a commercially used antioxidant. Although addition of 0.05 mM EDTA already showed some impact on the lipid oxidation, a clear inhibition of the lipid oxidation during the total storage period was observed in the emulsions with 0.1 mM EDTA (**Figure 6.4**). This result is in agreement with the fact that EDTA binds to Fe^{2+} in a 1:1 ratio (Hu et al., 2004; Mozuraityte et al., 2016), implying that all free Fe^{2+} was

bound to EDTA and thus no substantial amount was available to catalyze the lipid oxidation. Despite the fact that emulsions with 0.1 mM EDTA contained a lower number of negatively chargeable carboxyl groups, being approximately 0.40 mM COO^-, compared to the emulsions with 1% P13 (the pectin sample with the highest antioxidant capacity), being approximately 32 mM COO^-, the emulsion with 0.1 mM EDTA exhibited clearly lower peroxide values. This indicated a much higher Fe^{2+}-binding capacity for EDTA compared to low DM citrus pectin, confirming the clearly higher lipid antioxidant capacity of EDTA. In addition, the binding constant of EDTA (approximately $4.9.10^8$ M^{-1}) is tremendously higher than observed for P13 in Chapter 5 (0.4 M^{-1}, see **Table 5.1**) (Andjelković et al., 2006). In view of replacing synthetic antioxidants by natural ones, using pectin as an alternative for EDTA will be challenging given that EDTA is more effective in chelating Fe^{2+}.

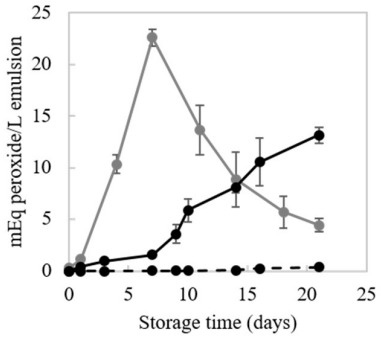

Figure 6.4: Peroxide concentration (mEq peroxide/L emulsion) with standard deviation as a function of storage time (days) of the linseed/sunflower oil (LSSO) emulsions without EDTA (grey), with 0.05 mM (black) and with 0.1 mM (black dotted) EDTA. All LSSO emulsions contained 0.1 mM Fe^{2+}.

6.4 CONCLUSION

This chapter explored the influence of citrus pectin structural properties, particularly the degree of methylesterification (DM) and absolute degree of blockiness (DB_{abs}), on the physical and oxidative stability of linseed/sunflower oil (LSSO) emulsions, previously stabilized by Tween 80. Pectin was most probably located in the aqueous phase of LSSO emulsions, however, its presence on the oil-water interface could not be excluded based on the results of this study. The addition of pectin to the emulsion systems caused physical instability, which was concentration dependent. Particularly flocculation of oil droplets and subsequent creaming was observed, which led to coalescence when a high concentration of pectin (1% w/v) was added due to stronger osmotic attractions between the oil droplets. The DM of pectin, which determines its anionic nature, did not play a role in the physical stability of the LSSO emulsions. Nevertheless, pectin DM clearly influenced the oxidative stability of LSSO emulsions. Low DM pectin (≤ 33%), especially with high DB_{abs} values, exhibited a higher lipid antioxidant capacity compared to high or intermediate DM pectin (≥ 58%), which was concentration dependent. The pectin lipid antioxidant activity can be mainly attributed to its capacity to chelate the pro-oxidant Fe^{2+}, which can be established by ionic interaction with the negatively chargeable carboxyl groups. The DB_{abs}, as a measure of the distribution pattern of non-methylesterified carboxyl groups, influenced the lipid antioxidant capacity of pectin as enzymatically demethylesterified pectins (high DB_{abs}) of a given DM delayed the lipid oxidation to a higher extent than alkaline demethylesterified pectins (low DB_{abs}). It might be possible that the emulsion instability is partly responsible for this reduced lipid oxidation. For instance, in destabilized emulsions, Fe^{2+} in the serum layer might be separated from the oil droplets in the cream layer, which could possibly reduce the interaction between Fe^{2+} and the lipid radicals. Further investigation of this aspect is necessary for optimization of the pectin antioxidant capacity, for use as an additive in emulsions. Nevertheless, given the clearly observed effect of pectin DM on the lipid oxidation, it is assumed that the emulsion instability only played a minor role in the lipid oxidation in this doctoral thesis. Despite EDTA exhibited a much higher lipid antioxidant capacity, the results of this chapter suggest that citrus pectin, especially with low DM and high DB_{abs}, can contribute to the delay of lipid oxidation in foods. Moreover, it would be worthwhile to study combinations of pectin and EDTA order to reduce the EDTA concentrations in emulsion-based foods. Nevertheless, since pectin may cause emulsion instability, food formulation should be carried out carefully to obtain stable emulsion-based food products, in which pectin functionalities such as a natural lipid antioxidant can be exhibited optimally.

PART III: GENERAL CONCLUSIONS AND PERSPECTIVES

CHAPTER 7

GENERAL CONCLUSIONS AND FUTURE PERSPECTIVES

The cation-binding capacity of pectin, which is reported to be largely determined by its degree and pattern of methylesterification (DM and DB or DB_{abs}, respectively), plays a major role in the most common pectin functionalities, such as gelation. To this extent, the influence of pectin DM and DB (or DB_{abs}) on pectin-Ca^{2+} interactions has been extensively explored with regard to the structure build-up in foods. Although Ca^{2+} has received main focus so far, given that this cation is more commonly used in cation-associated food applications, the potential of binding other cations, including essential minerals such as Fe^{2+} or Zn^{2+}, has been suggested. Exploring the binding of other cations to pectin could potentially provide multiple pectin functionalities when pectin is used as a food ingredient. For instance, chelation of Fe^{2+} could contribute to decreased lipid oxidation, implying a possible natural antioxidant capacity of pectin. However, the cation-binding ability of pectin could also have negative effects, including the possible reduction of mineral bioaccessibility during digestion as a consequence of pectin's non-digestibility. This could result in a decrease in the availability of minerals for absorption, potentially contributing to mineral deficiencies. With regard to the use of pectin as an ingredient and given consumer demands for more natural foods, possessing a high nutritional value, an in-depth understanding of the cation-chelating capacity of pectin is important in order to optimize its functionality, particularly promoting desired antioxidant capacity or structure build-up without compromising the mineral bioaccessibility. In this context, exploring the role of pectin structural properties, in particular its degree and pattern of methylesterification, is of main interest towards providing fundamental insights

into the structure-function relation of pectin. Therefore, this doctoral thesis aimed to gain insights into the effect of pectin degree and pattern of methylesterification on the interaction with cations and associated functionalities, particularly its antioxidant capacity and role in mineral bioaccessibility.

To achieve this research objective, a range of pectin structures with distinct DM and DB_{abs} values were first generated through enzymatic or alkaline demethylesterification of pectin, starting from commercial high methylesterified citrus pectin. The interaction of the generated pectins with Zn^{2+}, Ca^{2+}, as well as Fe^{2+} was then studied using equilibrium adsorption experiments to determine the maximum cation-binding capacity and associated interaction energy. Despite adsorption isotherms could provide fundamental insights into pectin-cation interactions, they have been scarcely used in understanding these interactions by the interaction energy and binding capacities of Zn^{2+}, Ca^{2+}, or Fe^{2+} as a function of pectin structural properties, including DM and DB_{abs}. In addition to equilibrium adsorption experiments, the Zn^{2+}-binding capacity of the pectin samples was studied by isothermal titration calorimetry (ITC) in order to gain insights into the binding thermodynamics (e.g., enthalpy or entropy change) between pectin and Zn^{2+}. Based on the information of the Zn^{2+}-binding capacity as influenced by the DM and DB_{abs} of the distinct pectin samples, the influence of these pectin properties on the Zn^{2+} bioaccessibility was explored through *in vitro* simulated digestion. The role of pectin DM and DB_{abs} in Fe^{2+}-binding and possible associated lipid antioxidant capacity of pectin in oil-in-water emulsions was also explored. The following subsections describe the main conclusions of each research part, together with the future perspectives. The major results are also schematically presented in **Figure 7.1**.

Generation and characterization of citrus pectin samples with distinct degrees and patterns of methylesterification

Since the degree and pattern of methylesterification are reported to play a major role in pectin cation-chelating capacity, pectins with distinct DM and DB_{abs} were produced through enzymatic (using plant pectin methylesterase) or alkaline (using NaOH) demethylesterification of commercial high methylesterified citrus pectin (CP95). Characterization of weight average molar mass, galacturonic acid (GalA) content and neutral sugar composition revealed no significant differences between the produced pectin samples. Only changes in DM were exhibited and for a given DM, enzymatically demethylesterified pectins were characterized by a higher estimated DB_{abs} compared to alkaline demethylesterified pectins, due to the blockwise compared

to random removal of methylesters, respectively. The enzymatically and alkaline demethylesterified pectins samples, denoted as P- and C-pectins, respectively, were used in subsequent sections to explore the effect of the DM and DB_{abs} on pectin functionality, particularly its role in Zn^{2+} bioaccessibility and lipid antioxidant capacity. In this doctoral thesis, it was decided to generate pectin samples mainly consisting of homogalacturonan, which typically represents commonly used commercial pectin, e.g., citrus or apple pectin, with distinct DM and DB_{abs} as those are hypothesized to largely influence the cation-binding capacity. Nevertheless, it might be worthwhile for future purposes to study other pectin structural properties in relation to the cation binding, e.g., degree of branching, degree of acetylation or degree of polymerization. As such, it approaches a more realistic system with *in situ* pectin functionality since natural food products mostly contain more structural complex pectin. Moreover, addition of pectin to food systems might induce the viscosity. In some products, such a viscosity increase is however not desired. Insights into the functionalities of pectin with decreased molar mass are therefore of particular interest as the addition of those pectin structures is assumed to reduce the viscosity increase.

Pectin-cation interactions as influenced by pectin degree and pattern of methylesterification

The study of the Zn^{2+}-, Ca^{2+}-, and Fe^{2+}-binding capacity of the pectin samples was performed through equilibrium adsorption experiments, in which adsorption isotherms were generated and fitted using the Langmuir adsorption model. This Langmuir model is typically characterized by a maximum binding capacity (q_{max}) and a Langmuir constant (K_L), with the latter being a measure for the interaction energy or in other words, the strength of the interaction. Based on the adsorption isotherms obtained, it was found that the cation binding was promoted by decreasing DM or increasing DB_{abs} of pectin, irrespective of cation type (**Figure 7.1**). With regard to specific adsorption parameters, the maximum binding capacity was mainly determined by DM, since no significant differences in q^G_{max} (mol cation/mol GalA) were observed between P- and C-pectins of a given DM. Besides, the interaction energy was largely determined by pectin DB_{abs}, as P-pectins exhibited significantly higher K_L values than C-pectins for a given DM. Based on this equilibrium adsorption experiment, on the one hand, the binding between very low DM or high DB_{abs} pectin and any cation type explored suggested a dimerization between pectin chains in which a cation is entrapped by two non-methylesterified GalA residues of opposite pectin chains, resulting in a binding capacity of approximately 0.5 mol cation/mol COO^-

(q^{C}_{max}). Pectin samples characterized by lower DB_{abs} values or higher DMs, on the other hand, exhibited binding capacities higher than 0.5 mol cation/mol COO^-, suggesting binding with cations via monocomplexation. This was particularly observed for P-pectins. These high binding capacities (above 0.5 mol cation/mol COO^-) possibly indicate additional interactions e.g., via hydroxyl groups in addition to binding via COO^- groups. With regard to cation type, the highest maximum binding capacity and interaction energy were exhibited for Zn^{2+} compared to Ca^{2+} and Fe^{2+}. This could be explained by possible binding of Zn^{2+} to other functional groups (such as OH^-) in addition to carboxylate groups. This observation is of particular interest with regard to competition between distinct cation types in binding with pectin, as the higher interaction energy observed for Zn^{2+} might suggest the preference for pectin to interact with Zn^{2+} compared to Ca^{2+} or Fe^{2+}. The competition between distinct cation for binding to pectin is an interesting research gap to further investigate, as different cation types in varying concentrations are likely to be present in real food matrices. This would allow a more realistic evaluation of the cation-binding capacity of pectin towards the use of pectin as an ingredient.

Besides equilibrium adsorption experiments, the Zn^{2+}-binding capacity of pectin was further explored by isothermal titration calorimetry (ITC). ITC was used to gain insights into the binding thermodynamics such as enthalpy or entropy change in addition to the binding capacity and binding constant. ITC results revealed that Zn^{2+}-binding to pectin occurred via a two-step binding mechanism: monocomplexation and the formation of point-like cross-links at low Zn^{2+} concentrations, followed by dimerization at increasing Zn^{2+} concentrations. Moreover, it could be concluded that the pectin-Zn^{2+} interaction is an entropy-driven process, implying a positive entropy change which dominated the unfavorable endothermic enthalpy change. Decreasing DM or increasing DB_{abs} promoted the interaction with Zn^{2+}, in analogy to the results of the equilibrium adsorption study. Despite ITC and equilibrium adsorption experiments showing similar trends in the strength of binding between the pectins and Zn^{2+} (denoted by interaction energies), some discrepancies in binding capacities were observed between the two methods. In the case of ITC, P-pectins exhibited significantly higher binding capacities compared to C-pectins, while no differences in maximum binding capacities between P- and C-pectins were observed in the equilibrium adsorption study as mentioned before (**Figure 7.1**). The differences observed between the two methods might be explained by the difference in parameters measured, being the free Zn^{2+} concentration (in the equilibrium adsorption study) versus the heat absorbed (ITC) during the pectin-Zn^{2+} interaction. Moreover, it was suggested that ITC measurements were probably influenced by gelling, particularly

for the low DM pectin samples which are generally more sensitive to gelling in presence of cations. For future purposes, careful selection and optimization of low DM pectin concentrations and cation concentrations is necessary in order to obtain better insights into the interaction. Nonetheless, in general, ITC was found to be a useful technique to understand the pectin-cation binding thermodynamics. Therefore, the use of this tool for exploring the thermodynamics of pectin interaction with other cations, such as Ca^{2+} or Fe^{2+} is recommended. With regard to Fe^{2+}, it should be noted that oxidation to Fe^{3+} might play a role in the binding with pectin and elimination of oxygen is thus advised, although this could be challenging.

Based on results of this section, it can generally be concluded that regardless of the technique used, both the DM and DB_{abs} of pectin largely influence its cation-binding capacity. While data from equilibrium adsorption isotherms can be faster obtained but are less extensive, ITC provides fundamental insights into the thermodynamics of binding parameters. Moreover, this section showed that targeted modification of pectin DM or DB_{abs} can be exploited to obtain desired cation-binding ability.

Zn^{2+} bioaccessibility as influenced by pectin degree and pattern of methylesterification

Based on the insights obtained into the influence of the DM and DB_{abs} on the Zn^{2+}-binding capacity of pectin, the effect of these pectin properties on the *in vitro* Zn^{2+} bioaccessibility was explored. Insights into the Zn^{2+} bioaccessibility are of interest as Zn^{2+} is considered to be an essential mineral for humans and its deficiency, resulting in e.g., retarded skeletal disorders, is reported as a highly prevalent nutritional problem worldwide. In general, increased Zn^{2+}-binding to pectin, due to decreasing DM or increasing DB_{abs}, was associated with lower Zn^{2+} bioaccessibility (**Figure 7.1**). At low Zn^{2+} concentrations (0.3 mM), Zn^{2+} bioaccessibility was mainly determined by DB_{abs}, while it was more determined by DM at higher Zn^{2+} contents (1 and 3 mM). Relating the Zn^{2+} bioaccessibilities with the established maximum Zn^{2+}-binding capacities of the pectin samples revealed that when samples were enriched with high Zn^{2+} concentration (3 mM, exceeding maximum binding capacity) prior to the *in vitro* digestion, generally higher amounts of Zn^{2+} were bound than estimated based on the maximum binding capacity study, thus not bioaccessible. This was attributed to the bile salts and probably enzymes added during *in vitro* simulated digestion binding substantial amounts of Zn^{2+}. For a more in-depth understanding of the influence of pectin on Zn^{2+} or cation bioaccessibility, the binding potential of components added during digestion should be explored.

In view of real food matrices, the competition between cations for binding to pectin and associated bioaccessibility was also investigated. In this doctoral thesis the possible competition between Ca^{2+} and Zn^{2+} was explored and revealed that addition of low Ca^{2+} levels (approximately 0.33 mM) had no clear influence on Zn^{2+} bioaccessibility (**Figure 7.1**). Nevertheless, higher Ca^{2+} concentrations (although not explored in this study) could affect the Zn^{2+} bioaccessibility by displacing the Zn^{2+} bound to pectin and as such possibly contribute to a higher Zn^{2+} bioaccessibility. Moreover, the competition experiment can be extended to Fe^{2+}, as its deficiency is also considered to be very common. In this sense, the cation binding studies revealed the highest affinity of pectin for Zn^{2+} compared to Ca^{2+} or Fe^{2+}, which might suggest the lowest bioaccessibilities for Zn^{2+} after digestion of food matrices which are rich in low DM pectin and a combination of those minerals. Additionally, the complexity of the *in vitro* digestion procedure could be increased in future, such as including simulated gastric or intestinal fluids, approaching a more realistic digestion. Furthermore, exploration of the digestion beyond the small intestine phase, i.e., in the colon (potential fermentation), and the associated release of minerals (if any) could promote a wide view of pectin's potential to influence mineral bioaccessibility.

Pectin antioxidant capacity as influenced by its degree and pattern of methylesterification

The use of natural antioxidants in emulsion-based products with the aim to reduce EDTA concentrations might contribute to food products which are more appealing for consumers. Insights obtained into the role of pectin DM and DB_{abs} in Fe^{2+}-interaction were therefore used in exploring the potential lipid antioxidant capacity of pectin in oil-in-water (o/w) emulsions. It was established that increased Fe^{2+}-binding, due to increased pectin concentration, decreased pectin DM, or increased DB_{abs}, promoted the lipid antioxidant capacity of pectin, as measured by the peroxide value (**Figure 7.1**). It was also suggested that the DB_{abs} plays an important role in the lipid antioxidant capacity since for a given DM, P-pectins (high DB_{abs}) retarded the lipid oxidation to a higher extent compared to C-pectins (low DB_{abs}). For future purposes, it is recommended to study the formation of secondary oxidation products in addition to the primary ones. This could be achieved by measurement of the volatiles formed using GC-MS, e.g., hexanal, 2-octenal, or 2-pentenal. As such, a more profound insight into the effect of pectin on the lipid oxidation could be obtained. Despite EDTA was found to be more effective in inhibiting the lipid oxidation, the results of this study evidence the potential of structurally modified citrus pectin to contribute as a natural antioxidant in o/w emulsions. Nevertheless, addition of pectin to o/w

emulsions caused emulsion destabilization probably due to depletion or bridging flocculation, independent of the pectin structural characteristics, which presents a challenge for use of pectin as an antioxidant.

General future outlook

This doctoral thesis clearly shows that pectin DM and DB_{abs} determine the divalent cation-binding capacity of pectin and associated functionalities. Depending on the intended application, targeted modification of pectin structure is important for optimization of this cation-binding capacity of pectin and associated functionalities. While pectin structural modifications leading to a high divalent cation-binding capacity promote the antioxidant capacity of pectin in emulsion-based food products, they reduce the bioaccessibility of divalent minerals in pectin solutions. It would be of interest to investigate if emulsions, containing pectin as antioxidant, would exhibit low mineral bioaccessibility in order towards optimization of both functionalities. Nevertheless, there is a challenge to eliminate phase separation when pectin is used as an antioxidant. A possible solution might be the addition of a combination of distinct pectin structures, in terms of DM and (weight average) molar mass (M_w), to o/w emulsions in order to possibly enhance both oxidative as well as physical emulsion stability. For instance, citrus pectin, particularly high DM, has recently been shown to exhibit emulsifying capacity, which is attributed to the adsorption onto the oil droplets via its hydrophobic methylesterified galacturonic acid units (Verkempinck et al., 2018). As such, high DM citrus pectin with low M_w (to enhance the mobility through the emulsion) is hypothetically suitable to achieve this emulsifying functionality, while low DM citrus pectin with high M_w (to increase viscosity of aqueous phase and higher Fe^{2+}-binding capacity) is more interesting for its antioxidant and emulsion stabilizing capacity.

The potential of pectin to retard the lipid oxidation is also recommended to evaluate in relation to that of EDTA, for replacing or supplementing the use of such artificial antioxidants. Given its wide variability in structure and functionalities, pectin can be used as a food additive (*ex situ*) and contribute to multiple functions simultaneously, for instance as a stabilizer and antioxidant in emulsion-based food products. As such, it is therefore interesting to study if the presence of pectin in lipid-based products for instance as a stabilizer, might additionally confer pectin an antioxidant capacity and thus potentially result in a decrease of required EDTA concentrations. Reduced EDTA concentrations can then be a first step in the production of more natural foods, which meets consumer demands. Furthermore, the insights in model systems obtained in this

doctoral thesis provide a fundamental basis for further investigation of the pectin structure-function relation in fruit- and vegetable-based food products, towards optimization of the (*in situ*) pectin functionalities.

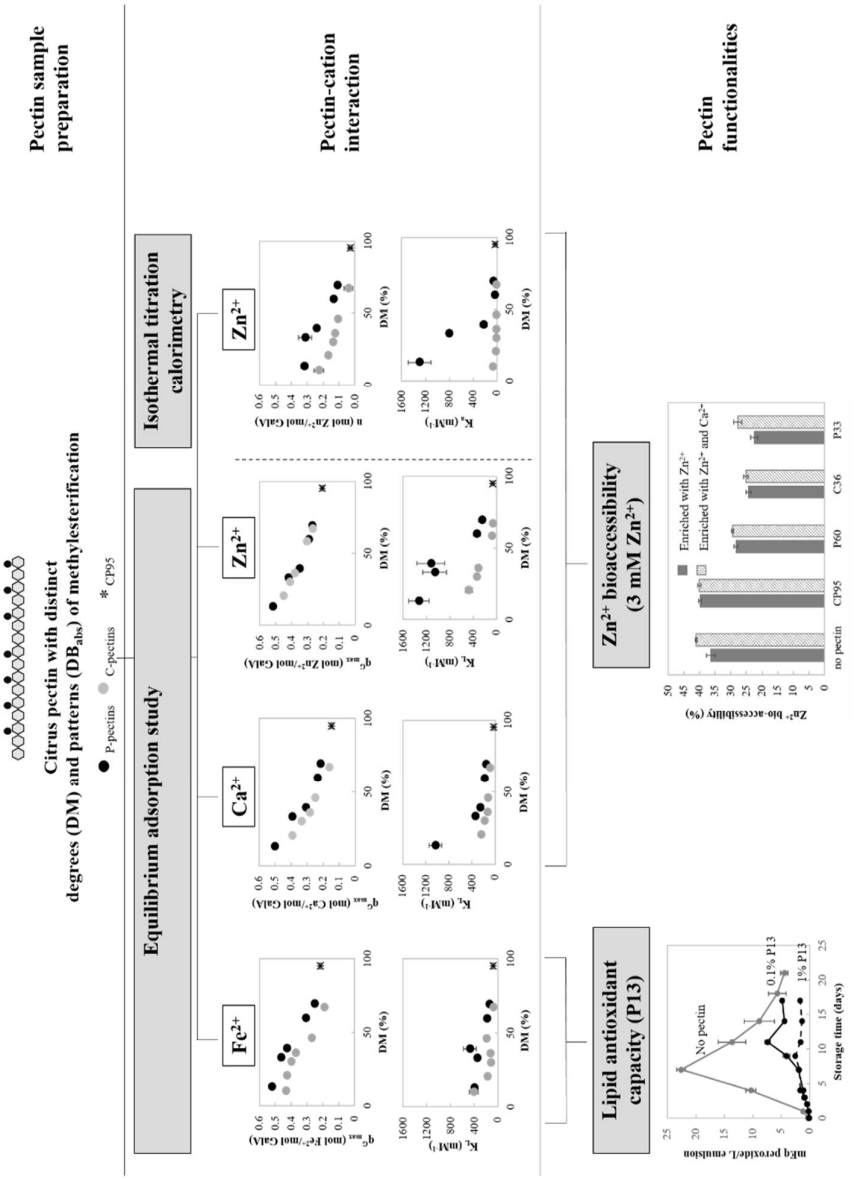

Figure 7.1: Schematic overview of the main results obtained in this doctoral thesis.

LIST OF REFERENCES

Ahmed, A. E. R., & Labavitch, J. M. (1977). A simplified method for accurate determination of cell wall uronide content. *Journal of Food Biochemistry*, *1*, 361–365.

Allred, A. L. (1961). Electronegativity values from thermochemical data. *Journal of Inorganic and Nuclear Chemistry*, *17*, 215–221.

Andjelković, M., Van Camp, J., De Meulenaer, B., Depaemelaere, G., Socaciu, C., Verloo, M., & Verhe, R. (2006). Iron-chelation properties of phenolic acids bearing catechol and galloyl groups. *Food Chemistry*, *98*(1), 23–31.

Assifaoui, A., Lerbret, A., Uyen, H. T. D., Neiers, F., Chambin, O., Loupiac, C., & Cousin, F. (2015). Structural behaviour differences in low methoxy pectin solutions in the presence of divalent cations (Ca^{2+} and Zn^{2+}): a process driven by the binding mechanism of the cation with the galacturonate unit. *Soft Matter*, *11*, 551–560.

Bagheri, S., & Guénguen, L. (1985). Effect of wheat bran and pectin on the absorption and retention of phosphorus, calcium, magnesium and zinc by the growing pig. *Reproduction Nutritional Development*, *25*, 705–716.

Blumenkrantz, N., & Asboe-Hansen, G. (1973). New method for quantitative determination of uronic acids. *Analytical Biochemistry*, *54*, 484–489.

Bosscher, D., Van Caillie-Bertrand, M., Van Cauwenbergh, R., & Deelstra, H. (2003). Availabilities of calcium, iron, and zinc from dairy infant formulas is affected by soluble dietary fibers and modified starch fractions. *Nutrition*, *19*(7–8), 641–645.

Braccini, I., & Pérez, S. (2001). Molecular basis of Ca^{2+}-induced gelation in alginates and pectins: the egg-box model revisited. *Biomacromolecules*, *2*, 1089–1096.

Braudo, E. E., Danilova, I. V., Dianova, V. T., Kobak, V. V., Plashchina, I. G., Sidorov, E. V., & Bogatyrev, A. N. (1996). Thermodynamic approach to the selection of polyuronide sequestrants for preventive and medicinal nutrition. *Die Nahrung*, *40*, 205–8.

Broxterman, S. E., Picouet, P., & Schols, H. A. (2017). Acetylated pectins in raw and heat processed carrots. *Carbohydrate Polymers*, *177*, 58–66.

Caffall, K. H., & Mohnen, D. (2009). The structure, function, and biosynthesis of plant cell wall pectic polysaccharides. *Carbohydrate Research*, *344*, 1879–1900.

Cameron, R. G., Kim, Y., Galant, A. L., Luzio, G. A., & Tzen, J. T. C. (2015). Pectin homogalacturonans: Nanostructural characterization of methylesterified domains. *Food Hydrocolloids*, *47*, 184–190.

Cameron, R. G., Luzio, G. A., Goodner, K., & Williams, M. A. K. (2008). Demethylation of a model homogalacturonan with a salt-independent pectin methylesterase from citrus: I. Effect of pH on demethylated block size, block number and enzyme mode of action. *Carbohydrate Polymers*, *71*(2), 287–299.

Capel, F., Nicolai, T., Durand, D., Boulenguer, P., & Langerdorff, V. (2005). Influence of chain length and polymer concentration on the gelation of (amidated) low-methoxyl pectin induced by calcium. *Biomacromolecules*, *6*(6), 2954–2960.

Castro, L., Blázquez, M. L., González, F., Muñoz, J. A., & Ballester, A. (2017). Biosorption of Zn(II) from industrial effluents using sugar beet pulp and *F. vesiculosus*: From laboratory tests to a pilot approach. *Science of the Total Environment*, *598*, 856–866.

Cervantes-Paz, B., Ornelas-Paz, J. de J., Ruiz-Cruz, S., Rios-Velasco, C., Ibarra-Junquera, V., Yahia, E. M., & Gardea-Béjar, A. A. (2017). Effects of pectin on lipid digestion and possible implications for carotenoid bioavailability during pre-absorptive stages: A review. *Food Research International*, *99*, 917–927.

Chen, B., McClements, D. J., & Decker, E. A. (2010). Role of continuous phase anionic polysaccharides on the oxidative stability of menhaden oil-in-water emulsions. *Journal of Agricultural and Food Chemistry*, *58*, 3779–3784.

Chodera, J. D., & Mobley, D. L. (2014). Entropy-enthalpy compensation: Role and ramifications in biomolecular ligand recognition and design. *Annual Review of Biophysics*, *42*, 121–142.

Christiaens, S., Mbong, V. B., Van Buggenhout, S., David, C. C., Hofkens, J., Van Loey, A. M., & Hendrickx, M. E. (2012). Influence of processing on the pectin structure-function relationship in broccoli purée. *Innovative Food Science and Emerging Technologies*, *15*, 57–65.

Christiaens, S., Uwibambe, D., Uyttebroek, M., Van Droogenbroeck, B., Van Loey, A. M., & Hendrickx, M. E. (2015a). Pectin characterisation in vegetable waste streams: A starting point for waste valorisation in the food industry. *LWT - Food Science and Technology*, *61*(2), 275–282.

Christiaens, S., Van Buggenhout, S., Houben, K., Kermani, Z. J., Moelants, K. R. N., Ngouémazong, E. D., Van Loey, A., & Hendrickx, M. E. G. (2015b). Process-structure-function relations of pectin in food. *Critical Reviews in Food Science and Nutrition*, *8398*, 37–41.

Coenen, G. J., Bakx, E. J., Verhoef, R. P., Schols, H. A., & Voragen, A. G. J. (2007). Identification of the connecting linkage between homo- or xylogalacturonan and rhamnogalacturonan type I. *Carbohydrate Polymers*, *70*(2), 224–235.

Cummings, J., & Macfarlane, G. (1991). The control and consequences of bacterial fermenation in the human colon. *Journal of Applied Bacteriology*, *70*, 443–459.

Daas, P. J. H., Meyer-Hansen, K., Schols, H. A., De Ruiter, G. A., & Voragen, A. G. J. (1999). Investigation of the non-esterified galacturonic acid distribution in pectin with endopolygalacturonase. *Carbohydrate Research*, *318*, 135–145.

De Vries, J. A., Rombouts, F. M., Voragen, A. G. J., & Pilnik, W. (1982). Enzymic degradation of apple pectins. *Carbohydrate Polymers*, *2*(1), 25–33.

Debon, S. J. J., & Tester, R. F. (2001). In vitro binding of calcium, iron and zinc by non-starch polysaccharides. *Food Chemistry*, *73*, 401–410.

Dickinson, E. (2003). Hydrocolloids at interfaces and the influence on the properties of dispersed systems. *Food Hydrocolloids*, *17*(1), 25–39.

Dongowski, G., Lorenz, A., & Proll, A. (2002). The degree of methylation influences the degradation of pectin in the intestinal tract of rats and in vitro. *Journal of Nutrition*, *132*(7), 1935–1944.

Dronnet, V. M., Renard, C. M. G. C., Axelos, M. A. V, & Thibault, J. F. (1996). Characterisation and selectivity of divalent metal ions binding by citrus and sugar-beet pectins. *Carbohydrate Polymers*, *30*, 253–263.

Eliaz, I., Hotchkiss, A. T., Fishman, M. L., & Rode, D. (2006). The effect of modified citrus pectin on urinary excretion of toxic elements. *Phytotherapy Research*, *20*, 859–864.

Espinal-Ruiz, M., Parada-Alfonso, F., Restrepo-Sánchez, L. P., Narváez-Cuenca, C. E., & McClements, D. J. (2014). Interaction of a dietary fiber (pectin) with gastrointestinal components (bile salts, calcium, and lipase): A calorimetry, electrophoresis, and turbidity study. *Journal of Agricultural and Food Chemistry*, *62*(52), 12620–12630.

Espitia, P. J. P., Du, W. X., Avena-Bustillos, R. de J., Soares, N. de F. F., & McHugh, T. H. (2014). Edible films from pectin: Physical-mechanical and antimicrobial properties - A review. *Food Hydrocolloids*, *35*, 287–296.

Fabbri, A. D. T., & Crosby, G. A. (2016). A review of the impact of preparation and cooking on the nutritional quality of vegetables and legumes. *International Journal of Gastronomy and Food Science*, *3*, 2–11.

Fang, Y., Al-Assaf, S., Phillips, G. O., Nishinari, K., Funami, T., & Williams, P. A. (2008). Binding behavior of calcium to polyuronates: Comparison of pectin with alginate. *Carbohydrate Polymers*, *72*(2), 334–341.

Fang, Y., Al-Assaf, S., Phillips, G. O., Nishinari, K., Funami, T., & Williams, P. A. (2009). Participation of ions in promoting intermolecular associations of cell wall polysaccharides. *Structural Chemistry*, *20*(2), 317–324.

Foo, K. Y., & Hameed, B. H. (2010). Insights into the modeling of adsorption isotherm systems. *Chemical Engineering Journal*, *156*, 2–10.

Fraeye, I., Colle, I., Vandevenne, E., Duvetter, T., Van Buggenhout, S., Moldenaers, P., Van Loey, A., & Hendrickx, M. (2010a). Influence of pectin structure on

texture of pectin-calcium gels. *Innovative Food Science and Emerging Technologies*, *11*(2), 401–409.

Fraeye, I., Doungla, E., Duvetter, T., Moldenaers, P., Van Loey, A., & Hendrickx, M. (2009). Influence of intrinsic and extrinsic factors on rheology of pectin-calcium gels. *Food Hydrocolloids*, *23*, 2069–2077.

Fraeye, I., Duvetter, T., Doungla, E., Van Loey, A., & Hendrickx, M. (2010b). Fine-tuning the properties of pectin-calcium gels by control of pectin fine structure, gel composition and environmental conditions. *Trends in Food Science and Technology*, *21*, 219–228.

Frankel, N. (1980). Lipid oxidation. *Progress in Lipid Research*, *19*, 1–22.

Freire, E., Schön, A., & Velazquez-Campoy, A. (2009). Isothermal titration calorimetry: General formalism using binding polynomials. In M. L. Johnson, J. M. Holt, & G. K. Ackers (Eds.), *Methods in Enzymology* (Vol. 455, pp. 127–155). Elsevier Inc.

Freyer, M. W., & Lewis, E. A. (2008). Isothermal titration calorimetry: Experimental design, data analysis, and probing macromolecule/ligand binding and kinetic interactions. *Methods in Cell Biology*, *84*(07), 79–113.

Gao, Z., Fang, Y., Cao, Y., Liao, H., Nishinari, K., & Phillips, G. O. (2017). Hydrocolloid-food component interactions. *Food Hydrocolloids*, *68*, 149–156.

Garnier, C., Axelos, M. A. V, & Thibault, J.-F. (1994). Selectivity and cooperativity by pectins in the binding of calcium ions. *Carbohydrate Research*, *256*, 71–81.

Gharibzahedi, S. M. T., & Jafari, S. M. (2017). The importance of minerals in human nutrition: bioavailability, food fortification, processing effects and nanoencapsulation. *Trends in Food Science and Technology*, *62*, 119–132.

Grant, G. T., Morris, E. R., Rees, D. A., Smith, P. J. C., & Thom, D. (1973). Biological interactions between polysaccharides and divalent cations: the egg-box model. *FEBS Letters*, *32*, 195–198.

Grundy, M. M.-L., Edwards, C. H., Mackie, A. R., Gidley, M. J., Butterworth, P. J., & Ellis, P. R. (2016). Re-evaluation of the mechanisms of dietary fibre and implications for macronutrient bioaccessibility, digestion and postprandial metabolism. *The British Journal of Nutrition*, *116*(5), 816–33.

Guerra-Rosas, M. I., Morales-Castro, J., Ochoa-Martínez, L. A., Salvia-Trujillo, L., & Martín-Belloso, O. (2016). Long-term stability of food-grade nanoemulsions from high methoxyl pectin containing essential oils. *Food Hydrocolloids*, *52*, 438–446.

Guillotin, S. E., Bakx, E. J., Boulenguer, P., Mazoyer, J., Schols, H. A., & Voragen, A. G. J. (2005). Populations having different GalA blocks characteristics are present in commercial pectins which are chemically similar but have different functionalities. *Carbohydrate Polymers*, *60*, 391–398.

Haahr, A. M., & Jacobsen, C. (2008). Emulsifier type, metal chelation and pH affect oxidative stability of n-3-enriched emulsions. *European Journal of Lipid Science and Technology*, *110*(10), 949–961.

Han, W., Meng, Y., Hu, C., Dong, G., Qu, Y., Deng, H., & Guo, Y. (2017). Mathematical model of Ca^{2+} concentration, pH, pectin concentration and soluble solids (sucrose) on the gelation of low methoxyl pectin. *Food Hydrocolloids*, *66*, 37–48.

Haug, A., & Smidsrød, O. (1970). Selectivity of some anionic polymers for divalent metal ions. *Acta Chemica Scandinavica*, *24*, 843–854.

Ho, Y. S., Huang, C. T., & Huang, H. W. (2002). Equilibrium sorption isotherm for metal ions on tree fern. *Process Biochemistry*, *37*, 1421–1430.

Houben, K., Jolie, R. P., Fraeye, I., Van Loey, A. M., & Hendrickx, M. E. (2011). Comparative study of the cell wall composition of broccoli, carrot, and tomato: Structural characterization of the extractable pectins and hemicelluloses. *Carbohydrate Research*, *346*(9), 1105–1111.

Hu, M., Li, Y., Decker, E. A., & McClements, D. J. (2010). Role of calcium and calcium-binding agents on the lipase digestibility of emulsified lipids using an in vitro digestion model. *Food Hydrocolloids*, *24*(8), 719–725.

Hu, M., McClements, D. J., & Decker, E. A. (2004). Impact of chelators on the oxidative stability of whey protein isolate-stabilized oil-in-water emulsions containing omega-3 fatty acids. *Food Chemistry*, *88*(1), 57–62.

Huang, P. H., Lu, H. T., Wang, Y. T., & Wu, M. C. (2011). Antioxidant activity and emulsion-stabilizing effect of pectic enzyme treated pectin in soy protein isolate-stabilized oil/water emulsion. *Journal of Agricultural and Food Chemistry*, *59*, 9623–9628.

Huynh, U. T. D., Chambin, O., Maire du Poset, A., & Assifaoui, A. (2018). Insights into gelation kinetics and gel front migration in cation-induced polysaccharide hydrogels by viscoelastic and turbidity measurements: Effect of the nature of divalent cations. *Carbohydrate Polymers*, *190*, 121–128.

Huynh, U. T. D., Lerbret, A., Neiers, F., Chambin, O., & Assifaoui, A. (2016). Binding of divalent cations to polygalacturonate: A mechanism driven by the hydration water. *Journal of Physical Chemistry B*, *120*, 1021–1032.

Hwang, J., & Kokini, J. L. (1992). Contribution of the side branches to rheological properties of pectins. *Carbohydrate Polymers*, *19*(1), 41–50.

Irani, A. H., Owen, J. L., Mercadante, D., & Williams, M. A. K. (2017). Molecular dynamics simulations illuminate the role of counterion condensation in the electrophoretic transport of homogalacturonans. *Biomacromolecules*, *18*(2), 505–516.

Jacobsen, C., Let, M. B., Nielsen, N. S., & Meyer, A. S. (2008). Antioxidant strategies for preventing oxidative flavour deterioration of foods enriched with

n-3 polyunsaturated lipids: a comparative evaluation. *Trends in Food Science and Technology*, *19*(2), 76–93.

Jaramillo, Á., Briones, L., Andrews, M., Arredondo, M., Olivares, M., Brito, A., & Pizarro, F. (2015). Effect of phytic acid, tannic acid and pectin on fasting iron bioavailability both in the presence and absence of calcium. *Journal of Trace Elements in Medicine and Biology*, *30*, 112–117.

Jolie, R. P., Duvetter, T., Houben, K., Clynen, E., Sila, D. N., Van Loey, A. M., & Hendrickx, M. E. (2009). Carrot pectin methylesterase and its inhibitor from kiwi fruit: Study of activity, stability and inhibition. *Innovative Food Science and Emerging Technologies*, *10*, 601–609.

Jolie, R. P., Duvetter, T., Van Loey, A. M., & Hendrickx, M. E. (2010). Pectin methylesterase and its proteinaceous inhibitor: A review. *Carbohydrate Research*, *345*(18), 2583–2595.

Kartel, M. T., Kupchik, L. A., & Veisov, B. K. (1999). Evaluation of pectin binding of heavy metal ions in aqueous solutions. *Chemosphere*, *38*, 2591–2596.

Katsuda, M. S., McClements, D. J., Miglioranza, L. H. S., & Decker, E. A. (2008). Physical and oxidative stability of fish oil-in-water emulsions stabilized with beta-lactoglobulin and pectin. *Journal of Agricultural and Food Chemistry*, *56*(14), 5926–5931.

Khotimchenko, M., Makarova, K., Khozhaenko, E., & Kovalev, V. (2017). Lead-binding capacity of calcium pectates with different molecular weight. *International Journal of Biological Macromolecules*, *97*, 526–535.

Khotimchenko, M. Y., Kolenchenko, E. A., & Khotimchenko, Y. S. (2008). Zinc-binding activity of different pectin compounds in aqueous solutions. *Journal of Colloid and Interface Science*, *323*, 216–222.

Khotimchenko, Y., Khozhaenko, E., Kovalev, V., & Khotimchenko, M. (2012). Cerium binding activity of pectins isolated from the seagrasses *Zostera marina* and *Phyllospadix iwatensis*. *Marine Drugs*, *10*(4), 834–848.

Kim, M. (1998). Highly esterified pectin with low molecular weight enhances intestinal solubility and absorption of ferric iron in rats. *Nutrition Research*, *18*, 1981–1994.

Kim, Y., Williams, M. A. K., Luzio, G. A., & Cameron, R. G. (2017). Introduction and characterization of charged functional domains into an esterified pectic homogalacturonan by a citrus pectin methylesterase and comparison of its modes of action to other pectin methylesterase isozymes. *Food Hydrocolloids*, *69*, 422–431.

Kohn, R. (1975). Ion binding on polyuronates - alginate and pectin. *Pure and Applied Chemistry*, *42*(3), 371–397.

Kohn, R. (1987). Binding of divalent cations to oligomeric fragments of pectin. *Carbohydrate Research*, *160*(C), 343–353.

Kohn, R., & Furda, I. (1968). Binding of calcium ions to acetyl derivates of pectin. *Collection of Czechoslovak Chemical Communications*, *33*, 2217–2225.

Kohn, R., & Luknár, O. (1977). Intermolecular calcium ion binding on polyuronates - Polygalacturonate and polyguluronate. *Collection of Czechoslovak Chemical Communications*, *42*, 731–744.

Kyomugasho, C., Christiaens, S., Shpigelman, A., Van Loey, A. M., & Hendrickx, M. E. (2015a). FT-IR spectroscopy, a reliable method for routine analysis of the degree of methylesterification of pectin in different fruit- and vegetable-based matrices. *Food Chemistry*, *176*, 82–90.

Kyomugasho, C., Christiaens, S., Van de Walle, D., Van Loey, A. M., Dewettinck, K., & Hendrickx, M. E. (2016). Evaluation of cation-facilitated pectin-gel properties: Cryo-SEM visualisation and rheological properties. *Food Hydrocolloids*, *61*, 172–182.

Kyomugasho, C., Gwala, S., Christiaens, S., Jamsazzadeh Kermani, Z., Van Loey, A. M., Grauwet, T., & Hendrickx, M. E. (2017). Pectin nanostructure influences pectin-cation interactions and in vitro-bioaccessibility of Ca^{2+}, Zn^{2+}, Fe^{2+} and Mg^{2+}-ions in model systems. *Food Hydrocolloids*, *62*, 299–310.

Kyomugasho, C., Munyensanga, C., Celus, M., Van de Walle, D., Dewettinck, K., Van Loey, A., & Hendrickx, M. E. (2018). Molar mass influence on pectin-Ca2+ adsorption capacity, interactions energy and associated functionality: gel microsctructure and stiffness. *Food Hydrocolloids*, *85*, 331–342.

Kyomugasho, C., Willemsen, K. L. D. D., Christiaens, S., Van Loey, A. M., & Hendrickx, M. E. (2015b). Pectin-interactions and invitro bioaccessibility of calcium and iron in particulated tomato-based suspensions. *Food Hydrocolloids*, *49*, 164–175.

Lanigan, R. S., & Yamarik, T. A. (2002). Final report on the safety assessment of EDTA, calcium disodium EDTA, diammonium EDTA, dipotassium EDTA, disodium EDTA, TEA-EDTA, tetrasodium EDTA, tripotassium EDTA, trisodium EDTA, HEDTA, and trisodium HEDTA. *International Journal of Toxicology*, *21*, 95–142.

Lei, K. Y., Davis, M., Fang, M. M., & Young, L. C. (1980). Effect of pectin on zinc, copper and iron balances in humans. *Nutrition Reports International*, *22*, 459–466.

Li, F. T., Yang, H., Zhao, Y., & Xu, R. (2007). Novel modified pectin for heavy metal adsorption. *Chinese Chemical Letters*, *18*(3), 325–328.

Limberg, G., Körner, R., Buchholt, H. C., Christensen, T. M. I. E., Roepstorff, P., & Mikkelsen, J. D. (2000). Analysis of different de-esterification mechanisms for pectin by enzymatic fingerprinting using endopectin lyase and endopolygalacturonase II from A. Niger. *Carbohydrate Research*, *327*(3), 293–307.

Limousin, G., Gaudet, J. P., Charlet, L., Szenknect, S., Barthès, V., & Krimissa, M. (2007). Sorption isotherms: A review on physical bases, modeling and measurement. *Applied Geochemistry*, *22*(2), 249–275.

Liners, F., Thibault, J.-F., & Van Cutsem, P. (1992). Influence of the degree of polymerization of oligogalacturonates and of esterification pattern of pectin on their recognition by monoclonal antibodies. *Plant Physiology*, *99*(3), 1099–1104.

Lips, A., Clark, A. H., Cutler, N., & Durand, D. (1991). Measurement of cooperativity of binding of calcium to neutral sodium pectate. *Food Hydrocolloids*, *5*, 87–99.

Löfgren, C., Guillotin, S., Evenbratt, H., Schols, H., & Hermansson, A. M. (2005). Effects of calcium, pH, and blockiness on kinetic rheological behavior and microstructure of HM pectin gels. *Biomacromolecules*, *6*(2), 646–652.

Lombardo, S., Eyley, S., Schütz, C., Van Gorp, H., Rosenfeldt, S., Van Den Mooter, G., & Thielemans, W. (2017). Thermodynamic study of the interaction of bovine serum albumin and amino acids with cellulose nanocrystals. *Langmuir*, *33*(22), 5473–5481.

Lootens, D., Capel, F., Durand, D., Nicolai, T., Boulenguer, P., & Langendorff, V. (2003). Influence of pH, Ca concentration, temperature and amidation on the gelation of low methoxyl pectin. *Food Hydrocolloids*, *17*(3), 237–244.

Luzio, G. A., & Cameron, R. G. (2008). Demethylation of a model homogalacturonan with the salt-independent pectin methylesterase from citrus: Part II. Structure-function analysis. *Carbohydrate Polymers*, *71*(2), 300–309.

Maire du Poset, A., Lerbret, A., Zitolo, A., Cousin, F., & Assifaoui, A. (2018). Design of polygalacturonate hydrogels using iron(II) as cross-linkers: A promising route to protect bioavailable iron against oxidation. *Carbohydrate Polymers*, *188*, 276–283.

Manzocco, L., Calligaris, S., & Nicoli, M. C. (2010). Methods for food shelf life determination and prediction. In E. A. Decker, R. J. Elias, & D. J. McClements (Eds.), *Oxidation in foods and beverages and antioxidant applications: Volume 1* (1st ed., p. 393). Woodhead publishing limited.

Massiot, P., Rouau, X., & Thibault, J.-F. (1988). Characterisation of the extractable pectins and hemicelluloses of the cell wall of carrot. *Carbohydrate Polymers*, *172*, 229–242.

Matsumura, Y., Egami, M., Satake, C., Maeda, Y., Takahashi, T., Nakamura, A., & Mori, T. (2003). Inhibitory effects of peptide-bound polysaccharides on lipid oxidation in emulsions. *Food Chemistry*, *83*(1), 107–119.

May, C. D. (1990). Industrial pectins: Sources, production and applications. *Carbohydrate Polymers*, *12*, 79–99.

McClements, D., & Decker, E. (2000). Lipid oxidation in oil-in-water emulsions: Impact of molecular environment on chemical reactions in heterogeneous food systems. *Journal of Food Science*, *65*(8), 1270–1282.

McClements, D. J. (2016). *Food emulsions* (3rd ed.). Boca Raton, Florida: CRC Press.

McClements, D. J., & Decker, E. (2018). Interfacial antioxidants: A review of natural and synthetic emulsifiers and coemulsifiers that can inhibit lipid oxidation. *Journal of Agricultural and Food Chemistry*, *66*(1), 20–25.

Mei, L., Decker, E. A., & McClements, D. J. (1998). Evidence of iron association with emulsion droplets and its impact on lipid oxidation. *Journal of Agricultural and Food Chemistry*, *46*(12), 5072–5077.

Minekus, M., Alminger, M., Alvito, P., Ballance, S., Bohn, T., Bourlieu, C., … Brodkorb, A. (2014). A standardised static in vitro digestion method suitable for food – an international consensus. *Food Function*, *5*, 1113–1124.

Miyada, T., Nakajima, A., & Ebihara, K. (2011). Iron bound to pectin is utilised by rats. *The British Journal of Nutrition*, *106*(1), 73–8.

Miyada, T., Nakajima, A., & Ebihara, K. (2012). Degradation of pectin in the caecum contributes to bioavailability of iron in rats. *The British Journal of Nutrition*, *107*, 1452–1457.

Mozuraityte, R., Kristinova, V., Rustad, T., & Storrø, I. (2016). The role of iron in peroxidation of PUFA: Effect of pH and chelators. *European Journal of Lipid Science and Technology*, *118*(4), 658–668.

Nair, B. M., Asp, N. G., Nyman, M., & Persson, H. (1987). Binding of mineral elements by some dietary fibre components in vitro (I). *Food Chemistry*, *23*, 295–303.

Naqash, F., Masoodi, F. A., Rather, S. A., Wani, S. M., & Gani, A. (2017). Emerging concepts in the nutraceutical and functional properties of pectin—A Review. *Carbohydrate Polymers*, *168*, 227–239.

Ngouémazong, D. E., Jolie, R. P., Cardinaels, R., Fraeye, I., Van Loey, A., Moldenaers, P., & Hendrickx, M. (2012a). Stiffness of Ca^{2+}-pectin gels: Combined effects of degree and pattern of methylesterification for various Ca^{2+} concentrations. *Carbohydrate Research*, *348*, 69–76.

Ngouémazong, D. E., Kabuye, G., Fraeye, I., Cardinaels, R., Van Loey, A., Moldenaers, P., & Hendrickx, M. (2012b). Effect of debranching on the rheological properties of Ca^{2+}-pectin gels. *Food Hydrocolloids*, *26*(1), 44–53.

Ngouémazong, D. E., Tengweh, F. F., Duvetter, T., Fraeye, I., Van Loey, A., Moldenaers, P., & Hendrickx, M. (2011). Quantifying structural characteristics of partially de-esterified pectins. *Food Hydrocolloids*, *25*, 434–443.

Ngouémazong, D. E., Tengweh, F. F., Fraeye, I., Duvetter, T., Cardinaels, R., Van Loey, A., Moldenaers, P., & Hendrickx, M. (2012c). Effect of de-methylesterification on network development and nature of Ca^{2+}-pectin gels: Towards understanding structure-function relations of pectin. *Food Hydrocolloids*, *26*, 89–98.

Ogawa, S., Decker, E. A., & McClements, D. J. (2003). Influence of environmental conditions on the stability of oil in water emulsions containing droplets stabilized by lecithin-chitosan membranes. *Journal of Agricultural and Food Chemistry*, *51*(18), 5522–5527.

Oosterveld, A., Beldman, G., Searle-Van Leeuwen, M. J. F., & Voragen, A. G. J. (2000). Effect of enzymatic deacetylation on gelation of sugar beet pectin in the presence of calcium. *Carbohydrate Polymers*, *43*(3), 249–256.

Parada, J., & Aguilera, J. M. (2007). Food microstructure affects the bioavailability of several nutrients. *Journal of Food Science*, *72*(2), 21–32.

Pérez, S., Mazeau, K., & Hervé du Penhoat, C. (2000). The three-dimensional structures of the pectic polysaccharides. *Plant Physiology and Biochemistry*, *38*, 37–55.

Platte, J. A., & Marcy, V. M. (1959). Photometric determination of zinc with zincon. Application to water containing heavy metals. *Analyical Chemistry*, *31*(7), 1226–1228.

Powell, D. A., Morris, E. R., Gidley, M. J., & Rees, D. A. (1982). Conformations and interactions of pectins II: Influence of residue sequence on chain association in calcium pectate gels. *Journal of Molecular Biology*, *155*(4), 517–531.

Privalov, P. L., & Gill, S. J. (1989). The hydrophobic effect: a reappraisal. *Pure and Applied Chemistry*, *61*(6), 1097–1104.

Qiu, C., Zhao, M., Decker, E. A., & McClements, D. J. (2015). Influence of anionic dietary fibers (xanthan gum and pectin) on oxidative stability and lipid digestibility of wheat protein-stabilized fish oil-in-water emulsion. *Food Research International*, *74*, 131–139.

Raes, K., Knockaert, D., Struijs, K., & Van Camp, J. (2014). Role of processing on bioaccessibility of minerals: Influence of localization of minerals and anti-nutritional factors in the plant. *Trends in Food Science & Technology*, *37*(1), 32–41.

Ralet, M. C., Crépeau, M. J., Buchholt, H. C., & Thibault, J. F. (2003). Polyelectrolyte behaviour and calcium binding properties of sugar beet pectins differing in their degrees of methylation and acetylation. *Biochemical Engineering Journal*, *16*(2), 191–201.

Ralet, M. C., Dronnet, V., Buchholt, H. C., & Thibault, J. F. (2001). Enzymatically and chemically de-esterified lime pectins: Characterisation, polyelectrolyte

behaviour and calcium binding properties. *Carbohydrate Research*, *336*, 117–125.

Ralet, M. C., Williams, M. A. K., Tanhatan-Nasseri, A., Ropartz, D., Quéméner, B., & Bonnin, E. (2012). Innovative enzymatic approach to resolve homogalacturonans based on their methylesterification pattern. *Biomacromolecules*, *13*, 1615–1624.

Renard, C. M. G. C., & Jarvis, M. C. (1999). Acetylation and methylation of homogalacturonans 2: effect on ion-binding properties and conformations. *Carbohydrate Polymers*, *39*(3), 209–216.

Ridley, B. L., O'Neill, M. A., & Mohnen, D. (2001). Pectins: Structure, biosynthesis, and oligogalacturonide-related signaling. *Phytochemistry*, *57*(6), 929–967.

Rolin, C., Nielsen, B. U., & Glahn, P.-E. (1998). Pectin. In S. Dimitriu (Ed.), *Polysaccharides: Structural integrity and functional versatility* (pp. 337–432). New York: Marcel Decker Inc.

Salvia-Trujillo, L., Decker, E. A., & McClements, D. J. (2016). Influence of an anionic polysaccharide on the physical and oxidative stability of omega-3 nanoemulsions: Antioxidant effects of alginate. *Food Hydrocolloids*, *52*, 690–698.

Schaich, K., Shahidi, F., Zhong, Y., & Eskin, N. A. M. (2013). Lipid oxidation. In N. A. M. Eskin & F. Shahidi (Eds.), *Biochemistry of foods* (p. 419). Elsevier Inc.

Schiewer, S., & Patil, S. B. (2008). Pectin-rich fruit wastes as biosorbents for heavy metal removal: Equilibrium and kinetics. *Bioresource Technology*, *99*(6), 1896–1903.

Schlemmer, U. (1989). Studies of the binding of copper, zinc and calcium to pectin, alginate, carrageenan and gum guar in HCO_3^--CO_2 buffer. *Food Chemistry*, *32*(3), 223–234.

Schmuhl, R., Krieg, H. M., & Keizer, K. (2001). Adsorption of Cu(II) and Cr(VI) ions by chitosan: Kinetics and equilibrium studies. *Water SA*, *27*, 1–7.

Shahidi, F. (2000). Antioxidants in food and food antioxidants. *Molecular Nutrition & Food Research*, *44*(3), 158–163.

Shantha, N. C., & Decker, E. A. (1994). Rapid, sensitive, iron-based spectrophotometric methods for determination of peroxides values of food lipids. *Journal of AOAC International*, *77*(2), 421–424.

Shimada, K., Okada, H., Matsuo, K., & Yoshioka, S. (1996). Involvement of chelating action and viscosity in the antioxidative effect of xanthan in an oil/water emulsion. *Bioscience Biotechnology and Biochemistry*, *60*(1), 125–127.

Shpigelman, A., Kyomugasho, C., Christiaens, S., Van Loey, A. M., & Hendrickx, M. E. (2014). Thermal and high pressure high temperature processes result in distinctly different pectin non-enzymatic conversions. *Food Hydrocolloids*, *39*, 251–263.

Siew, C. K., & Williams, P. A. (2005). New insights into the mechanism of gelation of alginate and pectin: Charge annihilation and reversal mechanism. *Biomacromolecules*, *6*, 963–969.

Sila, D. N., Van Buggenhout, S., Duvetter, T., Fraeye, I., De Roeck, A., Van Loey, A., & Hendrickx, M. (2009). Pectins in processed fruits and vegetables: Part II-Structure-function relationships. *Comprehensive Reviews in Food Science and Food Safety*, *8*, 86–104.

Slavov, A., Garnier, C., Crépeau, M. J., Durand, S., Thibault, J. F., & Bonnin, E. (2009). Gelation of high methoxy pectin in the presence of pectin methylesterases and calcium. *Carbohydrate Polymers*, *77*(4), 876–884.

Sousa, A. G., Nielsen, H. L., Armagan, I., Larsen, J., & Sørensen, S. O. (2015). The impact of rhamnogalacturonan-I side chain monosaccharides on the rheological properties of citrus pectin. *Food Hydrocolloids*, *47*, 130–139.

Spector, A. A. (1975). Fatty acid binding to plasma albumin. *Journal of Lipid Research*, *16*(2), 165–179.

Sriamornsak, P. (2003). Chemistry of pectin and its pharmaceutical uses: a review. *Silpakorn University International Journal*, *3*, 207–228.

Ström, A., Ribelles, P., Lundin, L., Norton, I., Morris, E. R., & Williams, M. A. K. (2007). Influence of pectin fine structure on the mechanical properties of calcium-pectin and acid-pectin gels. *Biomacromolecules*, *8*, 2668–2674.

Surabhi, A. K., Williams, P. A., & Elzagheid, M. I. (2017). Binding studies of pectin in presence of divalent cations. *Asian Journal of Chemistry*, *29*(5), 1141–1144.

Surh, J., Decker, E. A., & McClements, D. J. (2006). Influence of pH and pectin type on properties and stability of sodium-caseinate stabilized oil-in-water emulsions. *Food Hydrocolloids*, *20*(5), 607–618.

Tanhatan-Nasseri, A., Crépeau, M. J., Thibault, J. F., & Ralet, M. C. (2011). Isolation and characterization of model homogalacturonans of tailored methylesterification patterns. *Carbohydrate Polymers*, *86*(3), 1236–1243.

Tansel, B. (2012). Significance of thermodynamic and physical characteristics on permeation of ions during membrane separation: Hydrated radius, hydration free energy and viscous effects. *Separation and Purification Technology*, *86*, 119–126.

Thakur, B. R., Singh, R. K., Handa, A. K., & Rao, M. A. (1997). Chemistry and uses of pectin - A review. *Critical Reviews in Food Science and Nutrition*, *37*, 47–73.

Thibault, J.-F., & Ralet, M. C. (2003). Physico-chemical properties of pectins in the cel walls and after extraction. In A. G. J. Voragen, H. A. Schols, & R. Visser (Eds.), *Advances in pectin and pectinases research* (pp. 91–105). Dordrecht, The Netherlands: Kluwer Academic Publishers.

Thibault, J.-F., & Rinaudo, M. (1985). Interactions of mono- and divalent counterions with alkali- and enzyme-deesterified pectins in salt-free solutions. *Biopolymers*, *24*, 2131–2143.

Tibbits, C. W., MacDougall, A. J., & Ring, S. G. (1998). Calcium binding and swelling behaviour of a high methoxyl pectin gel. *Carbohydrate Research*, *310*, 101–107.

Van Buggenhout, S., Sila, D. N., Duvetter, T., Van Loey, A., & Hendrickx, M. (2009). Pectins in processed fruits and vegetables: Part III-Texture Engineering. *Comprehensive Reviews in Food Science and Food Safety*, *8*(2), 105–117.

van Dooren, C., Douma, A., Aiking, H., & Vellinga, P. (2017). Proposing a novel index reflecting both climate impact and nutritional impact of food products. *Ecological Economics*, *131*, 389–398.

Ventura, I., Jammal, J., & Bianco-Peled, H. (2013). Insights into the nanostructure of low-methoxyl pectin-calcium gels. *Carbohydrate Polymers*, *97*(2), 650–658.

Verkempinck, S. H. E., Kyomugasho, C., Salvia-Trujillo, L., Denis, S., Bourgeois, M., Van Loey, A. M., Hendrickx, M., & Grauwet, T. (2018). Emulsion stabilizing properties of citrus pectin and its interactions with conventional emulsifiers in oil-in-water emulsions. *Food Hydrocolloids*, *85*, 144–157.

Verrijssen, T. A. J., Christiaens, S., Verkempinck, S. H. E., Boeve, J., Grauwet, T., Van Loey, A. M., Salvia-Trujillo, L., & Hendrickx, M. E. (2016). In vitro β-Carotene bioaccessibility and lipid digestion in emulsions: Influence of pectin type and degree of methyl-esterification. *Journal of Food Science*, *81*(10), 2327–2336.

Vincken, J. P., Schols, H. A., Oomen, R. J. F. J., Beldman, G., Visser, R. G. F., & Voragen, A. G. J. (2003a). Pectin-the hairy thing. Evidence that homogalacturonan is a side chain of rhamnogalacturonan I. In A. G. J. Voragen, H. A. Schols, & R. Visser (Eds.), *Advances in pectin and pectinases research* (pp. 47–59). Dordrecht, The Netherlands: Kluwer Academic Publishers.

Vincken, J., Schols, H. A., Oomen, R. J. F. J., McCann, M. C., Ulvskov, P., Voragen, A. G. J., & Visser, R. G. F. (2003b). If homogalacturonan were a side chain of rhamnogalacturonan I. Implications for cell wall architecture. *Plant Physiology*, *132*(4), 1781–1789.

Viollier, E., Inglett, P. W., Hunter, K., Roychoudhury, A. N., & Van Cappellen, P. (2000). The ferrozine method revisited: Fe(II)/Fe(III) determination in natural

waters. *Applied Geochemistry*, *15*, 785–790.

Voragen, A. G. J., Coenen, G. J., Verhoef, R. P., & Schols, H. A. (2009). Pectin, a versatile polysaccharide present in plant cell walls. *Structural Chemistry*, *20*, 263–275.

Wicker, L., Kim, Y., Kim, M. J., Thirkield, B., Lin, Z., & Jung, J. (2014). Pectin as a bioactive polysaccharide - Extracting tailored function from less. *Food Hydrocolloids*, *42*, 251–259.

Willats, W. G. T., Knox, J. P., & Mikkelsen, J. D. (2006). Pectin: New insights into an old polymer are starting to gel. *Trends in Food Science and Technology*, *17*, 97–104.

Willats, W. G. T., Orfila, C., Limberg, G., Buchholt, H. C., Van Alebeek, G. J. W. M., Voragen, A. G. J., … Knox, J. P. (2001). Modulation of the degree and pattern of methyl-esterification of pectic homogalacturonan in plant cell walls: Implications for pectin methyl esterase action, matrix properties, and cell adhesion. *Journal of Biological Chemistry*, *276*(22), 19404–19413.

Xu, X., Liu, W., Luo, L., Liu, C., & McClements, D. J. (2017). Influence of anionic polysaccharides on the physical and oxidative stability of hydrolyzed rice glutelin emulsions: Impact of polysaccharide type and pH. *Food Hydrocolloids*, *72*, 185–194.

Yapo, B. M. (2011). Pectic substances: From simple pectic polysaccharides to complex pectins - A new hypothetical model. *Carbohydrate Polymers*, *86*(2), 373–385.

Zhao, F., Repo, E., Yin, D., & Sillanpää, M. E. T. (2013). Adsorption of Cd(II) and Pb(II) by a novel EGTA-modified chitosan material: Kinetics and isotherms. *Journal of Colloid and Interface Science*, *409*, 174–182.

Zhao, Z. Y., Liang, L., Fan, X., Yu, Z., Hotchkiss, A. T., Wilk, B. J., & Eliaz, I. (2008). The role of modified citrus pectin as an effective chelator of lead in children hospitalized with toxic lead levels. *Alternative Therapies*, *14*, 34–38.

LIST OF PUBLICATIONS

Publications in international peer-reviewed journals

Rousseau, S., Kyomugasho, C., **Celus, M**., Yeasman, N., Hendrickx, M., & Grauwet, T. (2018). Zinc bioaccessibility can be affected by the presence of calcium ions and pectin degree of methylesterification. Revisions submitted to *Food Hydrocolloids*.

Rousseau, S., Kyomugasho, C., **Celus, M**., Hendrickx, M., & Grauwet, T. (2018). Barriers impairing mineral bioaccessibility and bioavailability in plant-based foods and the perspectives for food processing. Submitted to *Critical Reviews in Food Science and Nutrition*.

Celus, M., Kyomugasho, C., Van Loey, A., Grauwet, T., & Hendrickx, M. (2018). Influence of pectin structural properties on interactions with divalent cations and its associated functionalities. *Comprehensive reviews in food science and food safety*, 17: 1576-1594.

Kyomugasho, C., Munyensanga, C., **Celus, M**., Van de Walle, D., Dewettinck, K., Van Loey, A., & Hendrickx, M. (2018). Molar mass influence on pectin-Ca^{2+} adsorption capacity, interaction energy and associated functionality: gel microstructure and stiffness. *Food Hydrocolloids,* 85: 331-342.

Celus, M., Kyomugasho, C., Lombardo, S., Thielemans, W., & Hendrickx, M. (2018). Isothermal titration calorimetry to study the influence of citrus pectin degree and pattern of methylesterification on Zn^{2+} interaction. *Carbohydrate Polymers*, 197: 460-468.

Celus, M., Kyomugasho, C., Salvia-Trujillo, L., Van Audenhove, J., Van Loey, A., Grauwet, T., & Hendrickx, M. (2018). Interactions between citrus pectin and Zn^{2+} or Ca^{2+} and associated *in vitro* Zn^{2+} bioaccessibility as affected by degree of methylesterification and blockiness. *Food Hydrocolloids,* 79: 319-330.

Celus, M., Salvia Trujillo, L., Kyomugasho, C., Maes, I., Van Loey, A., Grauwet, T., & Hendrickx, M. (2018). Structurally modified pectin for targeted lipid antioxidant capacity in linseed/sunflower oil-in-water emulsions. *Food Chemistry*, 241: 86-96.

Celus, M., Kyomugasho, C., Jamsazzadeh Kermani, Z., Roggen, K., Van Loey, A., Grauwet, T., & Hendrickx, M. (2017). Fe^{2+} adsorption on citrus pectin is influenced by the degree and pattern of methylesterification. *Food Hydrocolloids*, 73: 101-109.

Palmers, S., Grauwet, T., **Celus, M**., Kebede, B., Hendrickx, M., & Van Loey, A. (2015). Furan formation as a function of pressure, temperature and time conditions in spinach purée. *LWT - Food Science and Technology*, 64: 565-570.

Palmers, S., Grauwet, T., **Celus, M**., Wibowo, S., Kebede, B., Hendrickx, M., & Van Loey, A. (2015). A kinetic study of furan formation during storage of shelf-stable fruit juices. *Journal of Food Engineering*, 165:74-81.

Contributions to international conferences

Celus, M., Kyomugasho, C., Grauwet, T., Van Loey, A., & Hendrickx, M. Pectin-Cation Interactions and Associated Functional Properties as Influenced by Pectin Degree and Distribution of Methylesters. E-poster presentation at IFT18, July 15-18, 2018, Chicago, U.S.A.
At this conference, Miete Celus has been awarded the **1st place in the Carbohydrate Division Graduate Student Research Paper Poster Competition.**

Celus, M., Salvia Trujillo, L., Kyomugasho, C., Maes, I., Van Loey, A., Grauwet, T., & Hendrickx, M. Influence of citrus pectin nanostructure on the oxidative stability of oil-in-water emulsions. Oral presentation at 15th Euro Fed Lipid Congress, August 27-30, 2017, Uppsala, Sweden.

Palmers, S., Grauwet, T., **Celus, M**., Kebede, B.T., Hendrickx, M., & Van Loey, A. Furan formation throughout the food chain: prospects for furan mitigation. Oral presentation at the 12th International Congress on Engineering and Food: Bridging Science and Food Innovations, June 14-18, 2015, Québec City, Canada.

Contributions to national conferences

Celus, M., Kyomugasho, C., Jamsazzadeh Kermani, Z., Roggen, K., Grauwet, T., Van Loey, A., & Hendrickx, M. Role of degree and pattern of methylesterification of citrus pectin on Fe^{2+}-adsorption capacity. Oral presentation at National Symposium for Applied Biological Sciences, February 7, 2017, Leuven, Belgium.